

University of Montana

ScholarWorks at University of Montana

Graduate Student Theses, Dissertations, &
Professional Papers

Graduate School

2007

The role of Zinc and Reactive Oxygen Species in the Regulation of Endothelial Nitric Oxide Synthase

Jason Michael Wilham
The University of Montana

Follow this and additional works at: <https://scholarworks.umt.edu/etd>

Let us know how access to this document benefits you.

Recommended Citation

Wilham, Jason Michael, "The role of Zinc and Reactive Oxygen Species in the Regulation of Endothelial Nitric Oxide Synthase" (2007). *Graduate Student Theses, Dissertations, & Professional Papers*. 1077.
<https://scholarworks.umt.edu/etd/1077>

This Dissertation is brought to you for free and open access by the Graduate School at ScholarWorks at University of Montana. It has been accepted for inclusion in Graduate Student Theses, Dissertations, & Professional Papers by an authorized administrator of ScholarWorks at University of Montana. For more information, please contact scholarworks@mso.umt.edu.

THE ROLE OF ZINC AND REACTIVE OXYGEN SPECIES IN THE
REGULATION OF ENDOTHELIAL NITRIC OXIDE SYNTHASE

By

Jason Michael Wilham

B.S. Chemistry, Montana Tech of the University of Montana, Butte, MT, 2003

Dissertation

presented in partial fulfillment of the requirements
for the degree of

Doctor of Philosophy
in Toxicology

The University of Montana
Missoula, MT

Spring 2007

Approved by:

Dr. David A. Strobel, Dean
Graduate School

J. Douglas Coffin, Chair
Department of Biomedical and Pharmaceutical Sciences

Stephen M. Black, Co-Chair
Department

David Poulsen
Department of Biomedical and Pharmaceutical Sciences

Mark Pershouse
Department of Biomedical and Pharmaceutical Sciences

J.B. Alexander Ross
Department of Chemistry

The Role of Zinc and Reactive Oxygen Species in the Regulation of Endothelial Nitric Oxide Synthase

Chairperson: J. Douglas Coffin, Ph.D.

Co-Chairperson: Stephen M. Black, Ph.D.

Persistent pulmonary hypertension of the newborn (PPHN) is a very serious disease affecting nearly 5 in 1000 newborns each year. The development of PPHN has been linked to a decrease in the activity and expression of endothelial nitric oxide synthase (eNOS). Thus, it is critical to understand the mechanisms by which eNOS is regulated to identify new pathways and novel therapies for PPHN. eNOS is dynamically regulated at the transcriptional, post-transcriptional, post-translational, and developmental levels, however mechanisms of this regulation are unresolved. Our data indicates that increases in eNOS expression and activity correlate with increased cellular levels of labile zinc (Zn). In addition, our analysis of the eNOS promoter indicated the presence of a putative heavy metal response element (HRE) in the 5'-flanking sequence. We hypothesized that nitric oxide (NO) may be regulating eNOS expression and activity indirectly through its ability to regulate cellular levels of free Zn. Further, we hypothesized that Zn exerts an effect on eNOS at the transcriptional and post-translational levels. Our results suggested that both NO and hydrogen peroxide (H₂O₂) activate eNOS in a Zn-dependent manner by liberating cellular stores of Zn and activating the heavy metal-responsive transcription factor 1, MTF-1, which then would bind to the eNOS 5'-regulatory MRE. We found that basal zinc levels in endothelial cells (ECs) helped maintain eNOS promoter activity and total protein levels, but did not affect eNOS dimer levels. However, supplementing ECs with exogenous Zn increased eNOS total and dimer protein levels and activity, mostly through MTF-1. At higher, non-toxic doses of Zn, reactive oxygen species (ROS) production was much higher. eNOS was inhibited by high ROS levels through enzyme fragmentation. Lastly, an eNOS enzyme cofactor, tetrahydrobiopterin (BH₄), was found to help maintain eNOS protein due to its high antioxidant potential. In conclusion, eNOS appears to be regulated by NO and ROS through an increase in intracellular Zn, thus activating MTF-1, which binds to the 5' flanking region of the eNOS promoter.

ACKNOWLEDGMENTS

I would like to acknowledge my beautiful and wonderful wife, Laura, for her love and support through it all. I would like to thank the Department of Biomedical and Pharmaceutical Sciences and the Toxicology Department at the University of Montana for their support. Dr. Douglas Coffin, my co-advisor, was a big help in the final stages of this process and also inspired me to join the Toxicology program. I would also like to thank my advisor Dr. Stephen Black for his support and guidance. Thanks goes out to the former Vascular Biology Lab for their willingness to help me throughout this experience and for becoming such great friends in and out of the laboratory. These include Dr. Melisa Schlevan, Jon Welker, Dr. Dean Wiseman, Dr. Sanjiv Kumar, Dr. Albert Grobe, and Deborah Nycz. Last, but not least, a special thanks to my committee members, Dr. Stephen Black, Dr. J. Douglas Coffin, Dr. David Poulsen, Dr. Mark Pershouse, and Dr. Alexander Ross. This research was supported in part by grants 0515459Z from the American Heart Association Pacific Mountain Affiliates (to Jason Wilham), HL60190 (to Stephen Black), HL67841 (to Stephen Black), HL072123 (to Stephen Black), and HL070061 (to Stephen Black) from the National Institutes of Health.

COMMON INTRODUCTION

Persistent Pulmonary Hypertension of the Newborn (PPHN)

The foramen ovale, which links the two atria of the fetal heart, and the ductus arteriosus, which links the main pulmonary artery with the descending aorta, are both important in allowing fetal blood to bypass the pulmonary circuit and the collapsed non-functional fetal lungs. Prior to birth the open foramen ovale and ductus arteriosus cause the pulmonary vascular resistance (PVR) to be

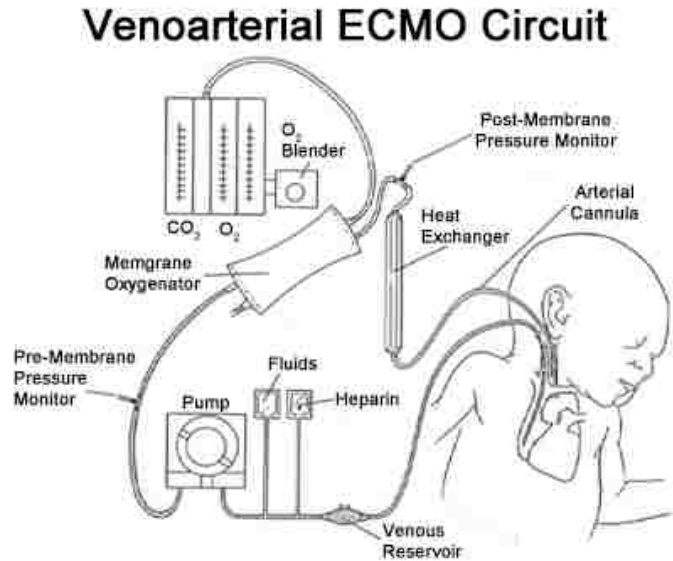


Figure 1: EMCO
(http://www.gla.ac.uk/surgicalpaediatrics/images/VA_ECMO_circuit_.jpg)

high, but at birth with the loss of the placenta PVR rapidly falls. Since pressure and flow are inversely related, this decrease is associated with an 8-10-fold increase in blood flow [1-3], allowing the fetal lungs to establish gas exchange. PVR then continues to fall gradually during the newborn's first month [4]. However, in a number of clinical cases in the term or near term infant, there is a failure of the pulmonary circulation to undergo the normal transition to postnatal life, resulting in persistent pulmonary hypertension of the newborn (PPHN). PPHN is a very serious disease that can be triggered by a number of events such as meconium aspiration syndrome, respiratory distress syndrome, pneumonia, sepsis, or severe hypoxia [4]. It is thought to be responsible for approximately 10% of admissions to neonatal intensive care units and affects nearly 5 in

1000 newborns each year [5]. The disorder is associated with significant morbidity and mortality [5].

Initially, these hypertensive infants are put on oxygen and if this is not sufficient, then they are given inhaled nitric oxide. Extra corporeal membrane oxygenation (ECMO) is considered the most advanced therapy for extreme cases. Essentially, ECMO is a heart lung bypass machine that is connected to the infant via an arterial cannula (Figure 1). Inhaled nitric oxide reduces the use of ECMO in these PPHN infants [6].

PPHN can be associated with extensive vascular remodeling. Figure 2 demonstrates this remodeling with arterial cross sections from normal and pulmonary hypertensive states. Obvious intima and adventitia hypoplasia is evident as well as thickening of the adventitia, media, and intima. These alterations result in a much smaller luminal diameter and therefore, a much lower blood flow.

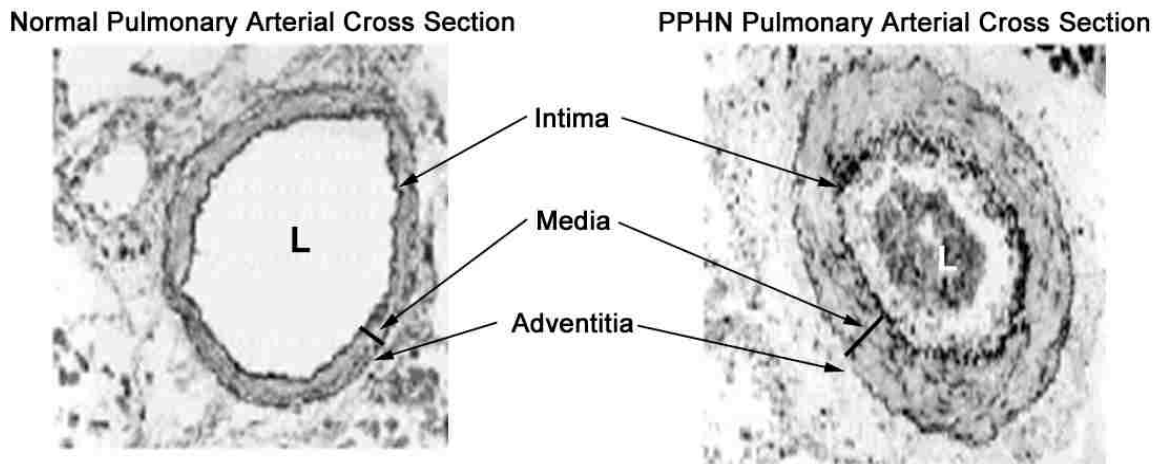


Figure 2. Arterial cross sections from normal and PPHN states. L labels the lumen of the vessels.

Endothelial Nitric Oxide Synthase (eNOS)

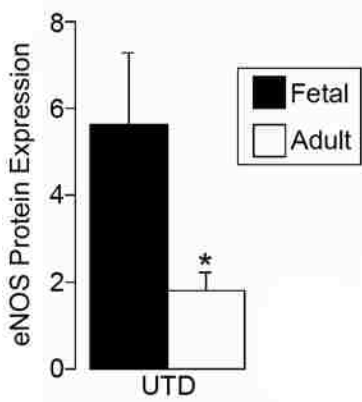


Figure 3. Ovine fetal endothelial cells have 5-6 fold higher eNOS protein levels compared to adult endothelial cells. Fetal and adult endothelial cells were grown to confluency. Protein was harvested and western blot analysis was used to look at eNOS protein levels. All values are mean \pm SEM (n=4). * $P < 0.05$ vs. Fetal.

The fetal to newborn transition is dependent on the functioning of the enzyme endothelial nitric oxide synthase (eNOS). In fact, the development of PPHN has been linked to a decrease in the activity and expression of eNOS. Endothelial NOS expression is largely tissue dependent. eNOS is predominantly expressed in

endothelial cells (EC), although studies have also shown eNOS expression in bronchiolar epithelial cells [7, 8]. eNOS helps to maintain vascular homeostasis by generating nitric oxide (NO). This NO keeps the vasculature dilated, protects the intima of the vessels from platelet aggregation and leukocyte adhesion and prevents proliferation of

vascular smooth muscle. Originally thought to be a constitutively expressed enzyme, eNOS is now known to be modulated by a variety of chemical, physical, and developmental stimuli [9]. The regulation of this enzyme's protein expression has been demonstrated at the developmental, transcriptional, post-transcriptional and post-translational levels [10-15]. However, the mechanisms of this regulation are yet to be resolved.

a. Developmental Regulation of eNOS

Basal and agonist-stimulated endothelial production of NO has been demonstrated in the fetal, newborn, and adult pulmonary vasculature [16-20]. Immunostaining for eNOS

is seen as early as 29% gestation in the fetal lamb lung and physiologic studies of intrapulmonary arteries and isolated lung preparations of the sheep reveal maturational increases in NO-mediated relaxation during the late fetal and early postnatal period [18, 19, 21, 22]. For example, in ovine intrapulmonary arteries, basal NO production rises 2-fold from late gestation to 1 week of life, and another 1.6-fold from 1-to-4 weeks of life [19]. Similarly, in the pig, there is an increase in NO-mediated relaxation during the first

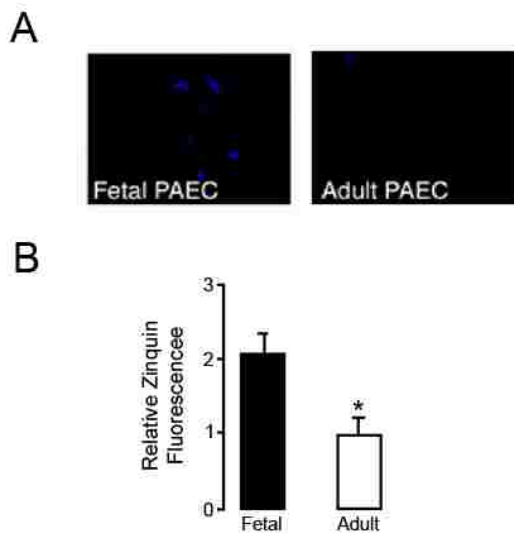


Figure 4. Ovine fetal endothelial cells have 2-fold higher free zinc levels compared to adult endothelial cells. Fetal and adult endothelial cells were grown to confluence. Cells were then loaded with zinquin ethyl ester and visualized using fluorescent microscopy. All values are mean \pm SEM (n=4). * $P < 0.05$ vs. Fetal.

two weeks of life, followed by a decrease. Coinciding with this physiologic data, eNOS mRNA and protein increase during late gestation and perinatal periods and decrease post-natally in a rat and sheep parenchyma [19, 21, 23-25].

Pitt and colleagues have carried out elegant studies indicating that NO donors can induce an increase in labile zinc in adult ovine PAECs [26, 27]. At least part of the mechanism

for this increase appears to be S-nitrosylation of metallothionein [27-29]. However, it is unknown if developmental differences in basal levels of labile zinc exist in endothelial cells. My data indicated that increased cellular levels of labile Zn, measured with the zinc fluorophore zinquin, correlate with increases in eNOS expression and activity

(Figure 3 & 4). These studies focused on the potential role played by the NO and zinc in regulating eNOS gene expression.

It is worth noting that the other two NOS isoforms, neuronal NOS (nNOS or NOS I) and inducible NOS (iNOS or NOS II) are also expressed in the lung and appear to be also

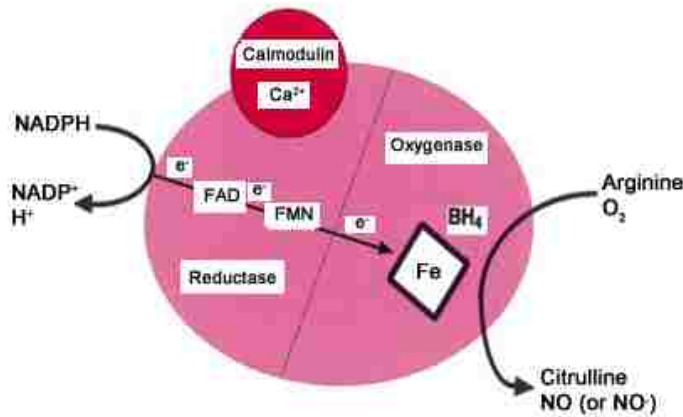


Figure 5. eNOS structure and cofactors.

developmentally regulated and differentially distributed in pulmonary vessels and airways of fetal lungs [20, 23, 25, 30].

However, we focused our studies on eNOS since it is intimately involved in the control of blood

pressure and its protein and activity levels are decreased in PPHN.

a. Transcriptional Regulation

Indeed, the eNOS promoter contains a plethora of putative cis-elements, including Sp-1 and GATA motifs, a sterol regulatory element, estrogen-responsive elements, a nuclear factor 1 element, a cAMP-responsive elements, and activator protein (AP-1 and -2) binding sites [24, 31, 32] that would allow eNOS to be regulated by many different signals. Basal eNOS expression has been shown to be regulated in ECs by a complex interaction between two tightly clustered cis-regulatory regions defined as positive regulatory domains I (-104/-95 relative to initiation site) and II (-144/-115) [33].

Data from our laboratory indicated that increases in eNOS expression and activity correlated with increases in the cellular levels of labile zinc (Zn) (Figures 3 & 4). In

addition, our analysis of the eNOS promoter indicated the presence of a putative heavy metal response element (HRE) located at -899/-893 in the 5'-flanking sequence of the human eNOS gene.

b. Post-translational Regulation

Recent evidence suggests that normal pulmonary vascular reactivity and vascular smooth muscle cell proliferation are regulated by a complex interaction of vasoactive substances produced by the endothelium [34-36]. Previously published research indicates that eNOS is only active as a dimeric enzyme and that the dimer is stabilized by the formation of a zinc tetrathiolate cluster, in which two cysteine thiolate ligands are contributed by each subunit [37-39]. When active and tightly coupled, eNOS catalyzes the oxidation reaction of L-arginine and molecular oxygen to L-citrulline and NO [40]. Once released from endothelial cells, NO diffuses into vascular smooth muscle cells and activates α_1 and β_1 subunits which catalyzes production of guanosine-3',5'-cyclic monophosphate (cGMP) from guanosine-5'-triphosphate. cGMP induces vascular smooth muscle relaxation through activation of a cGMP-dependent protein kinase [41]. Endothelium-derived NO (and the resulting cGMP) is an important mediator of vascular tone and an inhibitor of platelet aggregation and smooth muscle mitogenesis [42, 43].

However, under certain conditions, NOS may generate reactive oxygen species (superoxide and hydrogen peroxide) rather than NO. This process is referred to as NOS uncoupling, meaning that NADPH oxidation and NO synthesis have become uncoupled. It is important to note that a series of in vitro biochemical studies demonstrated that eNOS is the most tightly coupled of all the NOS isoforms [30, 37-39] and definitive in vivo and in vitro evidence that uncoupling of eNOS can occur is missing from the

literature. Thus, the mechanisms of eNOS uncoupling in ECs are not completely understood. Our data indicated that the addition of exogenous zinc to endothelial cells significantly increased NO generation.

c. Reactive Oxygen Species (ROS) Regulation

The development of hypertensive states in both the pulmonary and systemic circulatory systems is associated with increased vascular reactivity and the disruption of these regulatory mechanisms [44-49]. Inhibition of eNOS is one of the hallmarks of developing endothelial cell dysfunction [50-53]. The last several years have revealed that oxidative inactivation of NO is likely to be important in the development of several pathologic conditions including atherosclerosis, hypercholesterolemia, hypertension, and diabetes [54]. Studies have shown that in blood vessels, the balance existing between the steady state levels of NO and the superoxide anion appears to be disrupted resulting in a decrease in the bio-availability of NO [42, 54]. For example, large amounts of nitrogen oxides are released from vessels in an oxidatively degraded state in cholesterol-fed rabbits [55]. Treating these rabbits with polyethylene-glycosylated superoxide dismutase (SOD) dramatically increased endothelium-dependent vascular relaxation, suggesting a role for superoxide in oxidative inactivation of NO [56]. Vascular superoxide production in cholesterol-fed rabbits appeared to be from xanthine oxidase, because production was inhibited by the specific inhibitor oxypurinol [57]. Published results show increased levels of xanthine oxidase in the plasma of cholesterol-fed rabbits, and this circulating xanthine oxidase binds to heparin-binding sites on the vessel, where it acts to produce excess superoxide [57]. Evidence demonstrates that reactive oxygen species also diminish NO bioactivity in humans. For example, infusion of ascorbic acid improves

vascular responses to acetylcholine in cigarette smokers [58]. In the endothelium, cyclooxygenase [59], xanthine oxidase [60], and NADPH oxidase [61] have been identified as significant producers of superoxide. More recent studies have indicated that NOS itself may also be a significant producer of superoxide during the development of nitrate tolerance [48]. Interestingly, the use of PKC inhibitors was shown to decrease the production of superoxide in the tolerant vessels although the mechanism of this effect was not clear [48]. NOS may produce superoxide when the bioavailability of tetrahydrobiopterin or L-arginine are low [62]. Both superoxide and NO are free radicals (i.e., they contain an unpaired electron in their outer orbital). When exposed to each other, they undergo a facile radical-radical reaction that proceeds at a rate recently estimated to be $7 \times 10^9 \text{ mol}^{-1} \cdot \text{L} \cdot \text{s}^{-1}$ [63, 64]. This is approximately three times faster than the reaction rate for superoxide with either the Mn- or CuZn SOD. Thus, in a compartment in which both NO and SOD exist, there may be a propensity for superoxide to preferentially react with NO rather than SOD, depending on the relative concentrations of NO and SOD present.

Every cell type in the vascular wall, including fibroblasts [65], endothelial cells [66, 67], and smooth muscle cells [68], has been shown to produce and be regulated by ROS. This oxidant production plays an important role both in the normal functioning of the vascular system, as well as the pathogenesis of vascular disease.

A common property of the many stimuli that increase eNOS expression is the ability to increase the production of reaction oxygen intermediates (ROIs). In small amounts, these ROI can be stimulating, however, at high levels, our lab has shown them,

specifically hydrogen peroxide (H_2O_2) and nitric oxide (NO), to induce apoptosis and mitochondrial dysfunction in pulmonary aortic ECs [69, 70].

H_2O_2 , most commonly produced when superoxide ($O_2^{\cdot-}$) is dismutated by superoxide dismutase (SOD), is the most stable and long lasting of the ROS [71]. It has been previously shown that H_2O_2 , but not $O_2^{\cdot-}$ or hydroxyl radicals (OH^{\cdot}), increase eNOS expression by increasing both the rate of transcription of eNOS gene and the stability of the eNOS message once it is formed [9]. Previous studies done in a cell-free system have indicated that H_2O_2 releases zinc from metallothionein [72]. By exposing cells to certain levels of NO, either through exogenous NO [73, 74] or by upregulation of inducible nitric oxide synthase (iNOS) activity [75], other studies have also seen increases in intracellular labile zinc (Zn^{2+}) levels. We have previously demonstrated that maintaining zinc homeostasis is important in endothelial cell viability [69, 70].

Nitric Oxide and Zinc

Nitric oxide (NO) is a signaling molecule involved in several physiological processes such as vasodilation. NO can react with metal containing proteins (especially hemoproteins) at rates limited only by diffusion. These proteins may represent a primary target for NO. In fact the cellular effects of NO were initially believed to be due its affinity for heme and non-heme iron [76]. However, the number of pathophysiological pathways mediated by NO has been expanding to include processes that are independent of heme and non-heme iron. Alternative reaction pathways for NO have been proposed to account for these effects, most notably S-nitrosylation [77]. S-nitrosylation is the addition of NO to a sulfur group predominantly occurring on cysteine residues of protein.

Recent *in vitro* data has demonstrated that NO can S-nitrosylate metallothionein (MT) increasing labile zinc in endothelial cells [73, 78]. In certain cell types, MT is bound to >30% of cytosolic zinc. The interaction between MT and NO has been followed in real time using a fusion protein consisting of MT sandwiched between two mutant green fluorescent proteins [79]. *In vitro* studies with this protein demonstrated that observed fluorescent resonance energy transfer (FRET) changes are indicative of zinc release from MT. Imaging experiments have found that agents that increase cytoplasmic Ca^{2+} act via endogenously generated NO to rapidly and persistently release zinc from MT, an effect that can be mimicked by NO donors or exogenous NO gas [79]. Further, utilizing the zinc-sensitive fluorophore, Zinquin ethyl ester (Alexis), it has been shown that the exposure of endothelial cells to NO donors results in a rapid increase in labile zinc [73, 80, 81] and that the over-expression of MT can reduce this increase.

Heavy Metal Responsive Transcription Factor 1 (MTF-1)

Zinc binding proteins are the most abundant class of protein in the human cellular proteome [82]. Therefore, in theory, liberating enough zinc from these protein interactions to activate zinc binding transcription factors without inducing apoptotic or necrotic cell death should be relatively easy.

Heavy metal responsive transcription factor 1 (MTF-1) is one such transcription factor of interest. MTF-1 is a heavy metal-induced transcriptional activator [83-85] that is highly conserved from insects to vertebrates [86]. Targeted disruption of the MTF-1 gene results in death at embryonic day 14 due to liver degeneration, revealing a stage-specific developmental role [86]. Lichtlen et al. have engineered a mouse lacking

functional MTF-1 and discovered they die around day 14 of gestation due to acute decay of hepatocytes. Since MTF-1 conditional knock outs have not been developed yet, evidence of functional deficits in the vascular system alone are unknown. Also, under hypoxic-anoxic stress, MTF-1 helps to activate the transcription of the gene placental growth factor (PIGF), an angiogenic protein [86].

MTF-1 functions as a cellular zinc sensor, which coordinates the expression of genes involved in zinc homeostasis, as well as affording protection against metal toxicity and oxidative stress [87]. MTF-1 induces the expression of MT genes, which have the potential to act as chelators of heavy metals and scavenger of free radicals [88]. The current model suggests that the seven zinc-finger domain of MTF-1 directly and reversibly binds to zinc [83, 89]. This metallo-regulatory protein then adopts a DNA-binding conformation and translocates to the nucleus, where it binds to metal-responsive elements (MREs) in these gene promoters leading to increased transcription [87, 90]. Many genes contain putative MTF-1 binding sites that have been detected in the promoter sequences. These include MT itself [91], the zinc-transporter-1 (ZnT1) [92], and the gamma-glutamylcysteine synthetase heavy chain [93]. In addition, it has been shown that physiologic levels of NO can induce glutathione synthesis (GSH) in ECs and that this appears to be mediated via an increase in cGMP independent gamma-glutamylcysteine synthetase expression [94].

The mechanism by which zinc elicits MTF-1 conformational change, translocation to the nucleus, and synthesis of MT in a cell-free system has been outlined in a study by Zhang, et al. [72]. Hydrogen peroxide and certain heavy metals, such as cadmium, can disrupt zinc bound to MT. Being the so-called zinc sensor of the cell,

MTF-1 binds the free zinc that is released and becomes activated by undergoing a conformational change. Next, MTF-1 translocates to the nucleus, where it can act as a transcription factor and bind to various MREs, including MT. Zhang suggests that newly produced “apo-metallothionein” (non-zinc containing MT) will bind up free zinc, thus acting as a basic regulatory mechanism for activation of MTF-1 during cellular stress.

These MREs are DNA sequence motifs with the consensus binding site TGCRNC. MREs are present in a number of genes' promoters including metallothionein (MT) [95-97], the zinc transporter ZnT1 [92, 93, 98], and γ -glutamylcysteine synthetase heavy chain [93, 98]. Upon liberation of labile zinc, the eNOS HRE could be a likely target of MTF-1 binding. There are a limited number of studies that have explored the involvement of MTF-1 in the regulation of eNOS. We hypothesized that NO generation and ROS production increase cellular free Zn and activate MTF-1. This in turn causes MTF-1 nuclear translocation and increased expression of eNOS via the MRE located in the 5'-flanking region of the eNOS gene.

Endothelial cells in culture

Since our interest is in the regulation of eNOS activity and gene expression in the pulmonary system, a tractable model is needed. Thus, primary cultures of arterial endothelial cells from sheep and cow have been isolated and maintained in culture. These cells were obtained by scraping the main pulmonary artery and resistance vessels (<200 μ M). After a few days in culture, moderate-sized aggregates of cells were transferred using a micropipette, grown to confluence and maintained in culture. These cells take several passages to reach purity and can grow up to 20 passages before

reaching senescence. They exhibit contact inhibition, are tightly opposed, and are cobblestone in appearance.

Research Significance

It is critical to understand the mechanisms by which eNOS is regulated, not only to identify the pathways

responsible for the regulation of

eNOS, but also to develop new

treatments for PPHN. Certainly,

a large body of work has been

published in the regulation of

eNOS in the cell, but in reality,

still very little is known about

the exact mechanisms of eNOS

regulation. It is likely that

insights into the mechanisms of

eNOS regulation are impeded by

the fact that eNOS expression and

regulation appear to vary in different

EC cell lines. Little or no thought is given to the source of endothelial cell used in most

studies. Thus, studies are published using cells isolated from a variety of different

species that are isolated from a variety of different tissues. These studies will utilize low

passage ovine or bovine aortic endothelial cells.

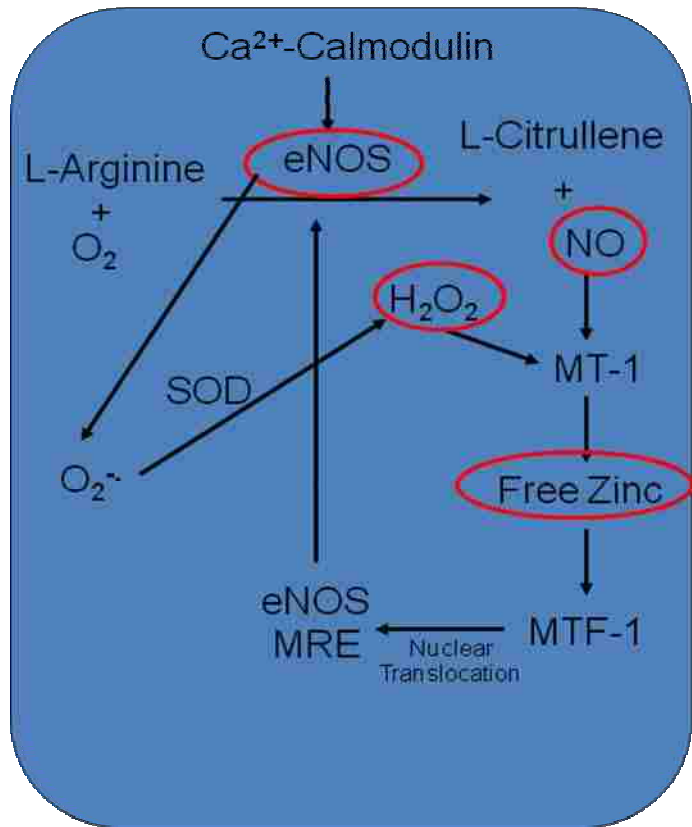


Figure 6. Hypothesized research pathway

We hypothesized that NO and ROS may be regulating eNOS expression and activity indirectly through their ability to alter cellular levels of free Zn. Further, we hypothesized that Zn exerts an effect on eNOS at the transcriptional and post-translational levels. These novel hypotheses will be tested in the four chapters of this dissertation.

Results from these studies indicated that non-toxic, low dose NO and H₂O₂ up-regulated eNOS promoter activity, mRNA, and total protein through the release of intracellular zinc, activation of MTF-1, and binding of MTF-1 to the eNOS HRE. The direct addition of low micro-molar amounts of zinc caused a dose-dependent increase in eNOS dimer levels and also significantly increased eNOS activity and total protein levels, mainly through activation of MTF-1. At higher levels it is associated with a large increase in ROS production. High levels of ROS significantly decreased eNOS activity by enzyme fragmentation. The eNOS cofactor, tetrahydrobiopterin (BH₄), one of the most potent naturally occurring reducing agents, was found to help protect eNOS protein levels and activity by acting as an antioxidant.

ENDOTHELIAL NITRIC OXIDE SYNTHASE REGULATION BY ZINC

Jason Wilham¹

Sanjiv Kumar²

Stephen M. Black²

¹Department of Biomedical & Pharmaceutical Sciences,

The University of Montana, Missoula MT 59812,

and

²Vascular Biology Center, Medical College of Georgia, Augusta, GA 30912

Short Title:

eNOS Regulation by Zinc

ABSTRACT

Persistent pulmonary hypertension of the newborn (PPHN) poses a serious health risk for the newborn, afflicting 5 in 1000 each year. The development of PPHN has been linked to a decrease in the activity and expression of the enzyme endothelial nitric oxide synthase (eNOS). Unpublished studies from our lab indicated that eNOS expression and activity correlated with cellular levels of labile zinc (Zn). In addition, our analysis of the eNOS promoter indicates the presence of a putative heavy metal response element (HRE) on the 5'-flanking sequence. Thus, this study sets out to define the mechanism by which zinc mediates eNOS expression at the transcriptional level and eNOS activity at the post-translational level. Low passage (P4-P6) fetal pulmonary aortic endothelial cells (FPAECs) were exposed to 0, 25, 50, and 100 μ M ZnCl₂ for 7hrs, or to zinc-depletion conditions, by virally transducing with metallothionein 1 (MT-1) adenovirus. Zinc exposure led to increases in eNOS dimer and total protein levels and eNOS activity as measured by nitric oxide (NO) production. It also activated the heavy metal responsive transcription factor 1 (MTF-1), causing a nuclear translocation of an MTF-1-GFP construct and binding to the eNOS promoter. Transduction with MT-1 decreased MTF-1 nuclear localization with or without the addition of zinc. It also led to decreased eNOS promoter activity. In summary, our results indicate that basal zinc levels are responsible for maintaining eNOS promoter activity and total protein levels, but once eNOS dimer is formed that it can withstand zinc depletion conditions. We propose that supplementation with zinc may help minimize symptoms of PPHN by increasing eNOS levels and activity prior to birth.

INTRODUCTION

The fetal to newborn transition is associated with a 10-fold increase in blood flow to the lungs and is dependent on the functioning of the enzyme endothelial nitric oxide synthase (eNOS). However, in a number of clinical conditions, there is a failure of the pulmonary circulation to undergo the normal transition to postnatal life, resulting in persistent pulmonary hypertension of the newborn (PPHN). PPHN is a serious disease that is thought to be responsible for approximately 10% of admissions to neonatal intensive care units and affects 5 in 1000 newborns each year [1]. The disorder is associated with significant morbidity and mortality [1]. The development of PPHN has been linked to a decrease in the activity and expression of eNOS. Thus it is critical to understand the mechanisms by which eNOS is regulated in the perinatal period, not only to identify pathways responsible for the developmental regulation of eNOS, but also to develop new treatments for PPHN.

In the vasculature, eNOS helps to maintain vascular homeostasis by generating nitric oxide (NO), which keeps the vascular resistance low, protects the intima of the vessels from platelet aggregation and leukocyte adhesion, and prevents proliferation of vascular smooth muscle. Previously thought of as a constitutively expressed enzyme, it is now becoming more apparent that eNOS is dynamically regulated at the transcriptional, post-transcriptional, post-translational, and developmental levels.

eNOS expression is largely tissue dependent, being predominantly expressed in endothelial cells, although studies have shown eNOS expression in bronchiolar epithelial cells [2, 3]. In recent years it has been shown that eNOS expression can be modulated by a variety of chemical, physical, and developmental stimuli. Indeed, the eNOS promoter

contains a plethora of putative *cis*-elements, including Sp-1 and GATA motifs, a sterol regulatory element, estrogen-responsive elements, a nuclear factor 1 element, a cAMP-responsive elements, and activator protein (AP-1 and -2) binding sites [4-6] that would allow eNOS to be regulated by many different signals. Basal eNOS expression has been shown to be regulated in ECs by a complex interaction between two tightly clustered *cis*-regulatory regions defined as positive regulatory domains I (-104/-95 relative initiation) and II (-144/-115) [7]. Our analysis of the eNOS promoter indicates the presence of a heavy metal response element (HRE) located at -899/-893 (TGCACTC) in the 5'-flanking sequence of the human eNOS gene. It is known that increases in zinc lead to increased activation of the heavy metal responsive transcription factor 1 (MTF-1), that binds to the HRE *cis*-elements [8]. Our initial studies indicated that the addition of exogenous zinc to endothelial cells significantly increased nitric oxide (NO) generation (ns).

Previously published research indicates that eNOS is only active as a dimeric enzyme and that the dimer is stabilized by the formation of a zinc tetrathiolate cluster, in which two cysteine thiolate ligands are contributed by each subunit [9-11]. When active and tightly coupled, eNOS produces NO. However, under certain conditions, NOS may generate reactive oxygen species (superoxide and hydrogen peroxide) rather than NO. This process is referred to as NOS uncoupling, meaning that NADPH oxidation and NO synthesis have become uncoupled. It is important to note that a series of *in vitro* biochemical studies demonstrated that eNOS is the most tightly coupled of all the NOS isoforms [9-12] and definitive *in vivo* and *in vitro* evidence that uncoupling of eNOS can

occur is missing from the literature. Thus, the mechanisms by which eNOS can become uncoupled in ECs are not completely understood.

In this study, we evaluated the effect of an acute zinc treatment on eNOS protein dimer levels, expression, and activity.

A large body of work has been published in the regulation of eNOS in the cell, but in reality, still very little is known about the exact mechanisms of eNOS regulation. The most important reason for this is that the majority of the data generated has been contradictory. Indeed, it is likely that insights into the mechanisms of eNOS regulation are impeded by the fact that eNOS expression and regulation appear to vary in different EC cell lines. Little or no thought is given to the source of endothelial cell used in most studies. Thus, studies are published using cells isolated from a variety of different species and tissues. Studies in this publication will utilize low passage (p4-p6) fetal pulmonary aortic endothelial cells (FPAECs).

MTF-1 functions as a cellular zinc sensor which coordinates the expression of genes involved in zinc homeostasis, as well as affording protection against metal toxicity and oxidative stress [13]. The current model suggests that the zinc-finger domain of MTF-1 directly and reversibly binds to zinc [14, 15]. This metallo-regulatory protein then adopts a DNA-binding conformation and translocates to the nucleus, where it binds to metal-responsive elements in these gene promoters leading to increased transcription [13, 16]. There are a number of genes in which putative MTF-1 binding sites have been detected in the promoter sequences, including metallothionein (MT) itself [17], the zinc transporter 1 (ZnT1) [18], and the gamma-glutamylcysteine synthetase heavy chain [19]. In addition, it has been shown that physiologic levels of NO can induce glutathione

synthesis (GSH) in endothelial cells (ECs). This appears to be mediated via an increase in gamma-glutamylcysteine synthetase expression that is independent of cGMP [20]. However, no studies have explored the involvement of MTF-1 in the regulation of eNOS.

We propose that the addition of zinc to FPAECs will activate MTF-1, causing nuclear translocation and binding to the HRE in the 5'-flanking region of the eNOS gene, which will increase eNOS protein expression. Since zinc holds the eNOS homo-dimer together, the addition of zinc will also cause increases in eNOS activity as measured by NO_x release.

MATERIALS AND METHODS

Cell Culture

Primary cultures of ovine fetal pulmonary arterial endothelial (FPAECs) cells were isolated as detailed previously [21]. Endothelial cell identity was confirmed by their typical cobblestone appearance, contact inhibition, specific uptake of 1,1'-dioctadecyl-1,3,3',3'-tetramethylindocarbocyanine perchlorate-labeled acetylated low-density lipoprotein (Molecular Probes, Eugene, OR), and positive staining for von Willebrand factor (Dako, Carpinteria, CA). FPAECs were grown in Eagles DMEM containing 1g/l glucose and phenol red (MediaTech, Herndon, VA), supplemented with 10% fetal bovine serum (Hyclone, Logan, UT), and antibiotic-antimycotic (MediaTech). Cells were incubated at 37°C in a humidified atmosphere of 95% air and 5% CO₂. Cells were used at passage 4-6. Zinc treatments were conducted in serum-free, phenol red free (SFPRF) media (MediaTech). Prior to experimental treatment (unless otherwise noted) cells were trypsinized, counted with a hemacytometer and replated in a 6, 24-, or 96-well plate (Costar, Corning, NY) at densities of approximately 10⁴/cm² and allowed to adhere for at least 18hrs.

Cell Death Analysis

FPAECs were cultured in 24-well plates and treated with various doses of zinc chloride or a vehicle control in serum free phenol red free (SFPRF) media for a 7hr time period. After the treatment period, the medium was collected and centrifuged for 5min at 500Xg, and the supernatant stored at 4°C until assayed. Relative cytotoxicity was quantified by measuring the release of the soluble cytoplasmic enzyme lactate

dehydrogenase (LDH) activity in the cell-free supernatant using a commercial kit (Rosche Applied Science, Indianapolis, IN). Briefly, in a fresh 96-well plate, 50 μ L aliquots of the cell-free medium and 50 μ L of reconstituted substrate mix were added to each well. The plate was put in a plate reader (keeping the plate in the dark at room temperature) and absorbance readings at 490nm were taken over 40min at 10min intervals. Each sample was measured in triplicate, with a minimum of three samples per experimental group. Relative toxicity was determined by comparison of absorbance of the experimental group with absorbance of a control cell group treated with 1% Triton X-100 cell lysis buffer according to the manufacturer's protocol.

Fluorescence Microscopy

A computer-based imaging system consisting of an Olympus IX51 microscope equipped with a charge-coupled device camera (Hamamatsu Photonics, Hamamatsu City, Japan) was used for acquisition of fluorescent images. Fluorescent-stained cells were observed with the appropriate excitation and emission, and the average fluorescent intensities (Integrated Optical Density or mean IOD) were quantified using ImagePro Plus imaging software (version 5.0, Media Cybernetics, Silver Spring, MD). FluoZin 3-AM (Molecular Probes), a fluorescent dye specific for the unassociated Zn²⁺, was used for labile zinc imaging. These were analyzed at 494-nm excitation and 516-nm emission. MTF-1-GFP nuclear translocation studies measured fluorescence at a 393-nm excitation and 509-nm emission.

eNOS Promoter Luciferase Activity Assay

1.6kb eNOS promoter constructs were generated by polymerase chain reaction (PCR) using human genomic DNA as a template. The reverse primer common to all constructs binds immediately upstream of the ATG initiation codon of eNOS (5' – GTTACTGTG CGT CCA CTCTGCTGCC). The forward primer was 5' – TGTAGTTTCCCTAGTCCCCC (840bp fragment). A 3-bp mutation was introduced into the metal response element sequence within the 840bp construct. The sequence -902 at -890 in the human eNOS promoter was changed to GCAattACTCTGG by site-directed mutagenesis.

FPAECs were grown to 70% confluence and dually transfected with 0.4 μ g β -gal (internal control) and 1.6 μ g eNOS promoter-luciferase construct using Effectene transfection kit (Qiagen, Velencia, CA).

Plates were rinsed with DPBS and 200 μ L 1X Reporter Lysis Buffer (Promega, Madison, WI) was added to each well. Plates were sealed with parafilm and frozen at -80 $^{\circ}$ C for 20min or until later analysis. Next, plates were taken out of the -80 and put in a 37 $^{\circ}$ C incubator for 30min. Plates were vortexed for 30s and cell solution was transferred to a new eppendorf tube. This tube was vortexed for an additional 15s and then spun at 14,000rpm for 10min at room temperature. The supernatant was transferred to a new set of tubes and put on ice until analysis.

To normalize for transfection efficiency, β -gal activity was measured first. Briefly, 5-10 μ L cell lysate was combined with 40-45 μ L 1X Reporter Lysis Buffer and 50 μ L β -gal substrate (Qiagen, Velencia, CA) for 100 μ L total. The 96-well plate was then allowed to incubate at 37 $^{\circ}$ C for 30min. Lastly, readings were taken on a Multiscan

plate reader at 405nm throughout the 30min incubation period as the substrate reacts with β -gal.

Luciferase activities were measured one sample at a time on a Fluoroscan plate reader set as a luminometer. 20 μ L of cell lysate was combined with 100 μ L luciferase substrate (Qiagen, Velencia, CA) and a reading on the luminometer was taken immediately.

Protein Extraction

FPAECs were grown to confluence on 6-well plates. Cells were treated with various doses of zinc or a vehicle control in SFPF media for 7hrs. Following treatment, cells were rinsed with DPBS (MediaTech) and RIPA lysis buffer added to each well. Cell were then collected and sheared with a 25-gauge needle 3X. Lastly, samples were spun at 14,000Xg for 10min and the supernatant was collected. Protein concentrations were analyzed using Bio-Rad protein assay (Bio-Rad, Hercules, CA) and Bovine Serum Albumin (BSA) for the protein standard curve.

Western Blotting

Western Blot analysis was performed as previously described [21]. Total protein extracts (~20 μ g) were resuspended in 5X Laemmli protein sample buffer and boiled for 5min. Total protein was then separated on a 4-20% Tris-SDS-HEPES polyacrylamide gel (Gradiopore, Frenchs Forest, Australia) and electrophoretically wet-transferred to a Hybond-PVDF membrane (Amersham, Arlington Hts., IL). The membranes were blocked with 5% nonfat dry milk in Tris buffered saline containing 0.1% Tween-20

(TBST) overnight at 4⁰C. After blocking, the membranes were incubated at room temperature for 2 hrs with the primary antibody (1:1,000 for α -eNOS, BD Biosciences), washed 3X with TBST, and incubated with a mouse anti-rabbit IgG-horseradish peroxidase conjugated secondary antibody (Pierce, Rockford, IL) for 1 hr. After washing, immunolabeled protein bands were visualized using chemiluminescence (SuperSignal West Fempto Substrate Kit, Pierce) on a Kodak Image Station 440CF with Kodak 1D Molecular Imaging Software and normalized to immunolabeled β -actin (1:1000, Sigma) on the same blot.

Low Temperature Poly Acrylamide Gel Electrophoresis (LT-PAGE)

LT-PAGE was used to analyze eNOS dimer levels. Briefly, cells were treated with zinc or a vehicle control in SFPP media for 7hrs and then were rinsed 2X with DPBS. Cells were harvested and protein concentrations measured as stated in the Western Blot section above. However, samples were not boiled as in a regular Western Blot prior to loading. Equal protein was loaded onto a denaturing Polyacrylamide gel and run on ice at 30v for approximately 7hrs. Transfer, blocking, and probing were performed similar to the Western Blot method above.

Assay for NOS Activity

NOS activity was determined by measuring NO_x levels in the media using a NO_x specific probe (Apollo 4000 Free Radical Analyzer, World Precision Instruments, Inc.). Briefly, following treatment with zinc or a vehicle control, media was collected and NO_x

levels were measured. Potassium Nitrate solutions, made in media, were used to make a standard curve for determining NO_x levels.

Generation of MT-1 Adenoviral Expression Construct

An adenoviral vector expressing MT-1 was constructed with the pAd/pENTR System (Invitrogen) [22]. Briefly, a pAd/CMV plasmid containing an MT-1 cDNA (cDNA purchased from ATCC, Manassas, VA) was created and transfected into 293A cells. A selected clone was propagated and viral lysates were collected and titered per the manufacturer's protocol. The titer for the AdV.MT-1 preparation was 3.4e10¹⁰ plaque-forming units per mL. Infections on PAECs were performed for 120min with virus diluted in normal DMEM to the desired multiplicity of infection. Verification of transgene expression was performed using Western Blot analysis as described above using 20µg of protein extracts.

Quantification of Intracellular Zn²⁺ Levels

FPAECs were grown on glass cover slips in 6-well plates and treated with various doses of zinc chloride or a vehicle control in SFPRF media for 1hr at 37⁰C. After a 30min treatment, cells were loaded with 2.5µM FluoZin 3-AM (Molecular Probes), a fluorescent dye specific for the unassociated Zn²⁺. Following the treatment period, cells were washed twice with SFPRF media and incubated for an additional 30min in the dark at 37⁰C (in the incubator). Cell-coated glass cover slips were removed from the 6-well plate one at a time and put onto a glass slides. These slides were analyzed by fluorescent microscopy as described above.

MTF-1-GFP Nuclear Translocation

MTF-1 and GFP constructs were cloned into the pcDNA 3.1-Hygro (+) vector, and enzymatic digests were utilized to verify cloning products and their orientation. FPAECs were grown on glass cover slips in 6-well plates to 50-60% confluence, and were transfected with the MTF-1-GFP construct using Effectene transfection reagent (Qiagen, Valencia, CA). MTF-1-GFP translocation was determined using fluorescent microscopy as described above. A higher mean IOD correlated to more nuclear localization. A minimum of 3 field pictures were taken per well and averaged. The mean \pm standard deviation was calculated and a $P < 0.05$ was considered statistically significant from the control.

Statistical Analysis

Values are expressed as the means \pm standard error of the mean from at least three experiments. Statistical analysis between experimental groups was performed by one way ANOVA or T-test using the Graph Pad Prism 4.0 statistical analysis software program. A $P < 0.05$ was considered statistically significant.

RESULTS

Our initial experimental data for this publication evaluated the developmental differences in enzyme endothelial nitric oxide synthase (eNOS) protein and activity levels. Passage matched fetal (FPAECs) and adult pulmonary aortic endothelial cells (AdPAECs) were grown to confluence in regular DMEM media. Media was collected for NO_x levels and protein was harvested for eNOS levels. Results indicated that eNOS protein levels were 5-6 fold higher in fetal versus adult PAECs (not shown). This data correlated with previous studies from our lab indicating that eNOS expression is higher in the fetal stage and then decreases in the adult. However, NO_x generation was nearly 20-fold higher in FPAECs versus AdPAECs (data not shown). This suggests that eNOS is more tightly coupled in the fetal stage compared to the adult. Interestingly, developmental cellular free zinc levels from these cells correlated with eNOS expression, such that free zinc levels were nearly 2-fold higher in the fetal compared to the adult cells (data not shown). In addition, our analysis of the eNOS promoter indicated the presence of a putative heavy metal response element (HRE) on the 5'-flanking sequence. This led us to explore the role of zinc in eNOS regulation.

We wanted to determine whether modulating cellular zinc would alter eNOS at the transcriptional and post-translational levels in FPAECs. The development of persistent pulmonary hypertension of the newborn (PPHN) has been linked to a decrease in the activity and expression of eNOS. FPAECs were used instead of adult cells for these studies, since they are the cells that are intimately involved in the transition of a baby at birth.

We first determined whether the addition of exogenous zinc would increase eNOS dimer levels. FPAECs were treated with 0 and 50 μ M zinc chloride (ZnCl₂) for 0-9hrs. Protein was harvested from the cells. Low Temperature Polyacrylamide Gel Electrophoresis (LT-PAGE) and Western Blot analysis was used to examine eNOS protein dimer levels (data not shown). Following a 7hr zinc treatment, eNOS protein dimer levels dose dependently increased. We then set up another experiment using a 7h ZnCl₂ treatment of 0-100 μ M. Results indicated a dose dependent increase in eNOS dimer levels peaking at 25 and 50 μ M ZnCl₂ (Figure 1) and dropping off at the nontoxic (Lactate Dehydrogenase (LDH) release, data not shown) dose of 100 μ M .

Next we wanted to determine whether the 7hr ZnCl₂ treatment increased total eNOS protein levels. Western Blot analysis was carried out on the protein extracts from the first experiments in FPAECs and blots were probed with anti-eNOS. Total eNOS protein levels following zinc 7h treatment were not statistically different from the 0 μ M ZnCl₂ control (data not shown). Therefore, FPAECs were treated for 20hrs with the same doses of ZnCl₂ and protein was harvested. At the 20hr time point, eNOS protein was statistically higher than control in both the 25 and 50 μ M treatments (Figure 2).

To determine whether these zinc treatments were causing increases in levels of cellular free zinc, the cell permeable zinc fluorophore, FluoZin-3 AM, was used. FPAECs were grown on glass cover slips and were treated with ZnCl₂ for 1hr, rinsed, and loaded with FluoZin-3 AM. Fluorescent photographs were taken with an Olympus microscope using a GFP cube and quantitated with the Image Pro software. Zinc levels were significantly higher ($p < 0.05$) in the 25, 50, and 100 μ M ZnCl₂ treatments (Figure 3).

We next looked to see if eNOS activity as measured by NO_x release correlated with the increased levels of eNOS dimer and total protein levels. FPAECs were treated for 7hrs with ZnCl₂. Shear is known to activate eNOS; therefore as a positive control for increased eNOS activation, we used 15min shear on half of the samples in this experiment prior to analyzing NO_x levels. Shearing was accomplished with a shear plate viscometer at a level that is comparable to shear forces seen in vivo. Media was collected and immediately analyzed for NO_x levels using a NO_x specific membrane covered micro-probe system. eNOS activity was significantly higher ($p<0.05$) in the 25, 50, and 100 μ M ZnCl₂ treatments in both un-sheared and sheared cells (Figure 4).

The addition of exogenous zinc increased cellular free zinc levels, therefore, we wanted to determine the effect of this zinc on the nuclear translocation of heavy metal responsive transcription factor 1 (MTF-1). FPAECs were grown on glass cover slips in 6-well plates to ~60% confluence and then transfected with a MTF-1-GFP construct. After 24hrs, cells were treated for ~1hr with various doses of ZnCl₂. As described above, fluorescence microscopy and Image Pro software were used for analysis. Integrated Optical Density (IOD) was used to determine the average fluorescent intensity for each cell. A higher average correlates to increased MTF-1 nuclear localization. Average nuclear brightness per well was determined by averaging the three random fields. Concentrations of 25, 50, and 100 μ M ZnCl₂ all increased MTF-1-GFP nuclear translocation (Figure 5).

Next, we determined if depleting zinc, by virally transducing with metallothionein-1 (MT-1), would prevent basal MTF-1 nuclear localization. FPAECs were grown on glass cover slips in 6-well plates and transduced (MOI=1000) with either

a Lac Z viral control or MT-1 adenovirus. After 24hrs, cells were transfected with the MTF-1 GFP construct. Following an additional 24hrs, cells were exposed to 50 μ M ZnCl₂ for 1hr. Nuclear localization was scored similar to the previous experiment. As in untransduced cells, Lac Z transduced cells exhibited increased MTF-1 nuclear localization following zinc treatment (Figure 6). MT-1 significantly ($p < 0.05$) decreased MTF-1 nuclear localization basally and prevented the increase following zinc treatment (Figure 6).

Treating FPAECs with zinc increased total eNOS protein, so we next wanted to determine the affect of cellular zinc depletion with MT-1 transduction on total eNOS protein expression. FPAECs were grown to ~80% confluence and transduced with GFP or MT-1 adenovirus (MOI=1000). After 36hrs, protein was harvested and Western Blot analysis was used to measure total eNOS protein. MT-1 expression caused a significant decrease in total eNOS protein (Figure 7).

Our data indicated that the addition of zinc increased eNOS dimer levels, so we next looked at the effect of depleting zinc on eNOS dimer levels. Using protein extracts from the previous experiment, LT-PAGE and Western Blot analysis were used to analyze eNOS dimer levels. Interestingly, eNOS dimer/monomer ratio did not decrease with MT-1 transduction (data not shown).

Results showing that the addition of zinc increased eNOS protein levels and the depletion of zinc decreased eNOS protein levels, suggested that the addition of zinc to FPAECs would increase eNOS transcription. Constructs were made combining a luciferase reporter sequence with a 5' eNOS regulatory element (-840 to 0). Both a wild type (WT) and a metal response element (MRE)-mutated eNOS luciferase construct were

utilized. The WT construct was compared to a construct containing the mutation in the 5' regulatory region from -902 to -890, corresponding to the MRE. A β -gal construct was also made to use as a transfection control. FPAECs were co-transfected with either a WT or mutant eNOS promoter luciferase and a β -gal construct. 24hrs later, cells were treated for 7hrs with $ZnCl_2$. β -gal and luciferase expression were measured by adding their respective substrates and reading on a plate reader or luminometer, as detailed above. Treatment of FPAECs with $50\mu M ZnCl_2$ resulted in significantly increased eNOS luciferase activity in the WT transfectants ($p < 0.05$) (Figure 8 A). However, there was no significant increase in luciferase activity in FPAECs transfected with the MRE-mutated construct ($p < 0.05$) (Figure 8 B).

Since eNOS luciferase data suggested that zinc-dependent increases in eNOS transcription are MRE dependent (Figure 8), the next step was to determine what transcription factors are involved. FPAECs were transduced with a GFP viral control or a MT-1 adenovirus (MOI=1000). After 36hrs, cells were harvested and nuclear protein extracts were made. Bandshift analysis was used to determine if the transcription factors Sp-1 or MTF-1 were responsible for the zinc-dependent binding of eNOS promoter basally in FPAECs. Results indicate that overexpression of MT-1 affects the binding of the eNOS regulatory sequence by both SP-1 and MTF-1. It significantly decreases SP-1 binding by 35% (Figure 9 A & B), but to a greater extent, significantly decreases MTF-1 binding by 55% (Figure 10 A & B).

MTF-1 is a major zinc responsive transcription factor involved in basal eNOS transcription (Figure 10). Decreased the amount of cellular zinc available by transduction with MT-1 significantly decreased MTF-1 binding to the eNOS regulatory

domain (Figure 10), therefore, we next determined if treating FPAECs with $ZnCl_2$ would increase MTF-1 binding to the eNOS regulatory domain. FPAECs were treated with $ZnCl_2$ for 7hrs and nuclear protein extracts were made. These extracts were used for bandshift analysis to determine the effect on MTF-1 binding. Results indicated that treatment with $ZnCl_2$ increased MTF-1 binding to eNOS regulatory domain at both 25 and 50 μ M $ZnCl_2$ (Figure 11) in the three separate experiments.

To be sure that the band observed in Figures 10 and 11 is from MTF-1 binding, we used a supershift assay. Nuclear extract from untreated FPAECs were incubated with either 2 or 4 μ L α -MTF-1 antibody at 4⁰C overnight. Bandshift analysis was then performed on this extract. If MTF-1 was bound to the eNOS regulatory sequence DNA, then the MTF-1 antibody should bind to that MTF-1/DNA complex, increasing its molecular weight and shifting it up on the gel. Results indicate that a supershift occurred with both 2 and 4 μ L of MTF-1 antibody in the upper band (Figure 12).

To be sure that MTF-1 was binding to the MRE in the eNOS 5' regulatory sequence DNA, we mutated three bases in the MRE of the eNOS regulatory domain construct. Bandshift analysis was performed using untreated FPAEC nuclear extracts and the mutated MRE eNOS regulatory sequence DNA. Results found 45% decrease in MTF-1 binding with the mutated MRE eNOS 5' regulatory sequence DNA compared to WT (Figure 13).

DISCUSSION

In this study, we provide evidence of a pathway by which the addition of exogenous zinc in endothelial cells drives increases in endothelial nitric oxide synthase (eNOS) protein dimer, total eNOS protein, and eNOS activity. These increases are mainly due to the activation, nuclear localization, and binding of the heavy metal responsive transcription factor 1 (MTF-1) to the eNOS metal response element (MRE). Developmental studies found that eNOS protein and activity levels correlated with cellular labile zinc levels, which led us to further explore the regulation of eNOS by zinc. Our studies established that exposure of fetal pulmonary aortic endothelial cells (FPAECs) to exogenous $ZnCl_2$ results in: (1) Immediate increases in intracellular zinc, (2) Phasic increases in eNOS protein dimer levels, (3) Increases in total eNOS protein, (4) Increases in eNOS promoter luciferase activity, and (5) Enhancement of MTF-1 nuclear translocation and binding to the eNOS promoter. Depletion of basal zinc levels in the FPAECs by viral transduction with MT-1 adenovirus, produced decreases in total eNOS protein and MTF-1 nuclear translocation with no change in eNOS dimer levels. As a result, we conclude that our data proposes a role of zinc homeostasis in eNOS transcriptional and post-translational regulation mainly occurring through MTF-1 activation.

Initially, we verified data indicating that FPAECs have higher eNOS expression compared to AdPAECs. The results indicated that there was 2-fold higher eNOS protein in FPAECs versus AdPAECs (Figure 1). However, FPAECs produced nearly 20-fold higher NO versus AdPAECs, demonstrating that eNOS in FPAECs is much more tightly

coupled and active (data not shown). This agrees with previous studies from our laboratory [23].

Pitt and colleagues have carried out elegant studies indicating that NO donors can induce an increase in labile zinc in adult ovine PAECs [24, 25]. At least part of the mechanism of this labile zinc increase is S-nitrosylation of metallothionein (MT) by NO [13, 25, 26]. However, it is unknown if there are developmental differences in basal levels of labile zinc in ECs. Thus, our studies examined the labile zinc levels in ECs isolated from fetal and adult sheep. Since, fetal endothelial cells produce much higher NO compared to adult, the results obtained here indicated that zinquin fluorescence levels were 2-fold higher in fetal (ns), correlating well with Pitt's studies. The levels of labile zinc also correlated with eNOS protein levels, such that FPAECs had 2-3-fold higher compared to adult (ns), suggesting that NO production may be driving eNOS transcription through the release of free zinc.

A recent paper that we published explored alterations in zinc homeostasis that lead to cell toxicity and induction of apoptosis [27], however these utilized doses of zinc (250 μ M and greater) that were much higher than doses used here and caused induction of ROS production. These studies selected doses and time courses of ZnCl₂ treatment that were non-toxic in FPAECs. While certain compounds, most notably the zinc ionophore pyrithione [28], have been shown to enhance ZnCl₂ uptake into cells, we found adverse toxicity of the compound in FPAECs and therefore, precluded its use for these studies. The doses of ZnCl₂ used here (25-100 μ M) increased intracellular zinc levels within 15min as measured by FluoZin-3AM fluorescence (data shown for 1hr in Figure 3), therefore no zinc ionophore was necessary.

To date, a diverse set of physiological, nutritional, and biochemical functions have been attributed to zinc [29]. Zinc atoms are positioned at catalytic, structural and regulatory sites of enzymes (e.g. caspase-3, superoxide dismutase, NO synthase), transcription factors (TFIIIA) and structural proteins accounting for its importance in maintaining a wide variety of biological processes [30]. Pathologies linked to Zn^{2+} deficiency are well documented [31], and sufficient dietary uptake of zinc remains a nutritional issue of global dimensions [32].

Since zinc plays an integral role in the eNOS homodimer, linking the two monomers by a zinc tetrathiolate cluster, we determined whether the addition of zinc to fetal pulmonary aortic endothelial cells would increase eNOS dimer levels. After testing various doses and time courses, it was determined that the passage and lot of FPAECs used in this study responded to a 7hr $ZnCl_2$ exposure with increased eNOS dimer and total protein levels at 25 and 50 μ M followed by a decrease at 100 μ M (Figure 3). This indicated that the addition of zinc to FPAECs does increase eNOS dimer protein levels and supports the hypothesis that eNOS is regulated by zinc.

Zinc is very tightly regulated in the cell, as intracellular concentrations of Zn^{2+} ions have been measured in pico- or nanomolar concentrations [33], indicative of the requirement for strict sequestration. Metallothioneins (MT) are a family of proteins containing 20 cysteine residues and thus, play a crucial part in zinc homeostasis within mammalian cells. In fact, MT is believed to bind 5-10% of the total mammalian cellular zinc [34]. MT binds more tightly to zinc than other zinc binding proteins and it is believed to participate in intracellular signal transduction pathways via the regulation of

intracellular zinc trafficking and homeostasis, utilizing thiolate clusters within the MT protein [35].

SP-1 is ubiquitously expressed zinc-responsive transcription factor. The eNOS promoter does contain an SP-1 binding site at -103 that has been found to be necessary for basal eNOS transcription in endothelial cells [36], so it was expected to see that SP-1 played a role in the basal zinc dependent regulation of eNOS (Figure 14).

The zinc-sensitive, heavy metal response element binding transcription factor, MTF-1 plays a central role in transcriptional activation of MT gene in response to heavy metals and oxidative stress [8, 14]. Our analysis of the eNOS promoter indicated the presence of a putative heavy metal response element (HRE) located at -899/-893 in the 5'-flanking sequence of the human eNOS gene. As expected from studies in other cell types, the addition of ZnCl₂ to FPAECs resulted in increased nuclear translocation of MTF-1-GFP (Figure 8). To determine whether MTF-1 was involved in the regulation of eNOS, we next performed MTF-1 bandshift analysis. It was interesting to see that MTF-1 also seemed to be very critical for basal zinc dependent eNOS regulation. MTF-1 does work together with MT, the zinc sink in the cell; therefore we believe that it is a key transcription factor involved in the zinc dependent regulation of eNOS.

In summary, this study establishes a link between cellular zinc homeostasis and eNOS protein and activity. In lower doses, zinc can stimulate enzyme levels and activity and at higher doses, it can cause decreases in enzyme levels and activity. This data suggests that maintaining certain dietary levels of zinc could be important in maintaining endothelial function and that zinc supplementation during pregnancy may help minimize symptoms PPHN by increasing eNOS levels and activity prior to birth.

ACKNOWLEDGMENTS

This research was supported in part by grants 0515459Z from the American Heart Association Pacific Mountain Affiliates (to JW) and HL60190 (to SMB), HL67841 (to SMB), HL072123 (to SMB), and HL070061 (to SMB) from the National Institutes of Health.

REFERENCES

1. Hooper, W.C., et al., *Vascular endothelium summary statement V: Pulmonary hypertension and acute lung injury: Public health implications*. Vascul Pharmacol, 2006.
2. Kirsch, E.A., et al., *Estrogen acutely stimulates endothelial nitric oxide synthase in H441 human airway epithelial cells*. Am J Respir Cell Mol Biol, 1999. **20**(4): p. 658-66.
3. German, Z., et al., *Molecular basis of cell-specific endothelial nitric-oxide synthase expression in airway epithelium*. J Biol Chem, 2000. **275**(11): p. 8183-9.
4. Marsden, P.A., et al., *Structure and chromosomal localization of the human constitutive endothelial nitric oxide synthase gene*. J Biol Chem, 1993. **268**(23): p. 17478-88.
5. Venema, R.C., et al., *Organization of the bovine gene encoding the endothelial nitric oxide synthase*. Biochim Biophys Acta, 1994. **1218**(3): p. 413-20.
6. Teichert, A.M., et al., *Characterization of the murine endothelial nitric oxide synthase promoter*. Biochim Biophys Acta, 1998. **1443**(3): p. 352-7.
7. Karantzoulis-Fegaras, F., et al., *Characterization of the human endothelial nitric-oxide synthase promoter*. J Biol Chem, 1999. **274**(5): p. 3076-93.
8. Zhang, B., et al., *Activity of metal-responsive transcription factor 1 by toxic heavy metals and H₂O₂ in vitro is modulated by metallothionein*. Mol Cell Biol, 2003. **23**(23): p. 8471-85.
9. Ghosh, D.K., H.M. Abu-Soud, and D.J. Stuehr, *Domains of macrophage N(O) synthase have divergent roles in forming and stabilizing the active dimeric enzyme*. Biochemistry, 1996. **35**(5): p. 1444-9.
10. Rodriguez-Crespo, I. and P.R. Ortiz de Montellano, *Human endothelial nitric oxide synthase: expression in Escherichia coli, coexpression with calmodulin, and characterization*. Arch Biochem Biophys, 1996. **336**(1): p. 151-6.
11. Venema, R.C., et al., *Subunit interactions of endothelial nitric-oxide synthase. Comparisons to the neuronal and inducible nitric-oxide synthase isoforms*. J Biol Chem, 1997. **272**(2): p. 1276-82.
12. Sherman, T.S., et al., *Nitric oxide synthase isoform expression in the developing lung epithelium*. Am J Physiol, 1999. **276**(2 Pt 1): p. L383-90.
13. Lichtlen, P. and W. Schaffner, *The "metal transcription factor" MTF-1: biological facts and medical implications*. Swiss Med Wkly, 2001. **131**(45-46): p. 647-52.
14. Heuchel, R., et al., *The transcription factor MTF-1 is essential for basal and heavy metal-induced metallothionein gene expression*. Embo J, 1994. **13**(12): p. 2870-5.
15. Radtke, F., et al., *Functional domains of the heavy metal-responsive transcription regulator MTF-1*. Nucleic Acids Res, 1995. **23**(12): p. 2277-86.
16. Giedroc, D.P., X. Chen, and J.L. Apuy, *Metal response element (MRE)-binding transcription factor-1 (MTF-1): structure, function, and regulation*. Antioxid Redox Signal, 2001. **3**(4): p. 577-96.

17. Palmiter, R.D., *Regulation of metallothionein genes by heavy metals appears to be mediated by a zinc-sensitive inhibitor that interacts with a constitutively active transcription factor, MTF-1*. Proc Natl Acad Sci U S A, 1994. **91**(4): p. 1219-23.
18. Langmade, S.J., et al., *The transcription factor MTF-1 mediates metal regulation of the mouse ZnT1 gene*. J Biol Chem, 2000. **275**(44): p. 34803-9.
19. Lichtlen, P., et al., *Target gene search for the metal-responsive transcription factor MTF-1*. Nucleic Acids Res, 2001. **29**(7): p. 1514-23.
20. Moellering, D., et al., *The induction of GSH synthesis by nanomolar concentrations of NO in endothelial cells: a role for gamma-glutamylcysteine synthetase and gamma-glutamyl transpeptidase*. FEBS Lett, 1999. **448**(2-3): p. 292-6.
21. Black, S.M., et al., *Ventilation and oxygenation induce endothelial nitric oxide synthase gene expression in the lungs of fetal lambs*. J. Clin. Invest, 1997. **100**: p. 1448-1458.
22. Wiseman, D.A., et al., *Alterations in zinc homeostasis underlie endothelial cell death induced by oxidative stress from acute exposure to hydrogen peroxide*. Am J Physiol Lung Cell Mol Physiol, 2007. **292**(1): p. L165-77.
23. Wedgwood, S., et al., *Developmental differences in the shear stress-induced expression of endothelial NO synthase: changing role of AP-1*. Am J Physiol Lung Cell Mol Physiol, 2003. **284**(4): p. L650-62.
24. Liu, S., et al., *Nitric oxide-dependent pro-oxidant and pro-apoptotic effect of metallothioneins in HL-60 cells challenged with cupric nitrilotriacetate*. Biochem J, 2001. **354**(Pt 2): p. 397-406.
25. Pearce, L.L., et al., *Metallothionein, nitric oxide and zinc homeostasis in vascular endothelial cells*. J Nutr, 2000. **130**(5S Suppl): p. 1467S-70S.
26. Pearce, L.L., et al., *Role of metallothionein in nitric oxide signaling as revealed by a green fluorescent fusion protein*. Proc Natl Acad Sci U S A, 2000. **97**(1): p. 477-82.
27. Wiseman, D.A., et al., *Endothelial response to stress from exogenous Zn²⁺ resembles that of NO-mediated nitrosative stress, and is protected by MT-1 overexpression*. Am J Physiol Cell Physiol, 2006. **291**(3): p. C555-68.
28. Tang, Z.L., et al., *Role of zinc in pulmonary endothelial cell response to oxidative stress*. Am J Physiol Lung Cell Mol Physiol, 2001. **281**(1): p. L243-9.
29. Powell, S.R., *The antioxidant properties of zinc*. J Nutr, 2000. **130**(5S Suppl): p. 1447S-54S.
30. Stitt, M.S., et al., *Nitric oxide-induced nuclear translocation of the metal responsive transcription factor, MTF-1 is mediated by zinc release from metallothionein*. Vascul Pharmacol, 2006. **44**(3): p. 149-55.
31. Fraker, P.J., *Roles for cell death in zinc deficiency*. J Nutr, 2005. **135**(3): p. 359-62.
32. Shrimpton, R., et al., *Zinc deficiency: what are the most appropriate interventions?* Bmj, 2005. **330**(7487): p. 347-9.
33. Maret, W., *Cellular zinc and redox states converge in the metallothionein/thionein pair*. J Nutr, 2003. **133**(5 Suppl 1): p. 1460S-2S.
34. Buhler, R.H. and J.H. Kagi, *Human hepatic metallothioneins*. FEBS Lett, 1974. **39**(2): p. 229-34.

35. Maret, W., *Metallothionein/disulfide interactions, oxidative stress, and the mobilization of cellular zinc*. *Neurochem Int*, 1995. **27**(1): p. 111-7.
36. Zhang, R., W. Min, and W.C. Sessa, *Functional analysis of the human endothelial nitric oxide synthase promoter. Sp1 and GATA factors are necessary for basal transcription in endothelial cells*. *J Biol Chem*, 1995. **270**(25): p. 15320-6.

FIGURE LEGENDS

Fig. 1. A 7hr treatment with ZnCl₂ leads to an increase in eNOS dimer levels. FPAECs were exposed to ZnCl₂ for 7hrs in SFPRF media. LT-PAGE analysis indicated that eNOS dimer levels significantly increased at ZnCl₂ doses of 10, 25, and 50μM. All values are mean ± SEM (n=4). * *P*<0.05 vs. 0μM ZnCl₂ treatment.

Fig. 2. A 20hr treatment with ZnCl₂ leads to increases in total eNOS protein levels. FPAECs were exposed to ZnCl₂ for 20hrs in SFPRF media. Western blot analysis indicated that total eNOS levels increased at some doses of ZnCl₂. All values are mean ± SD (n=4). * *P*<0.05 vs. 0μM ZnCl₂ treatment.

Fig. 3. A 1hr treatment with ZnCl₂ leads to increases in cellular level of free zinc. FPAECs were exposed to ZnCl₂ for 1hr in SFPRF media. Cells were rinsed and then loaded with 1μM FluoZin-3. An Olympus fluorescent microscope with a GFP filter cube was used to take photographs. Image Pro Software was used to quantitate fluorescence. All values are mean ± SEM (n=5). * *P*<0.05 vs. 0μM ZnCl₂ treatment.

Fig. 4. A 7hr treatment with ZnCl₂ and shear both increased NO_x production in FPAECs. Sheared and unsheared FPAECs were exposed to increasing levels of ZnCl₂ for 7hr in SFPRF media. Sheared cells were exposed to flow stress with a shear plate viscometer for 15min. Media was collected and NO_x levels were analyzed using the NOII Analyzer. All values are mean ± SEM (n=4). * *P*<0.05 vs. 0μM ZnCl₂ treatment +/- shear.

Fig. 5. The addition of zinc to FPAECs induces nuclear translocation of MTF-1-GFP. FPAECs were transfected with MTF-1-GFP. 24hrs later, cells were treated for ~1hr with ZnCl₂. They were then visualized on an Olympus scope using a GFP cube. Nuclear localization is determined using Image Pro Software with a mean IOD measurement. All values are mean ± SEM (n=4). * *P*<0.05 vs. 0μM ZnCl₂.

Fig. 6. A 1hr treatment with ZnCl₂ leads to increases in MTF-1 nuclear localization, but is prevented by overexpression of MT-1. FPAECs were transduced with Lac Z or MT-1 adenovirus at MOI=1000. After 24hrs, they were transfected with MTF-1 GFP and then 24hrs later, they were exposed to 50μM ZnCl₂ for 1hr in SFPRF media. An Olympus fluorescent microscope and GFP cube filter were used to take pictures of MTF-1-GFP localization and nuclear localization was quantitated using Image Pro Software with a mean IOD measurement. All values are mean ± SEM (n=5). * *P*<0.05 vs. 0μM ZnCl₂ treatment and Lac Z transduction.

Fig. 7. Overexpression of MT-1 leads to a decrease in total eNOS protein levels. FPAECs were transduced with GFP or MT-1 adenovirus at MOI=1000. After 36hrs, total protein was harvested and Western Blot analysis was used to measure total eNOS protein. All values are mean ± SEM (n=3). * *P*<0.05 vs. GFP transduced sample.

Fig. 8. The addition of zinc to FPAECs leads to increased eNOS luciferase activity in WT, but not in the MRE-mutant. FPAECs were co-transfected with either WT (A) or mutant (B) eNOS luciferase and a β-gal constructs. After 24hrs, cells were treated for

7hrs with 50 μ M ZnCl₂. β -gal and luciferase activities were assayed in FPAECs by adding their respective substrates and measuring absorbance on a plate reader for β -gal and a luminometer for luciferase. All values are mean \pm SEM (n=9). * P <0.05 vs. 0 μ M ZnCl₂.

Fig. 9. Overexpression of MT-1 leads to a decrease in SP-1 binding to the eNOS regulatory region. FPAECs were transduced with a GFP or MT-1 adenovirus (MOI=1000). After 36hrs, nuclear protein extracts were made. Bandshift analysis was performed with the nuclear extracts. All values are mean \pm SEM (n=3). * P <0.05 vs. GFP transduced sample.

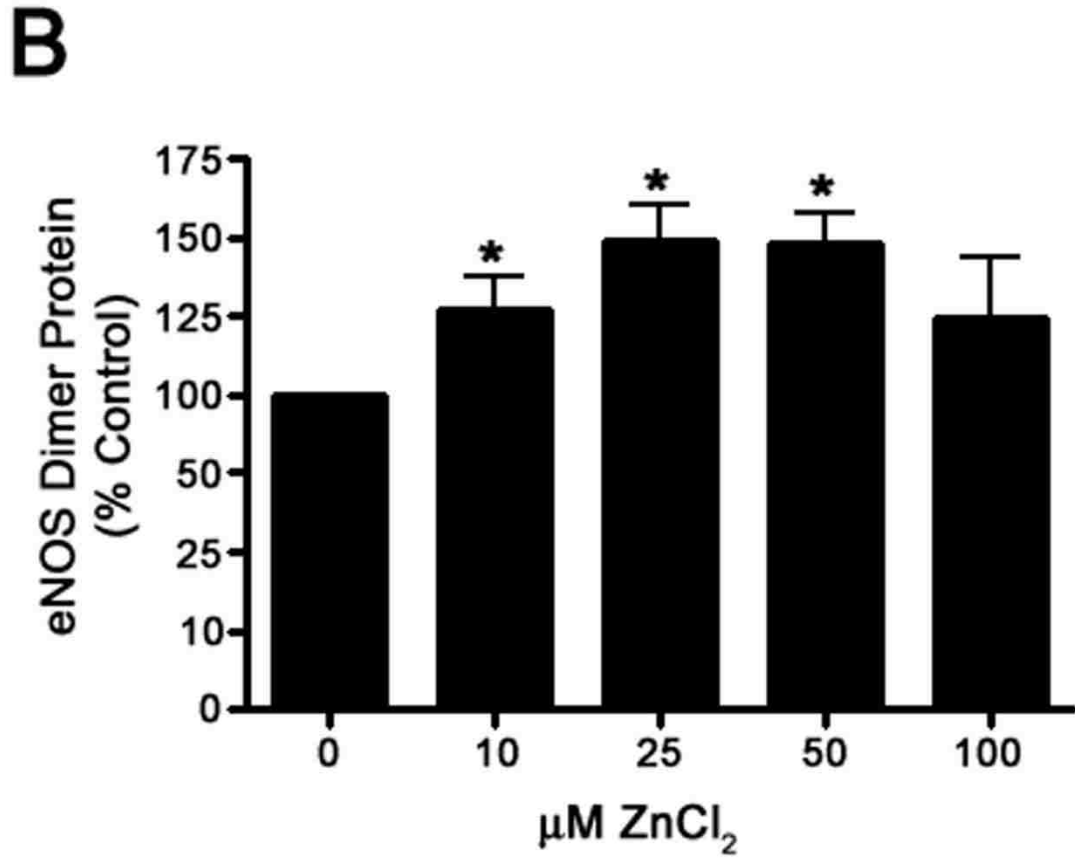
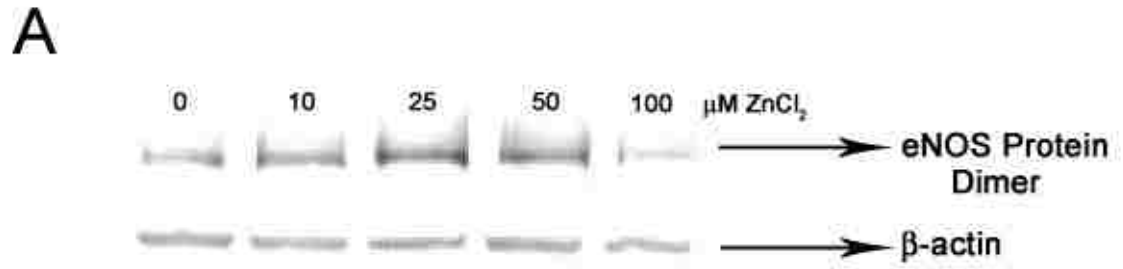
Fig. 10. Overexpression of MT-1 leads to a decrease in MTF-1 binding the eNOS promoter. FPAECs were transduced with GFP or MT-1 adenovirus (MOI=1000). After 36hrs, nuclear protein extracts were made. . Bandshift analysis was performed with the nuclear extracts. All values are mean \pm SD (n=3). * P <0.05 vs. GFP transduced sample.

Fig. 11. Treatment with ZnCl₂ leads to increases in MTF-1 binding to eNOS promoter. FPAECs were treated with ZnCl₂ for 7hrs and nuclear protein extracts were made. . Bandshift analysis was performed with the nuclear extracts. All values are mean \pm SEM (n=3). * P <0.05 vs. 0 μ M ZnCl₂ transduced sample.

Fig. 12. Supershift occurs with both 2 and 4 μ L MTF-1 antibody. FPAEC untreated nuclear extract is mixed with 0, 2, or 4 μ L MTF-1 antibody and allowed to react

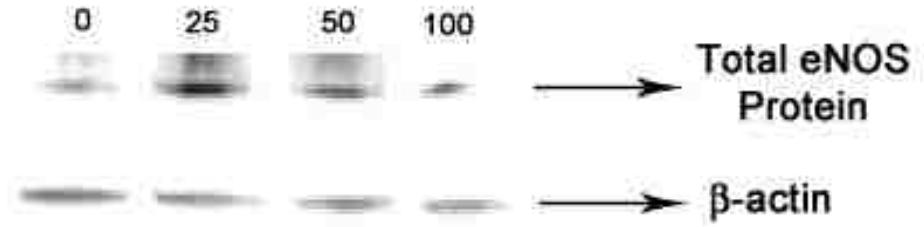
overnight at 4⁰C. Bandshift analysis was performed on reaction mixtures of MTF-1 antibody/eNOS 5' regulatory domain sequence DNA.

Fig. 13. Mutating the eNOS MRE causes a 45% decrease in MTF-1 binding. Bandshift analysis of untreated FPAEC nuclear extracts, utilizing an MRE-mutant eNOS 5' regulatory domain were performed. All values are mean \pm SD (n=3). * $P < 0.05$ vs. WT oligo sample.

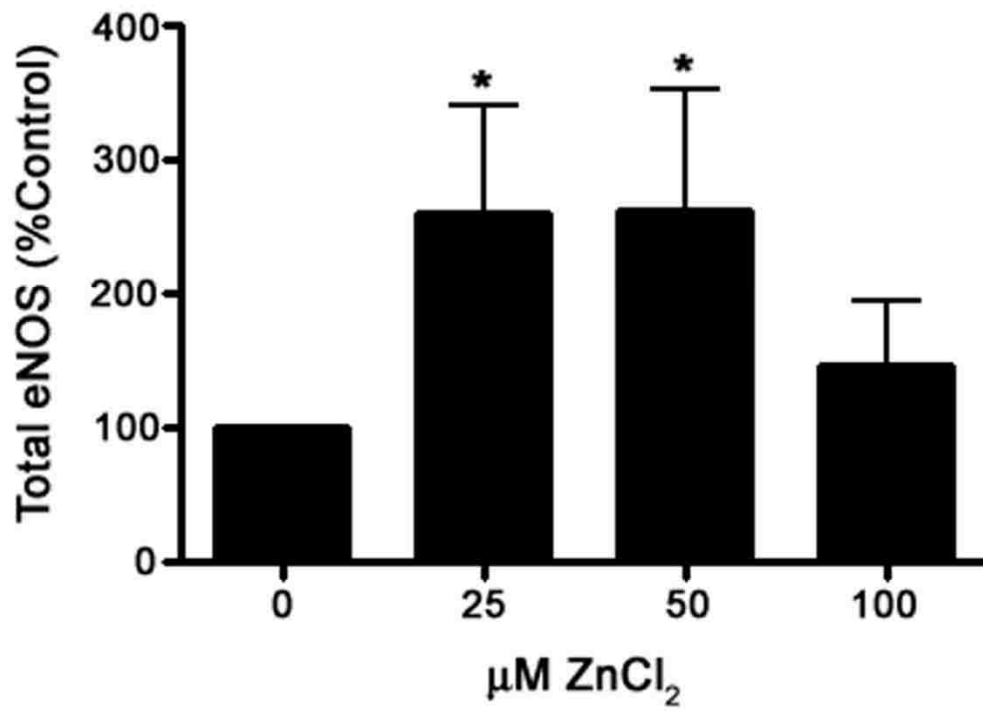


Wilham et al Fig. 1 A & B

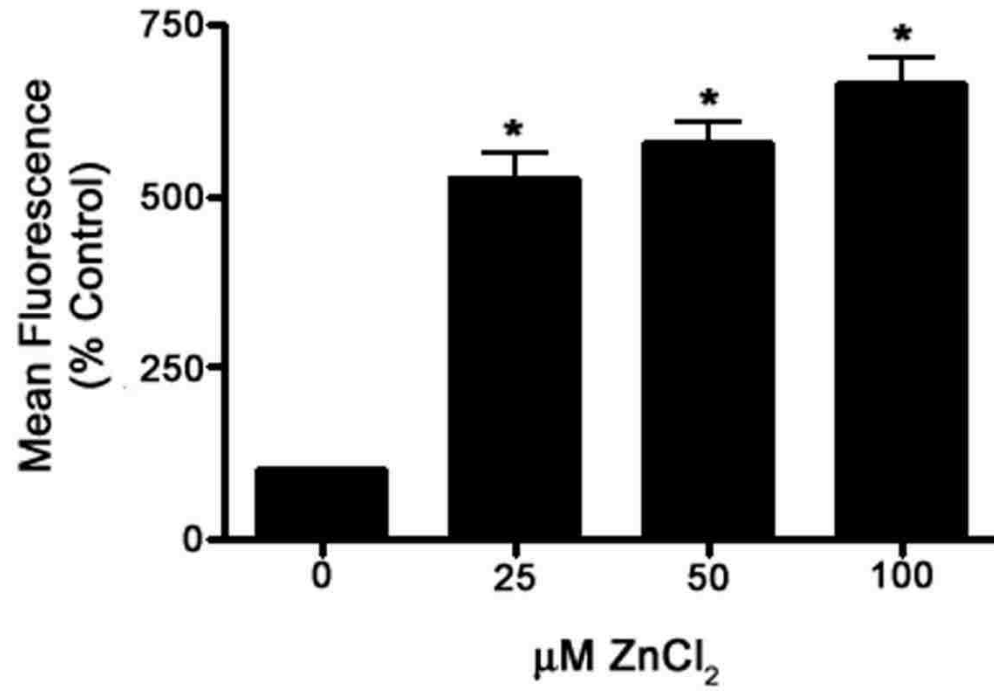
A



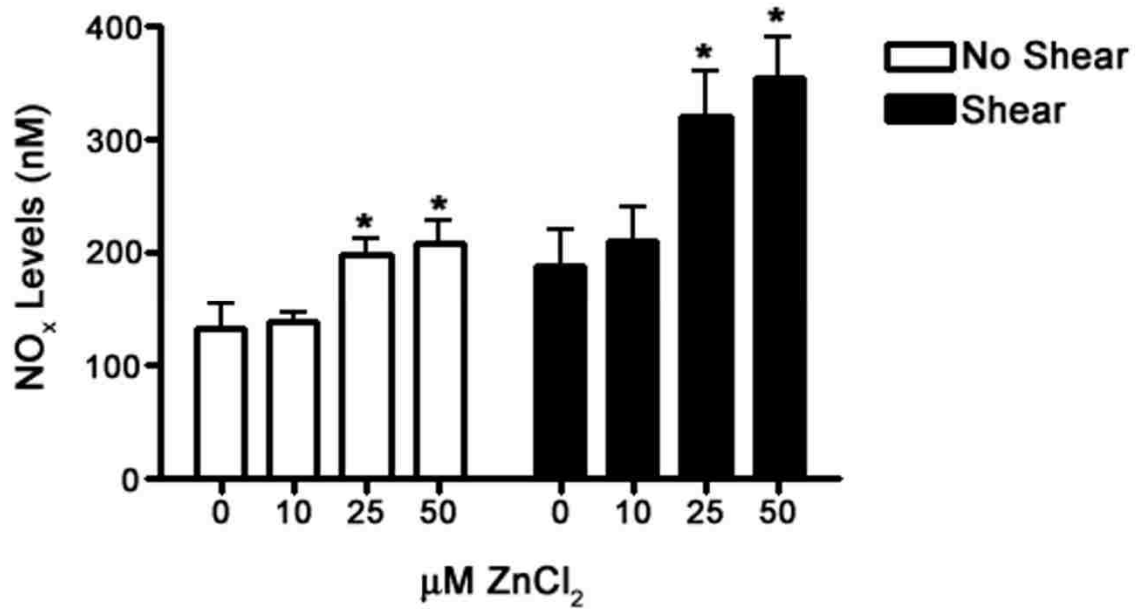
B



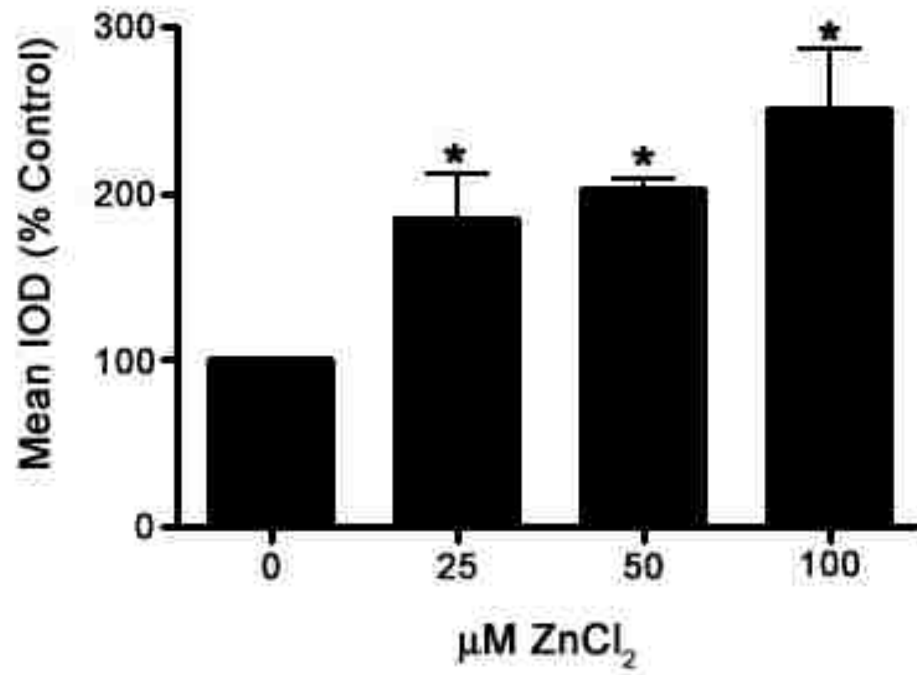
Wilham et al Fig. 2 A & B



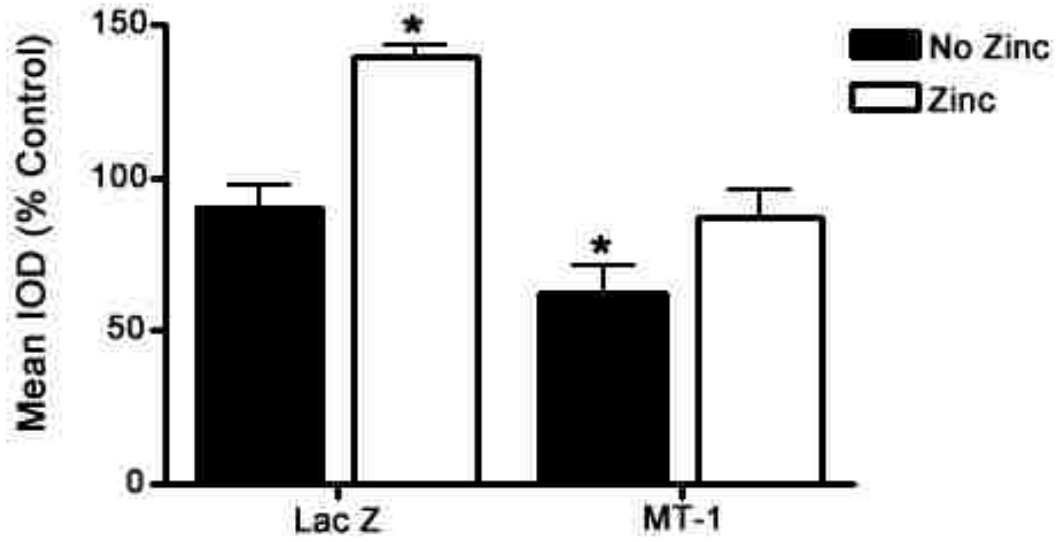
Wilham et al Fig. 3



Wilham et al Fig. 4

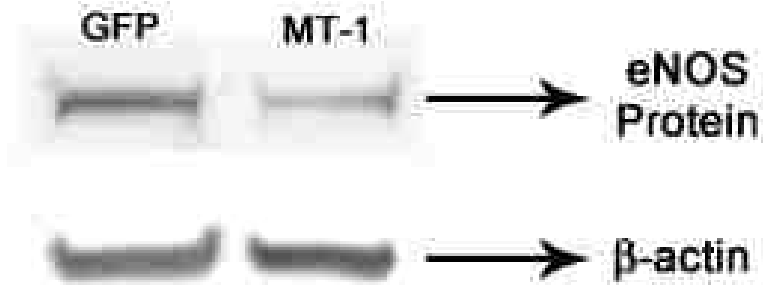


Wilham et al Fig. 5

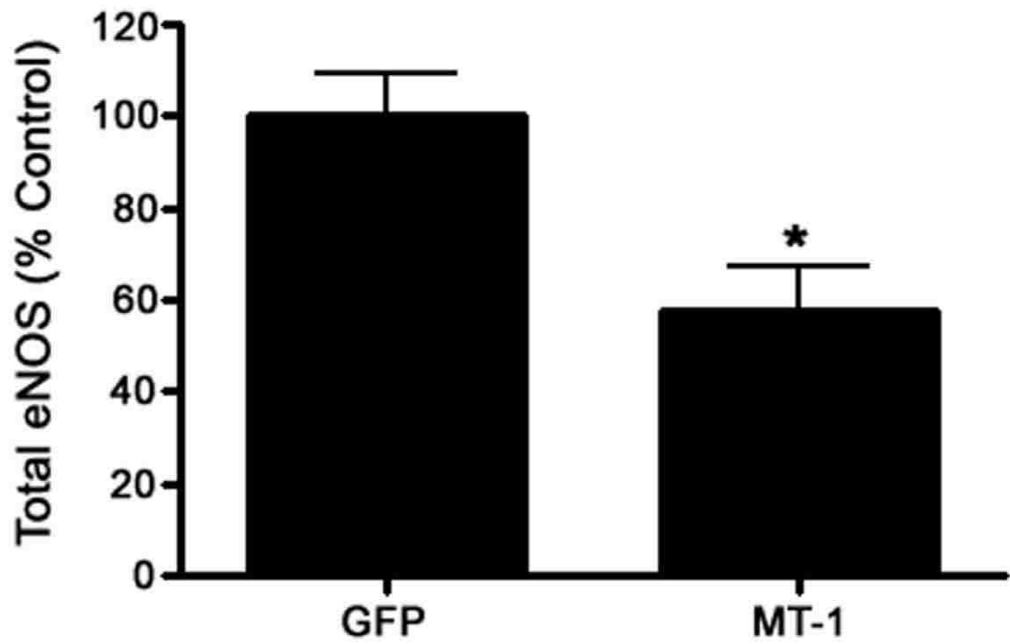


Wilham et al Fig. 6

A

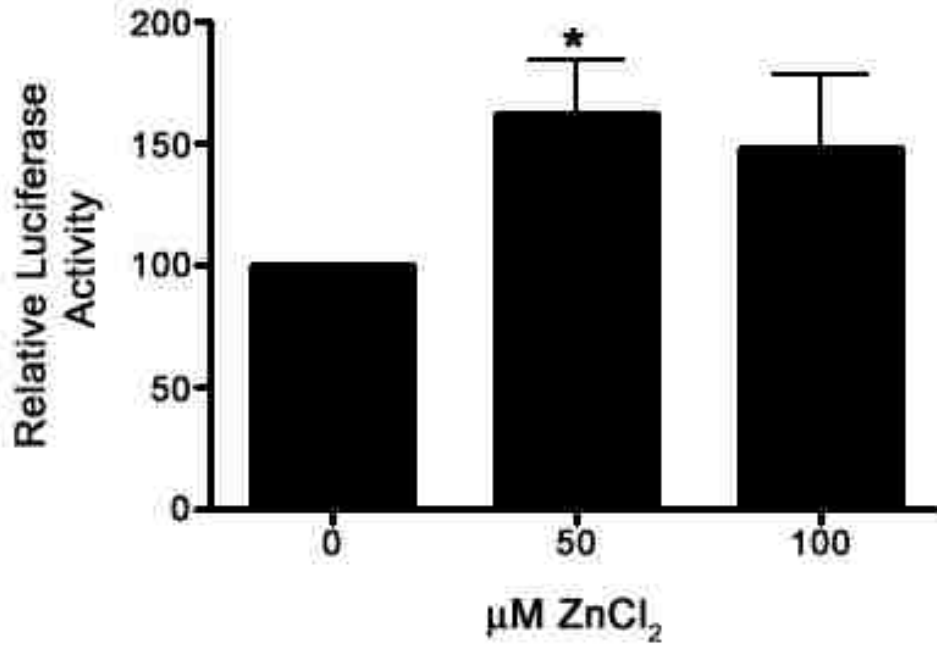


B

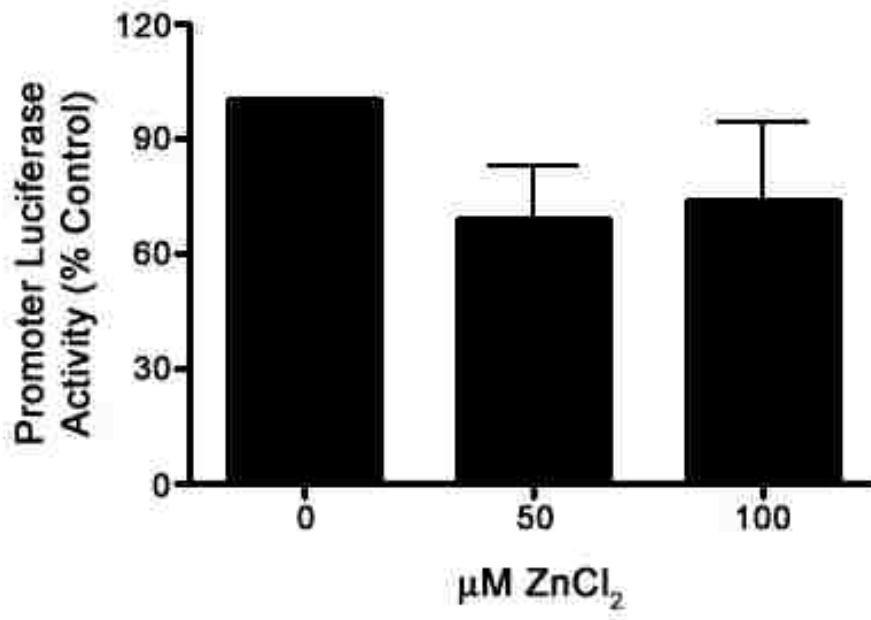


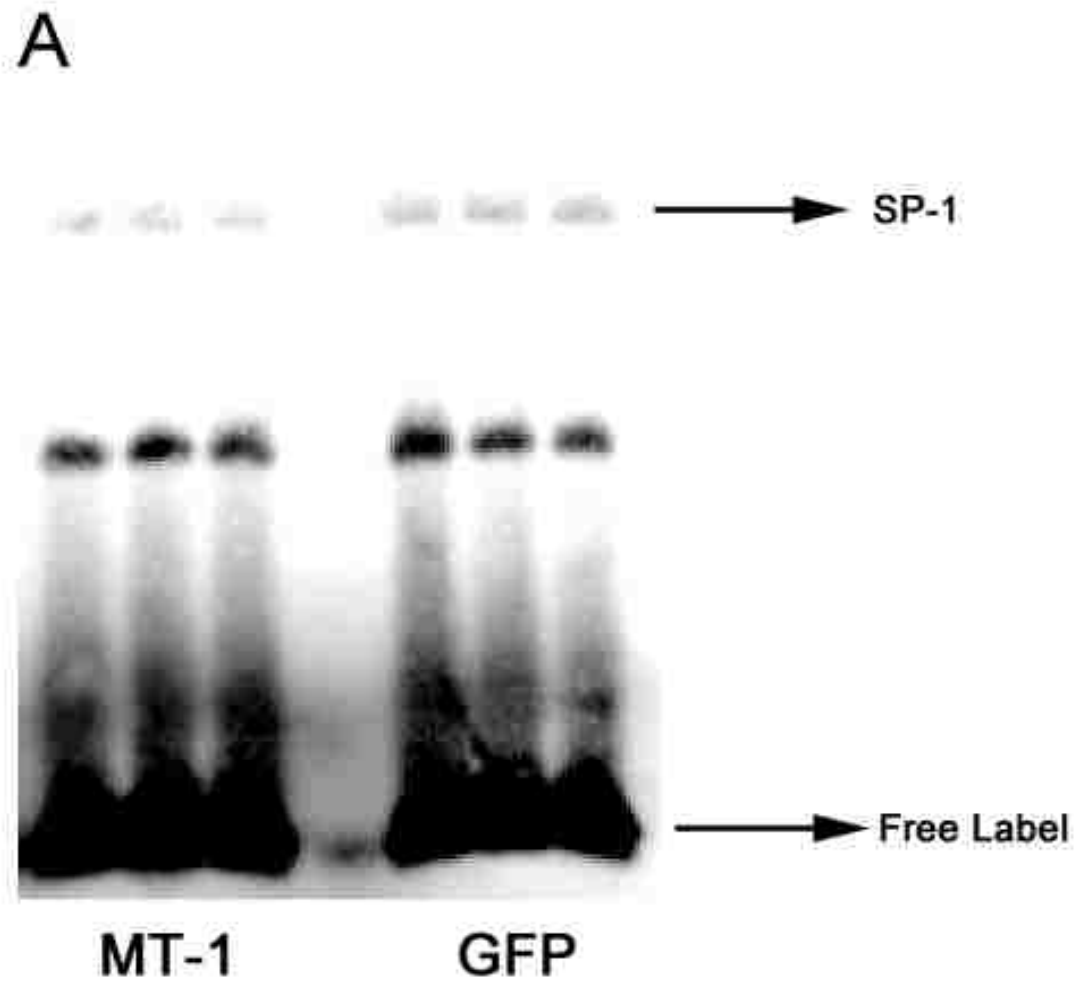
Wilham et al Fig. 7 A & B

A

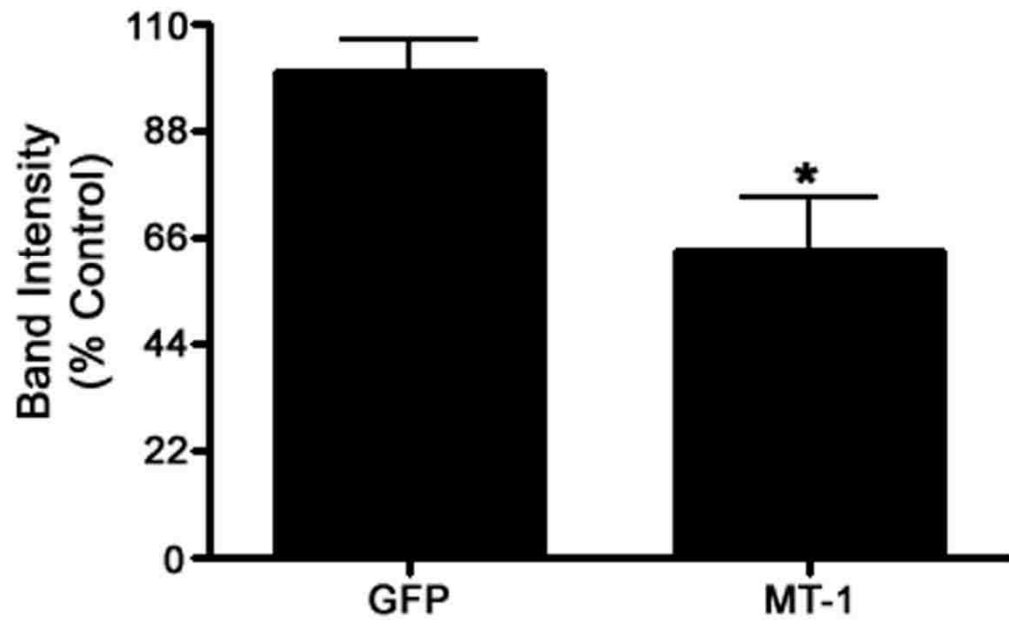


B



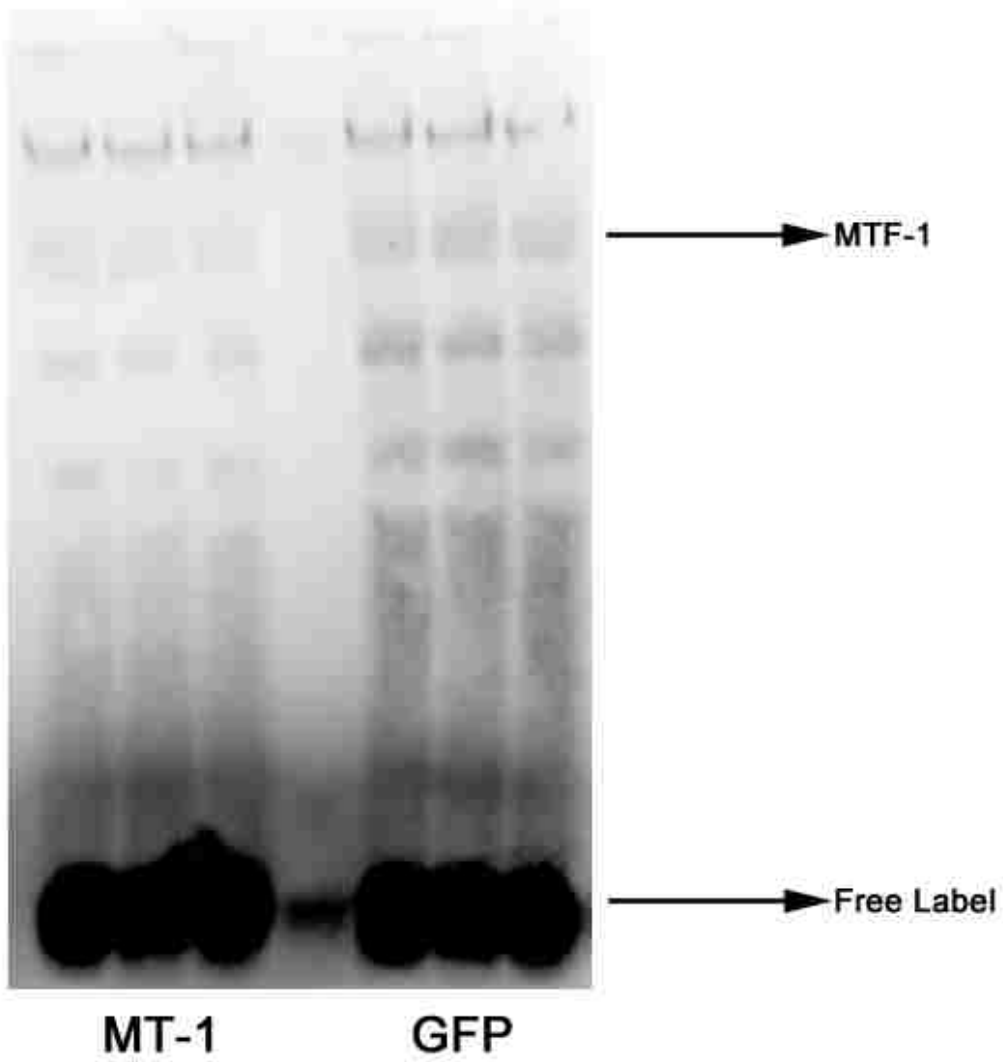


B

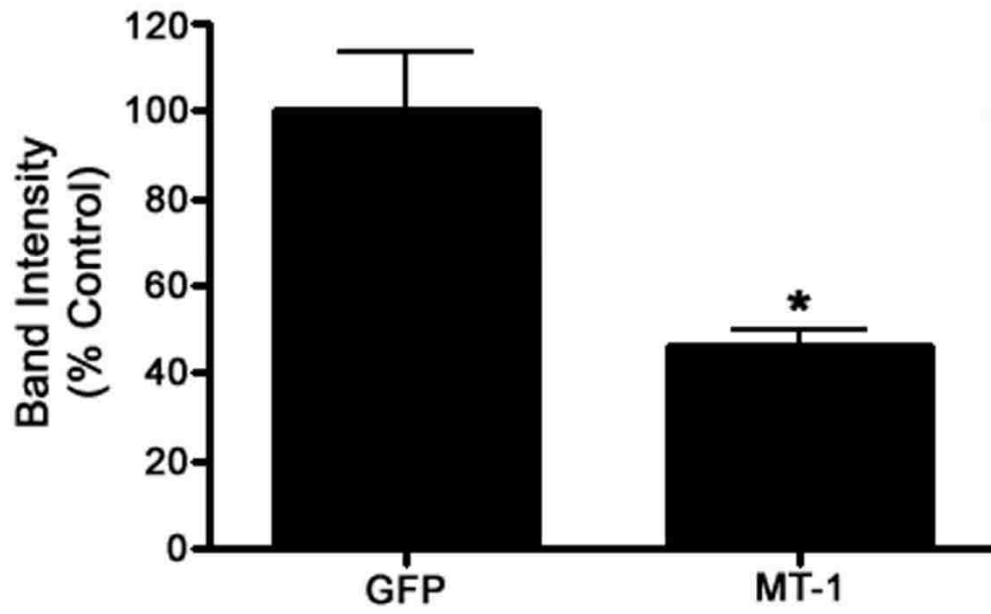


Wilham et al Fig. 9 A & B

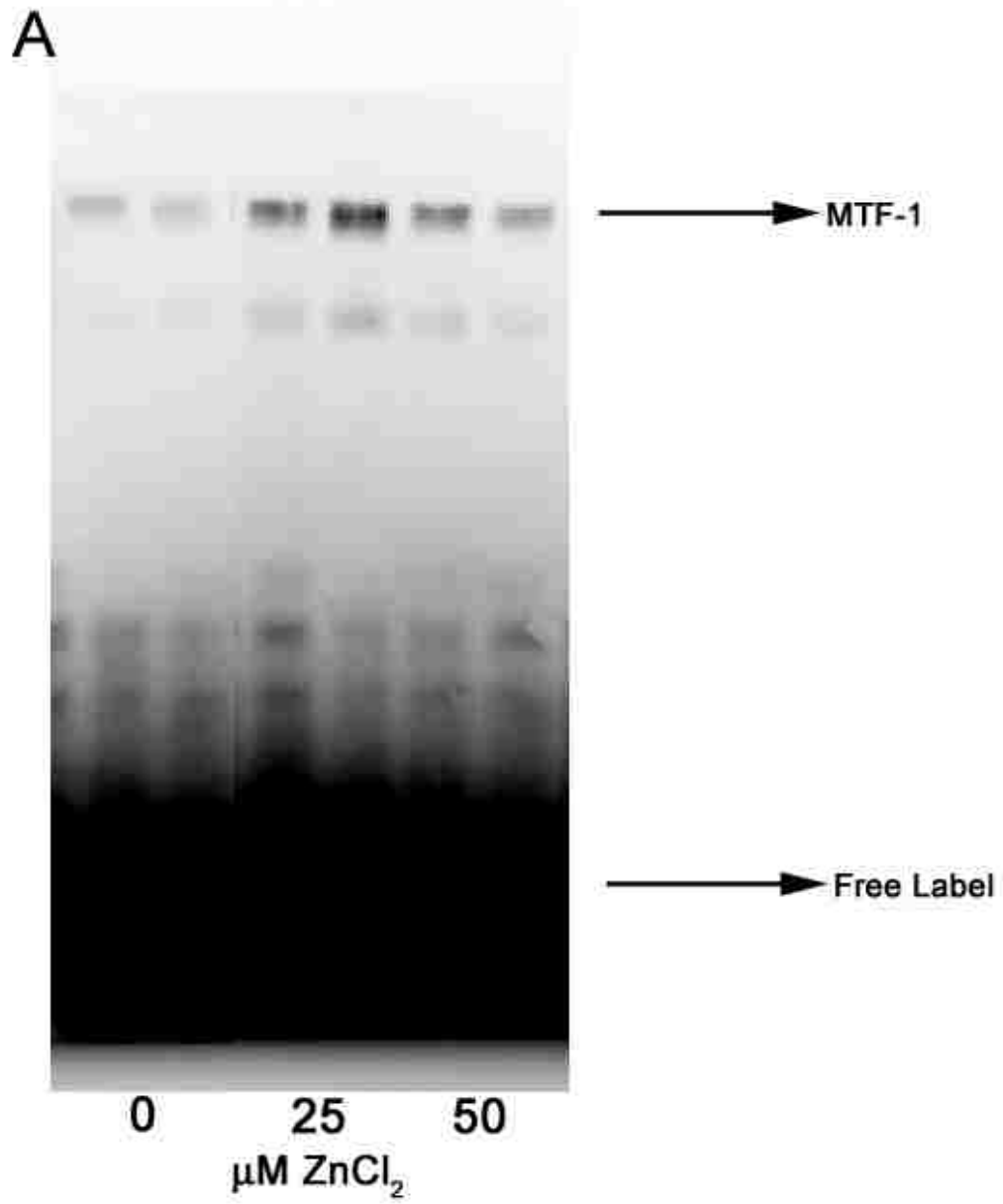
A



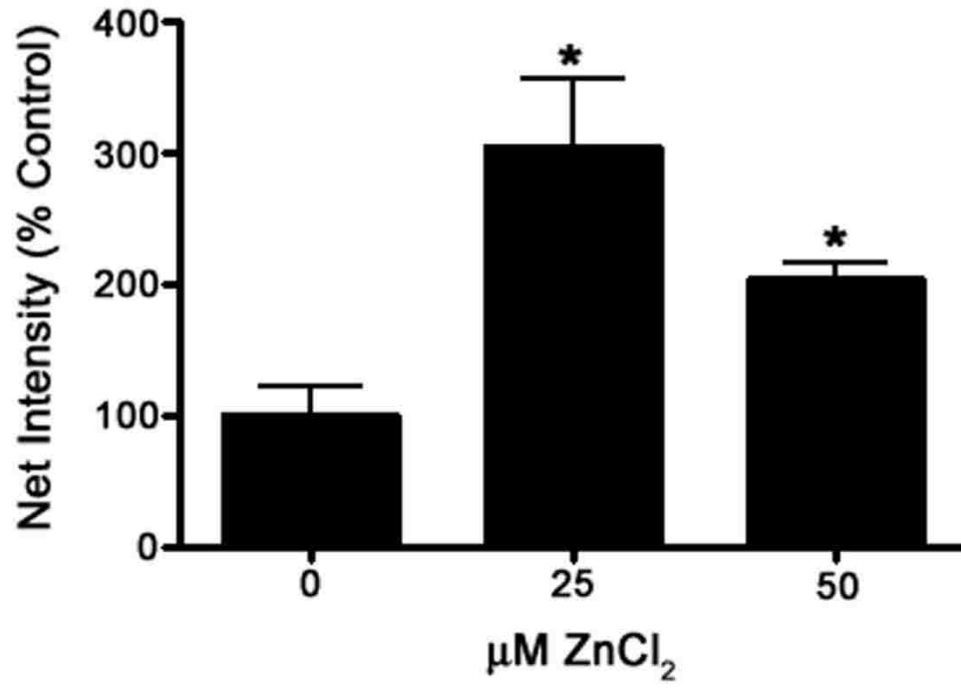
B



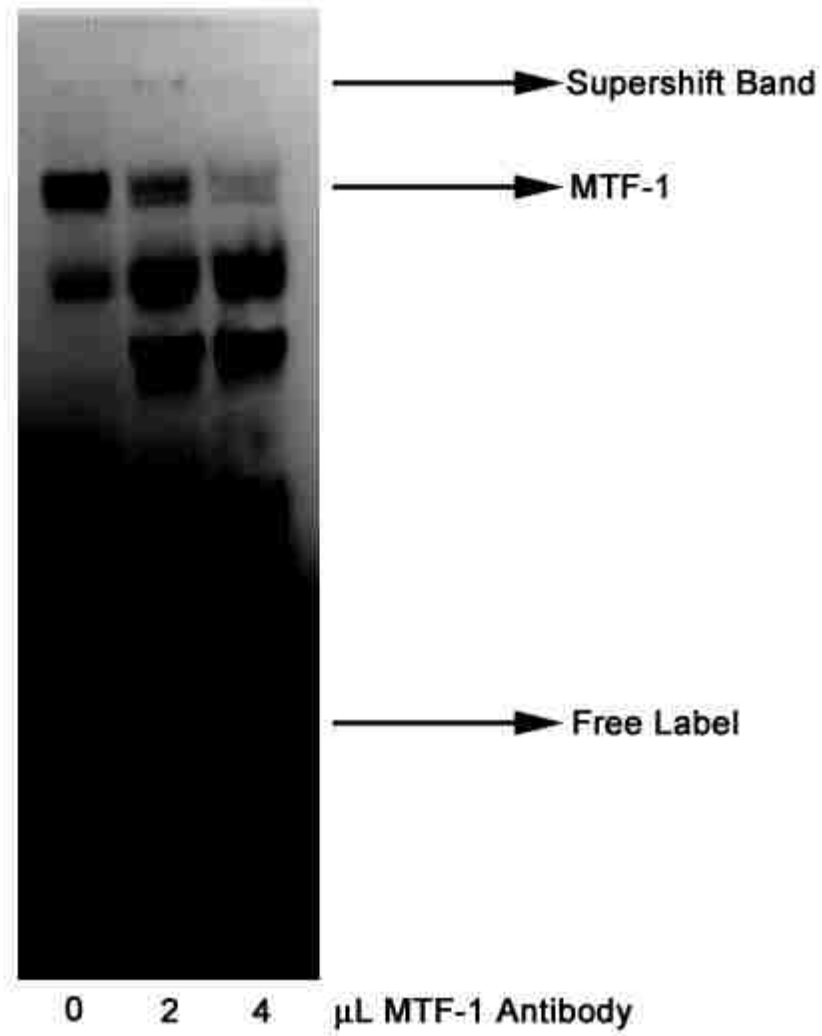
Wilham et al Fig. 10 A & B



B

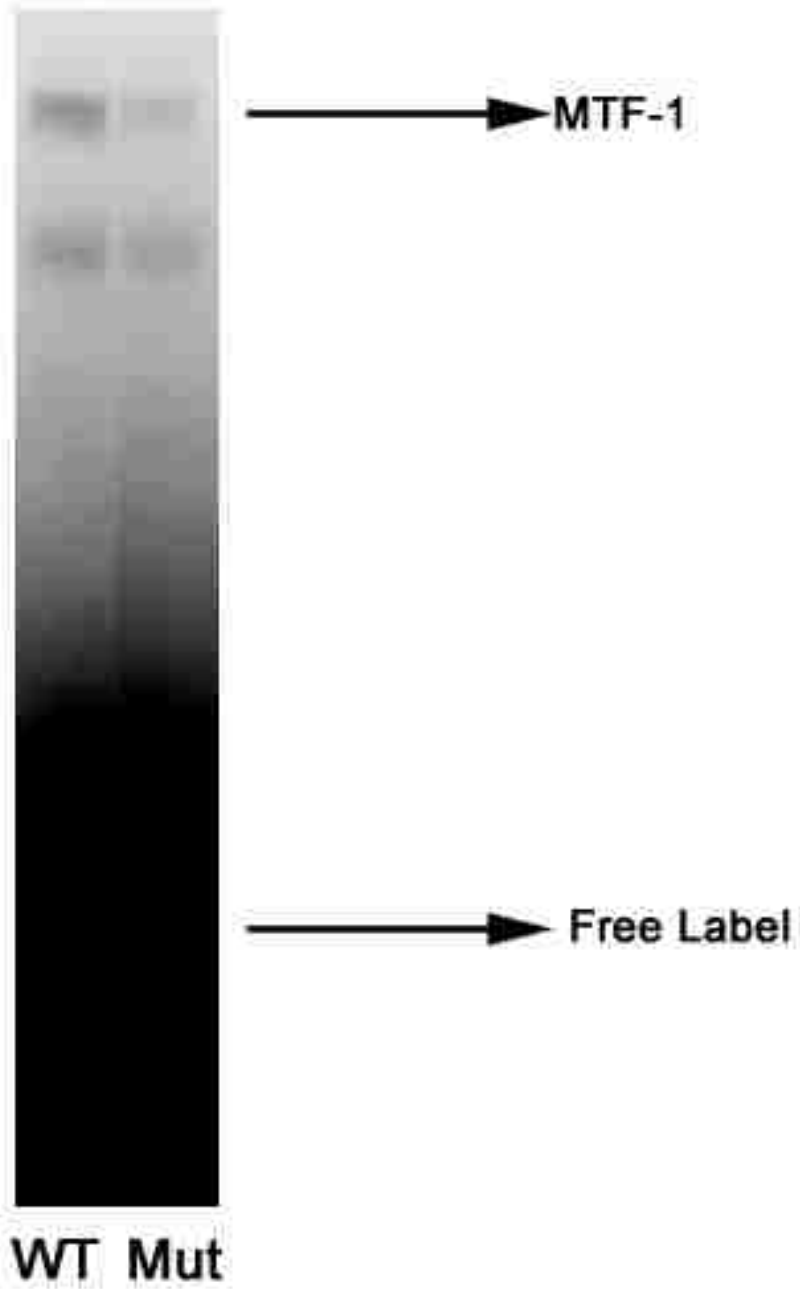


Wilham et al Fig. 11 A & B

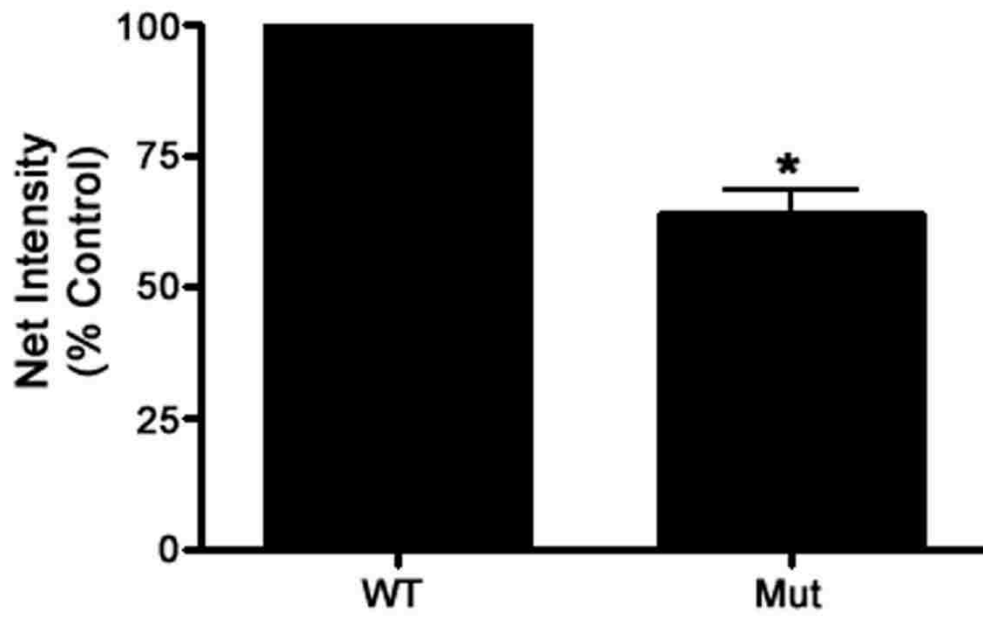


Wilham et al Fig. 12

A



B



Wilham et al Fig. 13 A & B

LOW DOSE HYDROGEN PEROXIDE AND NITRIC OXIDE ACTIVATE
ENDOTHELIAL NITRIC OXIDE SYNTHASE THROUGH RELEASE OF ZINC

Jason Wilham¹

Sanjiv Kumar²

Stephen M. Black²

¹Department of Biomedical & Pharmaceutical Sciences,
The University of Montana, Missoula MT 59812

and

²Vascular Biology Center, Medical College of Georgia, Augusta, GA 30912

Short Title:

Effect of H₂O₂ and NO on eNOS expression

ABSTRACT

Although endothelial nitric oxide synthase (eNOS) was originally thought to be a constitutively expressed enzyme, in recent years it has become clear that its expression can be modulated by a variety of chemical, physical, and developmental stimuli. Studies in our lab and others have shown that high doses of nitric oxide (NO) or hydrogen peroxide (H₂O₂) lead to decreases in eNOS expression and activity. However, at lower doses of H₂O₂, we have seen increases in eNOS expression and activity. Other studies have shown that NO donors lead to increases in eNOS expression and activity. Therefore, we set out to determine whether the NO donor spermine NONOate and H₂O₂ stimulate eNOS activity and expression in bovine aortic endothelial cells (BAECs) by increasing cellular free zinc levels and activating heavy metal responsive transcription factor 1 (MTF-1). Results indicated that BAECs stimulated for 1hr with either spermine NONOate or H₂O₂ had increased cellular labile zinc levels as indicated by FluoZin-3 AM fluorescence. An 18hrs treatment with either spermine NONOate or H₂O₂ yielded elevated levels of eNOS promoter activity, mRNA, and total protein levels. Using bandshift analysis and metallothionein (MT-1) viral transduction, we determined that both treatments led to zinc dependent increases in MTF-1 binding to the eNOS promoter. In conclusion, NO and H₂O₂ both appear to activate eNOS in a zinc dependent manner by liberating cellular stores of zinc and activating MTF-1, which binds to a region of the eNOS promoter that contains a metal response element.

INTRODUCTION

Under normal birth conditions, with the initiation of ventilation in the lungs, pulmonary vascular resistance decreases and pulmonary blood flow increases 8- to 10-fold [1-3]. However, in some instances, the normal transition does not occur, resulting in persistent pulmonary hypertension of the newborn (PPHN). The expression and activity of the enzyme endothelial nitric oxide synthase (eNOS), which is intimately involved in blood pressure control, is decreased in PPHN.

Originally thought to be a constitutively expressed enzyme, the regulation of eNOS has been demonstrated at the transcriptional, post-transcriptional and post-translational levels [4-9]. It is now known that eNOS can be modulated by a variety of chemical, physical, and developmental stimuli [10]. Studies in our lab have shown that high doses of nitric oxide (NO) or hydrogen peroxide (H_2O_2) induce apoptosis and mitochondrial dysfunction in pulmonary aortic endothelial cells [11, 12] and can decrease eNOS expression and activity [13].

H_2O_2 , most commonly produced when superoxide ($O_2^{\cdot-}$) is dismutated by superoxide dismutase (SOD), is the most stable and long lasting of the ROS [14]. It has been previously shown that H_2O_2 , but not $O_2^{\cdot-}$ or hydroxyl radicals (OH \cdot), increase eNOS expression by increasing both the rate of transcription of eNOS gene and the stability of the eNOS message once it is formed [10]. H_2O_2 has the ability to s-nitrosylate protein thiols. Previous studies carried out in a cell-free system have indicated that H_2O_2 releases zinc from metallothionein [15]. By exposing cells to certain levels of NO, either through exogenous NO [16, 17] or by upregulation of inducible nitric oxide synthase (iNOS) activity [18], studies have also demonstrated increases in intracellular labile zinc (Zn^{2+})

levels. Our laboratory has also previously demonstrated that maintaining zinc homeostasis is important in endothelial cell viability [11, 12].

We have previously shown that the addition of high levels of exogenous zinc to pulmonary aortic endothelial cells resulted in a dose dependent increase in ROS production, specifically $O_2^{\cdot-}$, producing mitochondrial dysfunction and inducing apoptotic cell death [12]. Heavy metal responsive transcription factor 1 (MTF-1) is an intracellular zinc sensor that works hand-in-hand with the zinc sink of the cell, metallothionein (MT). Upon binding of zinc, MTF-1 undergoes a conformational change, translocates to the nucleus, and binds to DNA sequence motifs with the consensus binding site TGCRCNC, known as metal response elements (MREs).

MREs are present in a number of genes' promoters including MT itself [19-21], the zinc transporter ZnT1 [22-24], and γ -glutamylcysteine synthetase heavy chain [22, 24]. Our analysis of the eNOS promoter indicated a putative MRE located at -899/-893 (TGCACTC) in the 5'-flanking sequence of the eNOS gene.

Therefore, the objective of this study was to evaluate the signaling effects of low, near physiologic doses of NO, from the NO donor spermine NONOate, and H_2O_2 on the stimulation of eNOS. We will then look specifically at the mechanism of this stimulation and if it's due to NO and H_2O_2 's ability to affect zinc storage. Results from this study indicated that non-toxic, low dose NO and H_2O_2 upregulated eNOS promoter activity, mRNA, and total protein through their ability to alter intracellular zinc levels and activate MTF-1, which then would bind to the eNOS MRE.

MATERIALS AND METHODS

Cell Culture

Primary cultures of Bovine pulmonary arterial endothelial cells (BAECs) were generously donated by Dr. J. Douglas Coffin at the University of Montana. Endothelial cell identity was confirmed by their typical cobblestone appearance, contact inhibition, specific uptake of 1,1'-dioctadecyl-1,3,3',3'-tetramethylindocarbocyanine perchlorate-labeled acetylated low-density lipoprotein (Molecular Probes, Eugene, OR), and positive staining for von Willebrand factor (Dako, Carpinteria, CA). BAECs were grown in Eagle DMEM containing 1g/l glucose and phenol red (MediaTech, Herndon, VA), supplemented with 10% fetal bovine serum (Hyclone, Logan, UT), and antibiotic-antimycotic (MediaTech). Cells were incubated at 37°C in a humidified atmosphere of 95% air and 5% CO₂. Prior to experimental treatment (unless otherwise noted) cells were trypsinized, counted with a hemacytometer and replated in a 6-, 24-, or 96-well plate (Costar, Corning, NY) at densities of approximately 10⁴/cm² and allowed to adhere for at least 18hrs.

Cell Death Analysis

BAECs were treated in serum-free, phenol red-free (SFPRF) media for an 18hr time period with various doses of spermine NONOate, hydrogen peroxide (H₂O₂), or a vehicle control. After the treatment period, the medium was collected and centrifuged for 5min at 500Xg, and the supernatant was stored at 4°C until assay. Relative cytotoxicity was quantified by measuring the release of the soluble cytoplasmic enzyme lactate dehydrogenase (LDH) activity in the cell-free supernatant using a commercial kit

(Rosche Applied Science, Indianapolis, IN). Briefly, in a fresh 96-well plate, 50 μ L aliquots of the cell-free medium and 50 μ L of reconstituted substrate mix were added to each well. LDH activity was determined spectrophotometrically using a Thermo Electron Multiscan by measuring absorbance at 490nm over a 40min period. Each sample was measured in triplicate, with a minimum of three samples per experimental group. Relative toxicity was determined by comparison of absorbance of all experimental groups with absorbance of a control cell group treated with 1% Triton X-100 cell lysis buffer according to the manufacturer's protocol. This experiment was performed six separate times for H₂O₂ and twelve for spermine NONOate.

Fluorescence Microscopy

A computer-based imaging system consisting of an Olympus IX51 microscope equipped with a charge-coupled device camera (Hamamatsu Photonics, Hamamatsu City, Japan) was used for acquisition of fluorescent images. Fluorescent-stained cells were observed with the appropriate excitation and emission, and the average fluorescent intensities (Integrated Optical Density or mean IOD) were quantified using ImagePro Plus imaging software (version 5.0, Media Cybernetics, Silver Spring, MD). A minimum of three field pictures were taken per well and averaged. FluoZin 3-AM (Molecular Probes), a fluorescent dye specific for the unassociated Zn²⁺, was used for labile zinc imaging. These were analyzed at 494-nm excitation and 516-nm emission. MTF-1-GFP nuclear translocation studies measured fluorescence at a 393-nm excitation and 509-nm emission.

eNOS Promoter Luciferase Activity Assay

1.6kb eNOS promoter constructs were generated by polymerase chain reaction (PCR) using human genomic DNA as a template. The reverse primer common to all constructs binds immediately upstream of the ATG initiation codon of eNOS (5' – GTTACTGTG CGT CCA CTCTGCTGCC). The forward primer was 5' – TGTAGTTTCCCTAGTCCCCC (840bp fragment). A 3-bp mutation was introduced into the metal response element sequence within the 840bp construct. The sequence -902 at -890 in the human eNOS promoter was changed to GCAattACTCTGG by site-directed mutagenesis.

BAECs were then grown to 70% confluence and transfected for 24hrs with 0.4 μ g β -gal (transfection efficiency control) and 1.6 μ g eNOS promoter-luciferase construct using an Effectene transfection kit (Qiagen, Velencia, CA). Cells were then treated for an additional 18hrs with various doses of spermine NONOate (0-100 μ M) or H₂O₂ (0-50 μ M).

Plates were rinsed with DPBS and 200 μ L 1X Reporter Lysis Buffer (Promega, Madison, WI) was added to each well. Plates were sealed with parafilm and frozen at -80°C for 20min or until subsequent analysis. Next, plates were put at 37°C for 30min. then vortexed for 30s and the cell solution transferred to a new eppendorf tube. This tube was vortexed for an additional 15s and then centrifuged at 12,000g for 10min at room temperature. The supernatant was then transferred to a new tube and placed on ice until analyzed.

To normalize for transfection efficiency, β -gal activity was measured. In a 96-well plate, 5-10 μ L cell lysate was combined with 40-45 μ L 1X Reporter Lysis Buffer and 50 μ L β -gal substrate (Qiagen, Valencia, CA) in 100 μ L total volume. The plate was then allowed to incubate at 37°C for 30min. Spectrophotometric readings were taken on a Thermo Electron Multiscan plate reader at 405nm throughout the 30min incubation period.

Luciferase activities were measured luminometrically using a Thermo Electron Fluoroscan plate reader set as a luminometer. Twenty microliters of cell lysate was combined with 100 μ L luciferase substrate (Qiagen, Valencia, CA) and a reading on the luminometer was taken immediately.

mRNA Extraction and Quantitation

eNOS mRNA levels were analyzed in BAECs following 18hr spermine NONOate or H₂O₂ treatment. Cells were grown in 6-well plates to confluence and treated in 10% fetal bovine serum containing medium for 18hr with various doses of spermine NONOate, H₂O₂, or a vehicle control. Following treatment, RNA was isolated using the RNeasy Kit (Qiagen, Valencia, CA). Final collection of RNA was in 40 μ L RNase free water. Throughout the isolation process, RNA was kept on ice to ensure minimal degradation. RNA concentrations were determined using 260 and 280nm readings from a Shimadzu spectrophotometer.

Next, cDNA was made from the RNA by following the Quantitect Reverse Transcriptase kit instructions (Qiagen, Valencia, CA). QuantiTect SYBR Green PCR kit (Qiagen, Valencia, CA) was used for PCR master mix. ROX (Invitrogen, Carlsbad, CA)

was used as a reference dye to normalize the fluorescent reporter signal from SYBR Green in the RT-PCR. 18S RNA was used to standardize sample concentration differences. A Multiplex Quantitative PCR System Mx4000 was used for the Real Time PCR.

Protein Extraction

BAECs were grown in 6-well plates to confluence and treated in regular serum media for 18hrs with various doses of spermine NONOate, H₂O₂, or a vehicle control. Following treatment, total protein was harvested. Briefly, cells were rinsed with DPBS (MediaTech) and RIPA lysis buffer added to each well. Cells were then collected and sheared with a 25-gauge needle 3X. Lastly, samples were spun at 14,000Xg for 10min and the supernatant was collected. Total protein concentrations were analyzed using Bio-Rad protein assay (Bio-Rad, Hercules, CA) and Bovine Serum Albumin (BSA) for the protein standard curve.

Western Blotting

Western Blot analysis was performed as previously described [25]. Total protein extracts (~20µg) were resuspended in 5X Laemmli protein sample buffer and boiled for 5min. Total protein was then separated on a 4-20% Tris-SDS-HEPES polyacrylamide gel (Gardipore, Frenchs Forest, Australia) and electrophoretically wet-transferred to a Hybond-PVDF membrane (Amersham, Arlington Hts., IL). The membranes were blocked with 5% nonfat dry milk in Tris buffered saline containing 0.1% Tween-20 (TBST) overnight at 4°C. After blocking, the membranes were incubated at room

temperature for 2 hrs with the primary antibody (1:1,000 for α -eNOS, BD Biosciences), washed 3X with TBST, and incubated with a mouse anti-rabbit IgG-horseradish peroxidase conjugated secondary antibody (Pierce, Rockford, IL) for 1 hr. After washing, immunolabeled protein bands were visualized using chemiluminescence (SuperSignal West Fempto Substrate Kit, Pierce) on a Kodak Image Station 440CF with Kodak 1D Molecular Imaging Software. Blots were stripped (Pierce Stripping Solution) and reprobed with β -actin (1:1000, Sigma) to normalize for loading.

Generation of MT-1 Adenoviral Expression Construct

An adenoviral vector expressing MT-1 was constructed using the pAd/pENTR System (Invitrogen). Briefly, a pAd/CMV plasmid containing an MT-1 cDNA (cDNA purchased from ATCC, Manassas, VA) was created and transfected into 293A cells. A selected clone was propagated and viral lysates were collected and tittered per the manufacturer's protocol. The titer for the AdV.MT-1 preparation was 3.4×10^{10} plaque-forming units per mL. Infections on BAECs were performed for 120min with virus diluted in normal DMEM to the desired multiplicity of infection. Verification of expression was performed using Western Blot analysis as described above using 20 μ g of protein extracts.

Quantification of Intracellular Zn²⁺ Levels

BAECs were grown on glass cover slips in 6-well plates and treated with various doses of spermine NONOate, H₂O₂, or a vehicle control in SFPRF media for 1hr at 37⁰C. After 30min of treatment, cells were loaded with 2.5 μ M FluoZin 3-AM (Molecular

Probes), a fluorescent dye specific for labile Zn^{2+} . Following the treatment period, cells were washed twice with SFPRF media and incubated for an additional 30min in the dark at 37°C (in the incubator). Cell-coated glass cover slips were removed from the 6-well plate one at a time and put onto a glass slides. These slides were analyzed by fluorescent microscopy as described above.

MTF-1-GFP Nuclear Translocation

An MTF-1 construct was cloned (Sal I and Xma I) upstream of a GFP construct (Xma I and Not I) into the pEntr1A gateway vector system (Invitrogen). Enzymatic digests were utilized to verify cloning products and their orientation.

BAECs were grown on glass cover slips in 6-well plates to 50-60% confluence, and were transduced with Lac Z (viral control) or MT-1 adenovirus at a multiplicity of infection (MOI) equal to 1000 for 24hrs. Then, they were transfected with the MTF-1-GFP construct using Effectene transfection reagent (Qiagen, Valencia, CA). MTF-1-GFP translocation was determined using fluorescent microscopy as described above. A higher mean IOD correlated to more nuclear localization. A minimum of 3 field pictures were taken per well and averaged. The mean \pm standard deviation was calculated and a $P < 0.05$ was considered statistically significant from the control.

Nuclear Extract Preparation and EMSA

BAECs were grown to 80% confluence and transduced with metallothionein 1 (MT-1) or a GFP transduction control adenovirus at a MOI equal to 1000. Twenty four hours post transduction, cells were treated for 18hr with 5 μ M H_2O_2 or 25 μ L spermine

NONOate. Following treatment, nuclear extracts were prepared using the NE-PER nuclear extraction kit (Pierce). Electrophoretic mobility shift assays (EMSA) were performed using biotinylated double stranded oligonucleotide corresponding to MRE site at -898 of eNOS promoter. We also utilized an MRE mutant oligonucleotide where 3 nucleotides at -898 were mutated from TGC to ATT in the human eNOS promoter. The single stranded oligonucleotides were biotinylated using Biotin 3' End DNA Labeling Kit (Pierce) to incorporate 1-3 biotinylated ribonucleotides (Biotin-11-UTP) onto the 3' end of DNA strands using terminal deoxynucleotidyl transferase (TdT) and then annealed to make it double stranded. Binding reactions involved incubating 7.5 µg of nuclear extract with biotinylated oligonucleotide and 1 µg poly(dI.dC) for 20min at room temperature. The DNA-protein complexes were resolved on a 5% nondenaturing polyacrylamide gel in 1X TBE buffer, then transferred to nylon membrane and biotinylated oligonucleotide was detected using a LightShift® Chemiluminescent EMSA kit (Pierce) and visualized on a Kodak Image station 440 CF (Eastman Kodak).

Statistical Analysis

Values are expressed as the means \pm standard error of the mean from at least three experiments. Statistical analysis between experimental groups was performed by one way ANOVA or T-test using the Graph Pad Prism 4.0 statistical analysis software program. The $P < 0.05$ was considered statistically significant.

RESULTS

Initial experiments determined cellular toxicity in bovine aortic endothelial cells (BAECs) to 18hr exposures of various doses of the nitric oxide (NO) donor spermine NONOate or hydrogen peroxide (H_2O_2) using lactate dehydrogenase release (LDH). LDH release was measured in the media of treated cells and normalized to Triton-X 100 lysed cells (100% cell death). No significant toxicity exists in BAECs following an 18hr H_2O_2 treatment at doses of $25\mu M$ and less (Figure 1), while doses of spermine NONOate at $100\mu M$ and less were not found to be toxic (Figure 2).

We next determined whether non-toxic doses of spermine NONOate and H_2O_2 would cause increases in cellular free zinc levels. Cells were grown on glass cover slips to minimize auto-fluorescence from the plastic and the zinc fluorophore, FluoZin-3 AM, was used to measure cellular labile zinc levels. Doses of $5\mu M$ H_2O_2 up to $50\mu M$ increased cellular free zinc 1.5-9.5 fold (Figure 2, $P < 0.05$). Doses of $25\mu M$ spermine NONOate up to $100\mu M$ increased cellular free zinc at least 2-fold (Figure 4, $P < 0.05$).

Knowing that H_2O_2 and NO can be detrimental at higher doses to eNOS, we next looked at the effect of the lowest doses of H_2O_2 and spermine NONOate that still significantly increased labile zinc levels on eNOS mRNA levels utilizing real time PCR. Cells were treated for 18hrs with $25\mu M$ spermine NONOate or $5\mu M$ H_2O_2 and then RNA was isolated using a Qiagen RNeasy kit. cDNA was made using the Qiagen QuantiTect Reverse Transcriptase kit and QuantiTect SYBR Green PCR kit was used for the master mix. 18s RNA was used to normalize cDNA loading. Results indicated that 18hr treatment with $5\mu M$ H_2O_2 increased eNOS mRNA (Figure 5), and that 18hr treatment with $25\mu M$ spermine NONOate increased eNOS mRNA (Figure 6).

Then, we followed up the mRNA experiments and looked at the effect of these treatments on total eNOS protein levels. Cells were grown to confluence, treated for 18hrs with 5 μ M H₂O₂ or 25 μ M spermine NONOate, and protein was harvested. Western Blot analysis indicated that total eNOS significantly increased with both treatments (Figure 7 and Figure 8 respectively).

Our initial analysis of the eNOS promoter indicated the presence of a putative heavy metal response element (HRE) located at -899/-893 in the 5'-flanking region of the human eNOS gene sequence. We wanted to determine whether increases in eNOS mRNA and protein levels following H₂O₂ or spermine NONOate treatments were due to eNOS transcriptional alterations through the eNOS MRE. This was done by using an eNOS promoter-luciferase activity assay with a wild type or MRE-mutant 1.6kb human eNOS promoter-luciferase construct. Using metallothionein (MT-1) adenovirus, we investigated whether alterations that may be found in eNOS promoter luciferase activity were due to increases in cellular free zinc. Cells were grown to 70% confluence and virally transduced with MT-1 adenovirus or a GFP viral control. Six to eight hours later, they were dually transfected with a β -gal transfection efficiency control construct and a WT or mutant eNOS promoter luciferase construct. After 24h, cells were treated with 5 μ M H₂O₂ or 25 μ M spermine NONOate for 18h. Lastly, they were harvested for eNOS promoter luciferase and β -gal activity assays. Our data indicate that 5 μ M H₂O₂ (Figure 9) and 25 μ M spermine NONOate (Figure 9) significantly increased eNOS promoter luciferase activity. MT-1 overexpression decreased basal eNOS promoter luciferase activity and abolished spermine NONOate and H₂O₂ stimulated eNOS promoter

luciferase activity (Figure 9). The MRE-mutated eNOS promoter luciferase construct resulted in decreased eNOS promoter luciferase activity in all samples (Figure 9).

We developed a MTF-1-GFP construct that can be transfected into cells to observe MTF-1 nuclear localization. Since MTF-1 is known to work directly with MT-1 and to be activated by alterations in labile zinc levels, we determined whether the MT-1 transduction decreased MTF-1 nuclear translocation. Cells were grown to 70% confluence on glass cover slips and transduced with MT-1 or a GFP viral control for 24h. Then, they were transfected with the MTF-1-GFP construct. Twenty four hours post transfection, fluorescence microscopy was used to quantitate nuclear translocation of MTF-1-GFP. MT-1 overexpression decreased MTF-1-GFP nuclear translocation (Figure 10).

Lastly, we wanted to determine whether our 18hr spermine NONOate and H₂O₂ treatments were causing zinc dependent activation of MTF-1 binding to the eNOS promoter. Therefore, we used MTF-1 bandshift analysis and MT-1 viral transduction. Cells were grown to 80% confluence and virally transduced with either a GFP control or MT-1 adenovirus. Twenty four hours post transduction; cells were treated for 18hrs with spermine NONOate or H₂O₂. Following treatment, nuclear extracts were prepared and MTF-1 bandshift analysis was carried out. Results indicated that both treatments lead to increased MTF-1 binding to the eNOS MRE and that these increases are abolished with MT-1 overexpression.

DISCUSSION

Persistent pulmonary hypertension of the newborn (PPHN) is associated with endothelial dysfunction, and endothelial cells have been shown to increase their generation of hydrogen peroxide and superoxide both from the “uncoupling” of endothelial nitric oxide synthase (eNOS) and from the activation of nicotinamide adenine dinucleotide phosphate-oxidase (NADPH) complex. Both eNOS mRNA and protein levels are decreased in PPHN, contributing to decreased levels of NO production. In the present study, we examined the effect of physiologic levels of spermine NONOate and hydrogen peroxide (H₂O₂) in bovine aortic endothelial cells (BAECs) on the eNOS expression. Under normal *in vivo* conditions, endothelial cells are continually exposed to low amounts of nitric oxide (NO) and H₂O₂. Findings from this study demonstrate a pathway of eNOS activation in BAECs by low dose treatments of the NO donor, spermine NONOate, and of H₂O₂ through free zinc release and heavy metal responsive transcription factor 1 (MTF-1) activation. Specifically, this study found that these exposures increased BAEC: (1) eNOS promoter activity, (2) eNOS mRNA, (3) total eNOS protein, (4) labile zinc, and (5) MTF-1 binding to eNOS promoter MRE. These results provide evidence of MTF-1 and zinc in the regulation of eNOS.

The mechanism by which NO regulates eNOS activity and gene expression is incompletely understood. In the vasculature, the free radical NO is produced mostly by the endothelial NOS isoforms, with a minor contribution from neuronal-type NOS in smooth muscle cells [7]. It can diffuse rapidly from the endothelium to adjacent cells, where it is important in maintaining vascular homeostasis through vasodilation by activation of soluble guanylate cyclase, production of cGMP, and ultimately, activation

of a variety of downstream effectors, including cGMP-dependent protein kinase, cGMP-modulated ion channels, and phosphodiesterases [27]. NO is also very important for preventing platelet aggregation and leukocyte adhesion, and lowering vascular smooth muscle proliferation. Many of the functions of endothelial –derived NO seem to prevent or inhibit atherosclerosis [8]. Its production is regulated by changes in eNOS enzyme activity and/or eNOS gene expression. Our toxicity results with the NO donor, spermine NONOate, in BAECs indicated no significant toxicity as measured by lactate dehydrogenase (LDH) release with an 18hr treatment and doses up to 100 μ M.

The mechanisms by which H₂O₂ regulates eNOS are complex and incompletely understood. Studies done by Drummond, et. al. have found concentration- and time-dependent increases in eNOS mRNA and protein induced by H₂O₂ through increases in transcription and mRNA stability [10]. Their studies utilized doses of 100 and 150 μ M H₂O₂ in BAECs for 24h exposures, while our studies found significant toxicity in BAECs at 50 μ M H₂O₂ for an 18h exposure (Figure 2). This contradiction could be due to cell passage or inter-animal differences. Our study utilized cells less than passage 10 and from the same animal. Despite varying doses and treatment times, results from our study had similar conclusions that H₂O₂ can increase eNOS mRNA and total protein.

Metallothioneins (MT) are small, cysteine-rich proteins that avidly bind to metals such as zinc, copper, and cadmium to reduce their concentration to a physiological or non-toxic level [15]. The concentration of exchangeable zinc in a cell is regulated by the sulfhydryl –rich MT, which is found in most organisms and tissues [28, 29]. In addition to regulating zinc, MT itself is involved in protecting against oxidative stress by virtue of its remarkably high content of cysteinyl residues [28, 30, 31].

Past studies have established that oxidizing compounds can cause release of zinc from proteins, such as MT, through oxidation of zinc-thiolate bonds [32, 33]. Both NO and H₂O₂ are compounds capable of oxidizing zinc-thiolate bonds and releasing free zinc. Interestingly, we found low, nontoxic doses of H₂O₂ and spermine NONOate for 1hr in BAECs to significantly increase intracellular labile zinc levels, 1.9-2.0-fold, as measured by the zinc fluorophore, FluoZin-3AM.

Zinc can have either positive or negative effects on cellular physiology depending on the local concentration, localization, and/or state [34]. Excess amounts of free zinc can be detrimental and exacerbate cellular damage both *in vivo* and *in vitro* [35-37]. However, at certain levels, zinc appears to protect against DNA damage and apoptosis caused by oxidative stress [38]. Zinc is very tightly regulated since it serves many essential cellular roles [39, 40]. Several hundred enzymes are known to require zinc for proper functioning and well over a thousand transcription factors contain zinc-binding sequences [41-43]. In fact, the zinc finger protein structure is the most prevalent DNA binding motif of transcription factors [44]. In a number of cell lines, zinc inhibits apoptosis and its depletion induces characteristic apoptotic death [45, 46].

Results from this study in BAECs found immediate increases in labile zinc following spermine NONOate or H₂O₂, followed by increased eNOS mRNA (1.6-2.9-fold), total protein (1.3-1.9-fold), and promoter activity (1.7-2.9-fold). This agrees with previous data from our lab that found an 18hr 6μM H₂O₂ treatment in BAECs significantly increased total eNOS protein levels [13]. Increases in eNOS promoter-luciferase activity with spermine NONOate and H₂O₂ treatment were zinc-dependent, since they were abolished with MT-1 viral transduction. MT-1 transduction also

decreased eNOS promoter-luciferase activity in untreated BAECs, suggesting that zinc is at least partially involved in basal eNOS promoter activity (Figure 11). We also looked at eNOS promoter luciferase activity with a mutated MRE in the eNOS promoter construct. Our results indicated that the MRE mutant lowered basal eNOS promoter activity as well as H₂O₂ and spermine NONOate induced eNOS promoter activity. MT-1 transduction also significantly decreased spermine NONOate and H₂O₂ treated levels of eNOS promoter luciferase activity.

Treatment with NO or H₂O₂ could induce zinc-activated transcription of genes encoding antioxidant proteins. One of the most obvious proteins involved would be MT since MT expression is induced by zinc and it is a potent antioxidant [28-30, 47, 48]. MTF-1 plays a central role in the transcriptional activation of the MT gene in response to heavy metals and oxidative stress [15, 49]. In our MTF-1 bandshift analysis, we found that low dose, 18h spermine NONOate and H₂O₂ treatments in BAECs both increased MTF-1 bound to the eNOS MRE. The H₂O₂ data agrees with recent data from Zhang, et al., which found that in a cell free system, MTF-1 could be activated indirectly by H₂O₂ through release of zinc from oxidized MT [15].

It is also becoming increasingly apparent that phosphorylation by multiple kinases including protein kinase C (PKC), c-Jun N-terminal kinase (JNK) and tyrosine kinase, is involved in the metal-dependent transactivation of MTF-1 [50-52]. However, further studies will need to be carried out to examine the involvement of these various kinases in MTF-1 transcriptional activation following low dose spermine NONOate and H₂O₂.

In conclusion, low dose NO and H₂O₂ both appear to activate eNOS in a zinc dependent manner by liberating cellular stores of zinc and activating MTF-1, which then binds to the eNOS promoter metal response element. Further studies will need to be done to look at the involvement of other zinc finger transcription factors, such as Sp-1. Studies here utilized an 18hr, low dose NO and H₂O₂ treatment and therefore did not mimic a disease state, such as PPHN, where there is a chronic, high production of oxidative species. However, an understanding of eNOS regulation may help to identify new pathways and novel therapies for diseases such as PPHN.

ACKNOWLEDGMENTS

This research was supported in part by grants 0515459Z from the American Heart Association Pacific Mountain Affiliates (to JW) and HL60190 (to SMB), HL67841 (to SMB), HL072123 (to SMB), and HL070061 (to SMB) from the National Institutes of Health.

REFERENCES

1. Dawes, G.S., et al., *Changes in the lungs of the new-born lamb*. J Physiol, 1953. **121**(1): p. 141-62.
2. Iwamoto, H.S., D. Teitel, and A.M. Rudolph, *Effects of birth-related events on blood flow distribution*. Pediatr Res, 1987. **22**(6): p. 634-40.
3. Rudolph, A.M., *Fetal and neonatal pulmonary circulation*. Annu Rev Physiol, 1979. **41**: p. 383-95.
4. Fleming, I. and R. Busse, *Molecular mechanisms involved in the regulation of the endothelial nitric oxide synthase*. Am J Physiol Regul Integr Comp Physiol, 2003. **284**(1): p. R1-12.
5. Fulton, D., J.P. Gratton, and W.C. Sessa, *Post-translational control of endothelial nitric oxide synthase: why isn't calcium/calmodulin enough?* J Pharmacol Exp Ther, 2001. **299**(3): p. 818-24.
6. Govers, R. and T.J. Rabelink, *Cellular regulation of endothelial nitric oxide synthase*. Am J Physiol Renal Physiol, 2001. **280**(2): p. F193-206.
7. Li, H., T. Wallerath, and U. Forstermann, *Physiological mechanisms regulating the expression of endothelial-type NO synthase*. Nitric Oxide, 2002. **7**(2): p. 132-47.
8. Searles, C.D., *Transcriptional and posttranscriptional regulation of endothelial nitric oxide synthase expression*. Am J Physiol Cell Physiol, 2006. **291**(5): p. C803-16.
9. Tai, S.C., G.B. Robb, and P.A. Marsden, *Endothelial nitric oxide synthase: a new paradigm for gene regulation in the injured blood vessel*. Arterioscler Thromb Vasc Biol, 2004. **24**(3): p. 405-12.
10. Drummond, G.R., et al., *Transcriptional and posttranscriptional regulation of endothelial nitric oxide synthase expression by hydrogen peroxide*. Circ Res, 2000. **86**(3): p. 347-54.
11. Wiseman, D.A., et al., *Alterations in zinc homeostasis underlie endothelial cell death induced by oxidative stress from acute exposure to hydrogen peroxide*. Am J Physiol Lung Cell Mol Physiol, 2007. **292**(1): p. L165-77.
12. Wiseman, D.A., et al., *Endothelial response to stress from exogenous Zn²⁺ resembles that of NO-mediated nitrosative stress, and is protected by MT-1 overexpression*. Am J Physiol Cell Physiol, 2006. **291**(3): p. C555-68.
13. Wedgwood, S. and S.M. Black, *Endothelin-1 decreases endothelial NOS expression and activity through ETA receptor-mediated generation of hydrogen peroxide*. Am J Physiol Lung Cell Mol Physiol, 2005. **288**(3): p. L480-7.
14. Boulden, B.M., et al., *Early determinants of H₂O₂-induced endothelial dysfunction*. Free Radic Biol Med, 2006. **41**(5): p. 810-7.
15. Zhang, B., et al., *Activity of metal-responsive transcription factor 1 by toxic heavy metals and H₂O₂ in vitro is modulated by metallothionein*. Mol Cell Biol, 2003. **23**(23): p. 8471-85.
16. Pearce, L.L., et al., *Metallothionein, nitric oxide and zinc homeostasis in vascular endothelial cells*. J Nutr, 2000. **130**(5S Suppl): p. 1467S-70S.

17. St Croix, C.M., et al., *Nitric oxide-induced changes in intracellular zinc homeostasis are mediated by metallothionein/thionein*. Am J Physiol Lung Cell Mol Physiol, 2002. **282**(2): p. L185-92.
18. Spahl, D.U., et al., *Regulation of zinc homeostasis by inducible NO synthase-derived NO: nuclear metallothionein translocation and intranuclear Zn²⁺ release*. Proc Natl Acad Sci U S A, 2003. **100**(24): p. 13952-7.
19. Mueller, P.R., S.J. Salser, and B. Wold, *Constitutive and metal-inducible protein:DNA interactions at the mouse metallothionein I promoter examined by in vivo and in vitro footprinting*. Genes Dev, 1988. **2**(4): p. 412-27.
20. Searle, P.F., *Zinc dependent binding of a liver nuclear factor to metal response element MRE-a of the mouse metallothionein-I gene and variant sequences*. Nucleic Acids Res, 1990. **18**(16): p. 4683-90.
21. Stuart, G.W., P.F. Searle, and R.D. Palmiter, *Identification of multiple metal regulatory elements in mouse metallothionein-I promoter by assaying synthetic sequences*. Nature, 1985. **317**(6040): p. 828-31.
22. Gunes, C., et al., *Embryonic lethality and liver degeneration in mice lacking the metal-responsive transcriptional activator MTF-1*. Embo J, 1998. **17**(10): p. 2846-54.
23. Langmade, S.J., et al., *The transcription factor MTF-1 mediates metal regulation of the mouse ZnT1 gene*. J Biol Chem, 2000. **275**(44): p. 34803-9.
24. Lichtlen, P., et al., *Target gene search for the metal-responsive transcription factor MTF-1*. Nucleic Acids Res, 2001. **29**(7): p. 1514-23.
25. Black, S.M., et al., *Ventilation and oxygenation induce endothelial nitric oxide synthase gene expression in the lungs of fetal lambs*. J. Clin. Invest, 1997. **100**: p. 1448-1458.
26. Stitt, M.S., et al., *Nitric oxide-induced nuclear translocation of the metal responsive transcription factor, MTF-1 is mediated by zinc release from metallothionein*. Vascul Pharmacol, 2006. **44**(3): p. 149-55.
27. Murad, F., et al., *Regulation and role of guanylate cyclase-cyclic GMP in vascular relaxation*. Prog Clin Biol Res, 1987. **249**: p. 65-76.
28. McKenna, I.M., et al., *Expression of metallothionein protein in the lungs of Wistar rats and C57 and DBA mice exposed to cadmium oxide fumes*. Toxicol Appl Pharmacol, 1998. **153**(2): p. 169-78.
29. Moffatt, P. and F. Denizeau, *Metallothionein in physiological and physiopathological processes*. Drug Metab Rev, 1997. **29**(1-2): p. 261-307.
30. Andrews, G.K., *Regulation of metallothionein gene expression by oxidative stress and metal ions*. Biochem Pharmacol, 2000. **59**(1): p. 95-104.
31. Vallee, B.L., *The function of metallothionein*. Neurochem Int, 1995. **27**(1): p. 23-33.
32. Aizenman, E., et al., *Induction of neuronal apoptosis by thiol oxidation: putative role of intracellular zinc release*. J Neurochem, 2000. **75**(5): p. 1878-88.
33. Jiang, L.J., W. Maret, and B.L. Vallee, *The glutathione redox couple modulates zinc transfer from metallothionein to zinc-depleted sorbitol dehydrogenase*. Proc Natl Acad Sci U S A, 1998. **95**(7): p. 3483-8.
34. Chen, C.J. and S.L. Liao, *Neurotrophic and neurotoxic effects of zinc on neonatal cortical neurons*. Neurochem Int, 2003. **42**(6): p. 471-9.

35. Choi, D.W., M. Yokoyama, and J. Koh, *Zinc neurotoxicity in cortical cell culture*. Neuroscience, 1988. **24**(1): p. 67-79.
36. Lees, G.J., et al., *The neurotoxicity of zinc in the rat hippocampus*. Neurosci Lett, 1990. **120**(2): p. 155-8.
37. Yokoyama, M., J. Koh, and D.W. Choi, *Brief exposure to zinc is toxic to cortical neurons*. Neurosci Lett, 1986. **71**(3): p. 351-5.
38. Leccia, M.T., et al., *Zinc protects against ultraviolet A1-induced DNA damage and apoptosis in cultured human fibroblasts*. Biol Trace Elem Res, 1999. **69**(3): p. 177-90.
39. Berg, J.M. and Y. Shi, *The galvanization of biology: a growing appreciation for the roles of zinc*. Science, 1996. **271**(5252): p. 1081-5.
40. Vallee, B.L. and D.S. Auld, *Zinc coordination, function, and structure of zinc enzymes and other proteins*. Biochemistry, 1990. **29**(24): p. 5647-59.
41. Heximer, S.P. and D.R. Forsdyke, *A human putative lymphocyte G0/G1 switch gene homologous to a rodent gene encoding a zinc-binding potential transcription factor*. DNA Cell Biol, 1993. **12**(1): p. 73-88.
42. Klug, A., *Zinc finger peptides for the regulation of gene expression*. J Mol Biol, 1999. **293**(2): p. 215-8.
43. Sukegawa, J. and G. Blobel, *A nuclear pore complex protein that contains zinc finger motifs, binds DNA, and faces the nucleoplasm*. Cell, 1993. **72**(1): p. 29-38.
44. Klug, A. and J.W. Schwabe, *Protein motifs 5. Zinc fingers*. Faseb J, 1995. **9**(8): p. 597-604.
45. Adler, M., R.E. Dinterman, and R.W. Wannemacher, *Protection by the heavy metal chelator N,N,N',N'-tetrakis (2-pyridylmethyl)ethylenediamine (TPEN) against the lethal action of botulinum neurotoxin A and B*. Toxicon, 1997. **35**(7): p. 1089-100.
46. Hyun, H.J., et al., *Depletion of intracellular zinc induces macromolecule synthesis- and caspase-dependent apoptosis of cultured retinal cells*. Brain Res, 2000. **869**(1-2): p. 39-48.
47. Chubatsu, L.S. and R. Meneghini, *Metallothionein protects DNA from oxidative damage*. Biochem J, 1993. **291** (Pt 1): p. 193-8.
48. Kling, P.G. and P. Olsson, *Involvement of differential metallothionein expression in free radical sensitivity of RTG-2 and CHSE-214 cells*. Free Radic Biol Med, 2000. **28**(11): p. 1628-37.
49. Heuchel, R., et al., *The transcription factor MTF-1 is essential for basal and heavy metal-induced metallothionein gene expression*. Embo J, 1994. **13**(12): p. 2870-5.
50. LaRochelle, O., et al., *Phosphorylation is involved in the activation of metal-regulatory transcription factor 1 in response to metal ions*. J Biol Chem, 2001. **276**(45): p. 41879-88.
51. Saydam, N., et al., *Nucleo-cytoplasmic trafficking of metal-regulatory transcription factor 1 is regulated by diverse stress signals*. J Biol Chem, 2001. **276**(27): p. 25487-95.
52. Yu, C.W., J.H. Chen, and L.Y. Lin, *Metal-induced metallothionein gene expression can be inactivated by protein kinase C inhibitor*. FEBS Lett, 1997. **420**(1): p. 69-73.

FIGURE LEGENDS

Fig. 1. 18hr treatment of BAECs with H_2O_2 leads to significant LDH release at doses of $50\mu M$ and higher. BAECs were grown to confluence and treated for 18hr with H_2O_2 in regular media. Media was harvested and LDH release was measured using a Rosche LDH colorometric assay kit and reading at 492nm on a Multiscan platereader. All values are mean \pm SEM (n=6). * $P<0.05$ vs. $0\mu M$ sample.

Fig. 2. 18hr treatment of BAECs with Spermine NONOate does not lead to significant LDH release at doses of $100\mu M$ and less. BAECs were grown to confluence and treated for 18hr with spermine NONOate in regular media. Media was harvested and LDH release was measured using a Rosche LDH colorometric assay kit and reading at 492nm on a Multiscan platereader. All values are mean \pm SEM (n=12). * $P<0.05$ vs. $0\mu M$ sample.

Fig. 3. A 1hr treatment with H_2O_2 leads to increases in cellular level of free zinc. BAECs were exposed to H_2O_2 for 1hr in SFPRF media. Cells were rinsed and then loaded with $1\mu M$ FluoZin-3. An Olympus scope and GFP cube were used to take pictures and Image Pro Software to quantitate fluorescence. Results found that $5\mu M$ H_2O_2 were sufficient to increase cellular free zinc levels. All values are mean \pm SD (n=6). * $P<0.05$ vs. $0\mu M$ H_2O_2 .

Fig. 4. A 1hr treatment with Spermine NONOate leads to increases in cellular level of free zinc. BAECs were exposed to Spermine NONOate for 1hr in SFPRF media. Cells were rinsed and then loaded with 1 μ M FluoZin-3. An Olympus scope with a GFP cube was used to take pictures and Image Pro Software to quantitate fluorescence. Results found that 25, 50, and 100 μ M Spermine NONOate were sufficient to increase cellular free zinc levels. All values are mean \pm SD (n=6). * $P < 0.05$ vs. 0 μ M Spermine NONOate.

Fig. 5. 4hr H₂O₂ treatment of BAECs leads to significant increase in eNOS mRNA levels. BAECs were treated for 4hrs with H₂O₂ in regular media. mRNA was isolated from the cells and cDNAs were made. Quantitative real time PCR and normalization to 18s RNA was used to quantitate the levels of eNOS mRNA. Results found that 5 μ M H₂O₂ is sufficient to significantly increase eNOS mRNA. All values are mean \pm SD (n=5). * $P < 0.05$ vs. 0 μ M H₂O₂.

Fig. 6. 4hr Spermine NONOate treatment of BAECs leads to significant increase in eNOS mRNA levels. BAECs were treated for 4hrs with Spermine NONOate in regular media. mRNA was isolated from the cells and cDNAs were made. Quantitative real time PCR and normalization to 18s RNA was used to quantitate the levels of eNOS mRNA. Results found that 25 μ M Spermine NONOate is sufficient to significantly increase eNOS mRNA. All values are mean \pm SD (n=5). * $P < 0.05$ vs. 0 μ M Spermine NONOate.

Fig. 7. A 4hr treatment with H₂O₂ leads to increases in total eNOS protein levels.

BAECs were exposed to H₂O₂ for 4hrs in SFPRF media. Western Blot analysis indicated that total eNOS levels increased at some doses of H₂O₂. All values are mean ± SD (n=5).

* *P*<0.05 vs. 0μM H₂O₂.

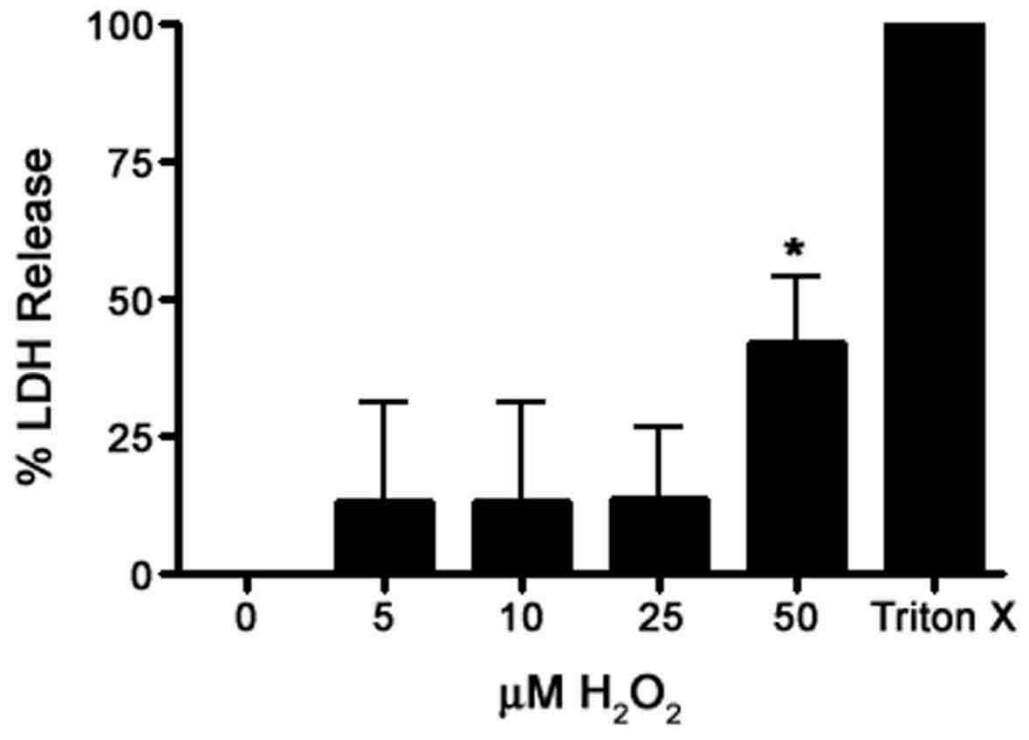
Fig. 8. A 4hr treatment with Spermine NONOate leads to increases in total eNOS protein levels. BAECs were exposed to Spermine NONOate for 4hrs in SFPRF media. Western Blot analysis indicated that total eNOS levels increased at some doses of Spermine NONOate. All values are mean ± SD (n=5). * *P*<0.05 vs. 0μM Spermine NONOate.

Fig. 9. Increases in eNOS promoter luciferase activity due to spermine NONOate or H₂O₂ treatments are zinc dependent and acting through the eNOS MRE. The overexpression of MT-1 decreases eNOS promoter luciferase activity in untreated, Spermine NONOate, and H₂O₂ treated samples. However, in the mutant, the overexpression of MT-1 also decreases eNOS promoter luciferase activity. BAECs were transduced with MT-1. 24hrs later, the BAECs were co-transfected with either WT or mutant eNOS promoter luciferase and β-gal. 24hrs later, cells were harvested and β-gal and luciferase activities were measured by adding their respective substrates and reading on a plate reader or luminometer. All values are mean ± SEM (n=3). * *P*<0.05 vs. GFP WT.

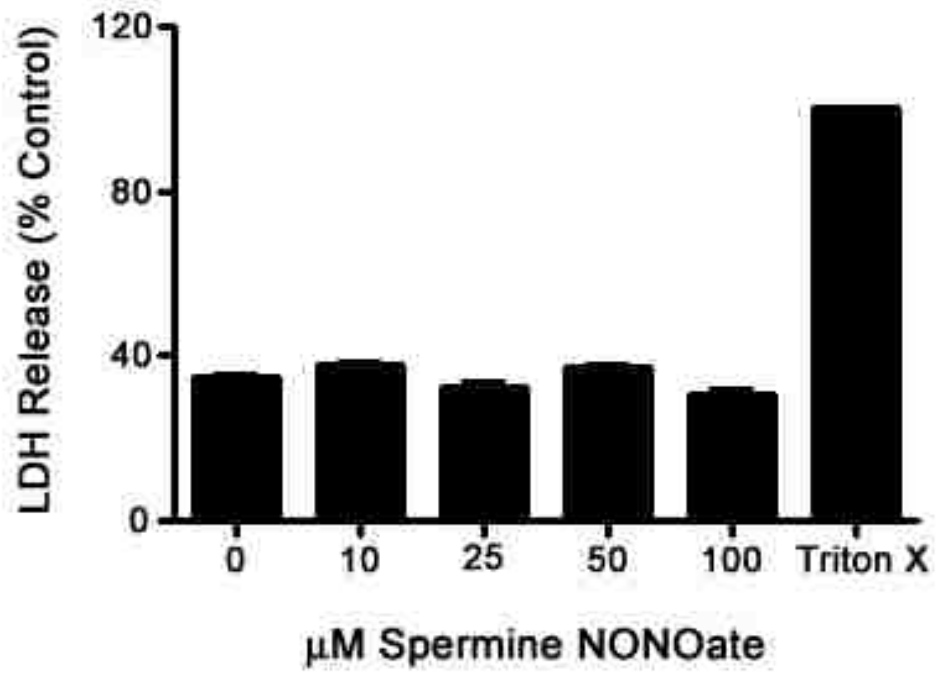
Fig. 10. Overexpression of MT-1 in BAECs leads to a decrease in MTF-1 nuclear localization. BAECs were transduced with Lac Z or MT-1 adenovirus at MOI=1000.

24hrs later, they were transfected with MTF-1 GFP. 24hrs more, an Olympus scope and GFP cube were used to take pictures of MTF-1-GFP localization and Image Pro software was used to quantitate nuclear brightness. All values are mean \pm SEM (n=5). * $P<0.05$ vs. Lac Z transduction.

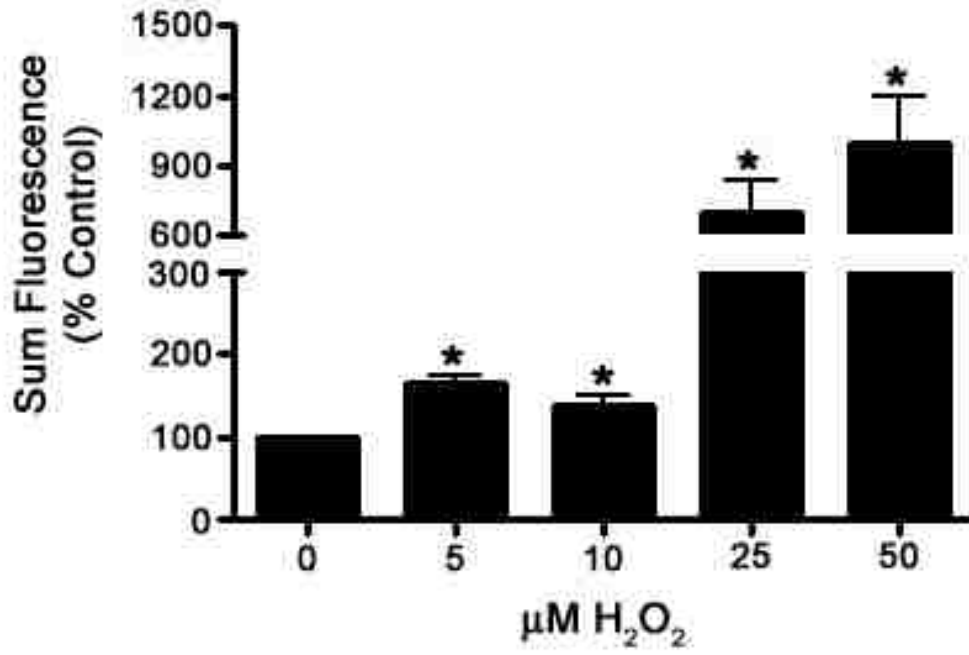
Fig. 11. Overexpression of MT-1 attenuates NO and H₂O₂ induced increases in MTF-1 bandshift levels. BAECs were grown to ~80% confluency and transduced with GFP or MT-1 adenovirus at MOI=1000. 24hrs later, cells were treated for 18hr with Spermine NONOate or H₂O₂. Nuclear protein extracts were made and bandshift analysis was performed. All values are mean \pm SEM (n=6). * $P<0.05$ vs. GFP UTD.



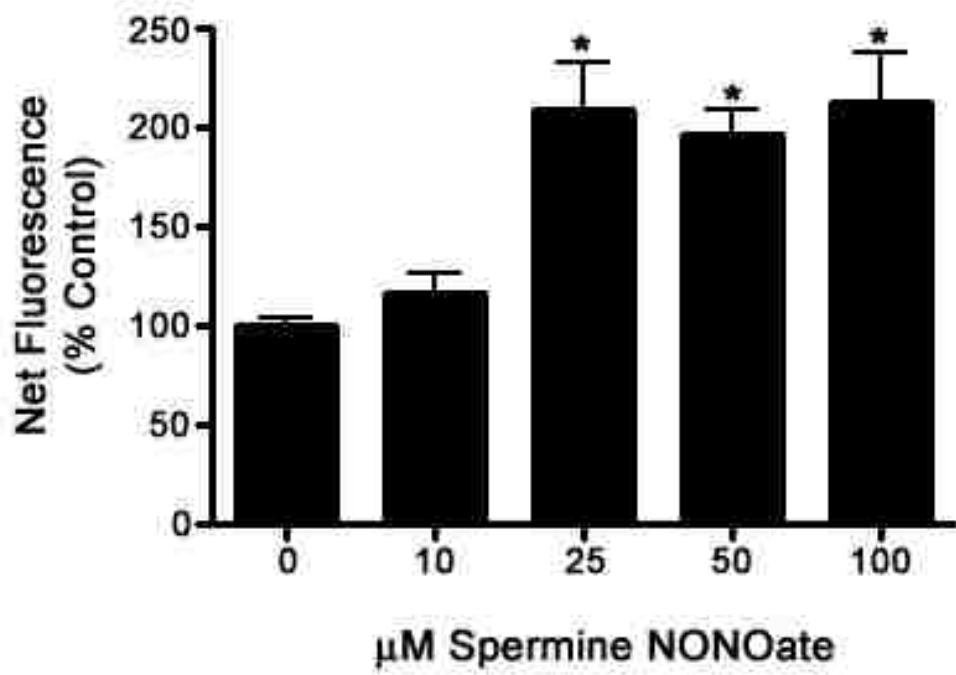
Wilham et al Fig. 1



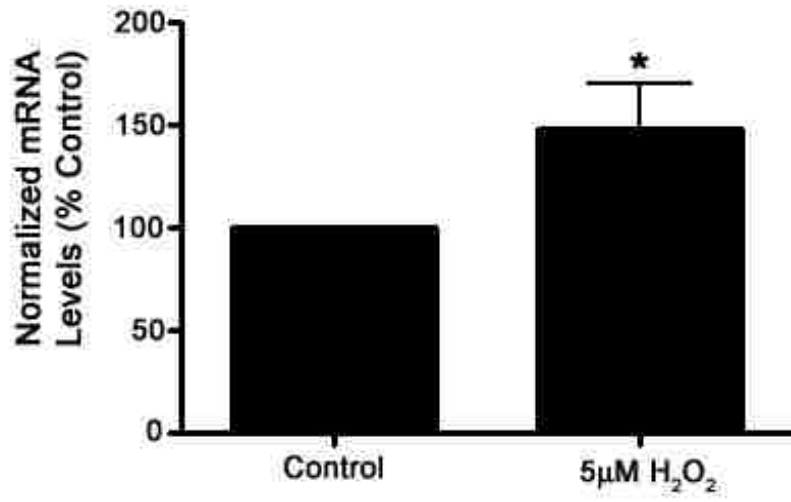
Wilham et al Fig. 2



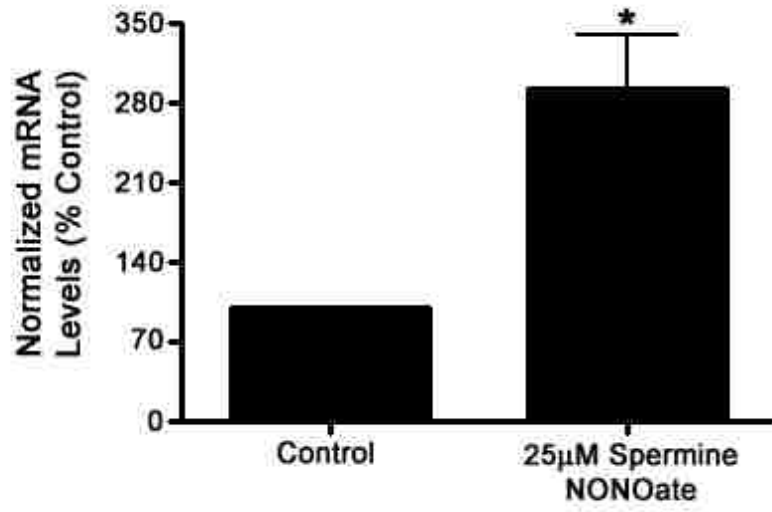
Wilham et al Fig. 3



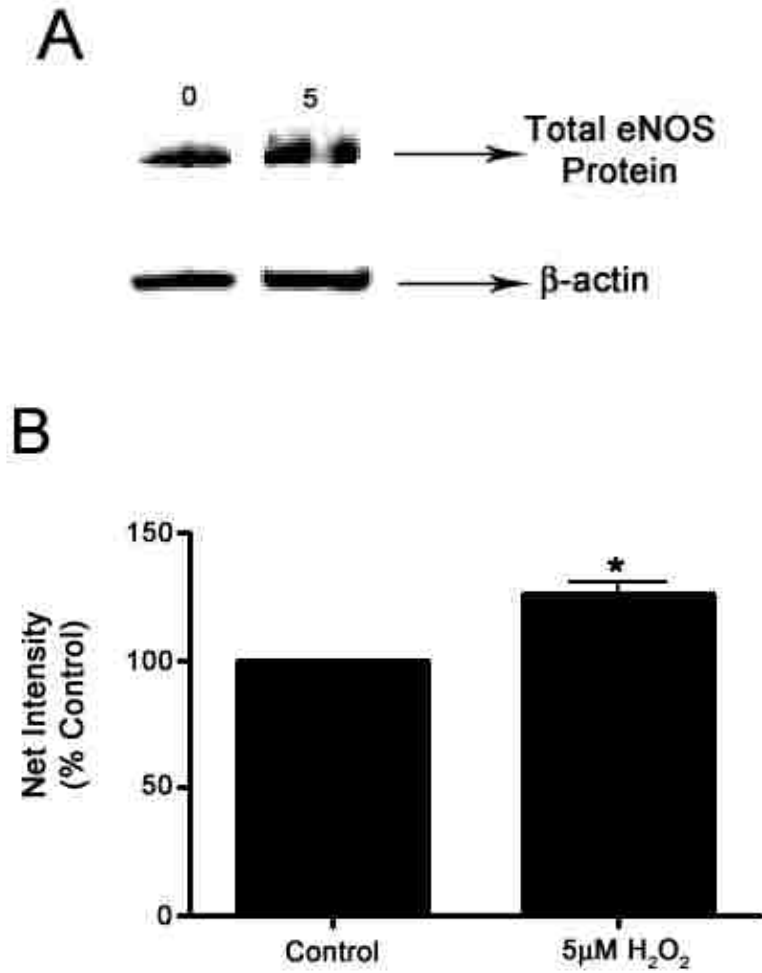
Wilham et al Fig. 4



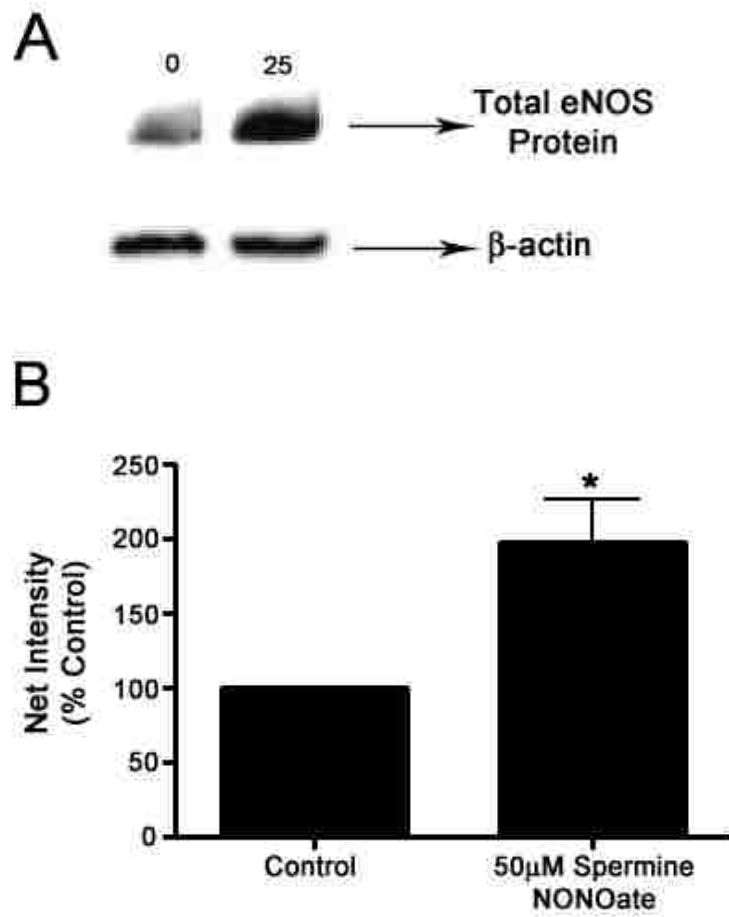
Wilham et al Fig. 5



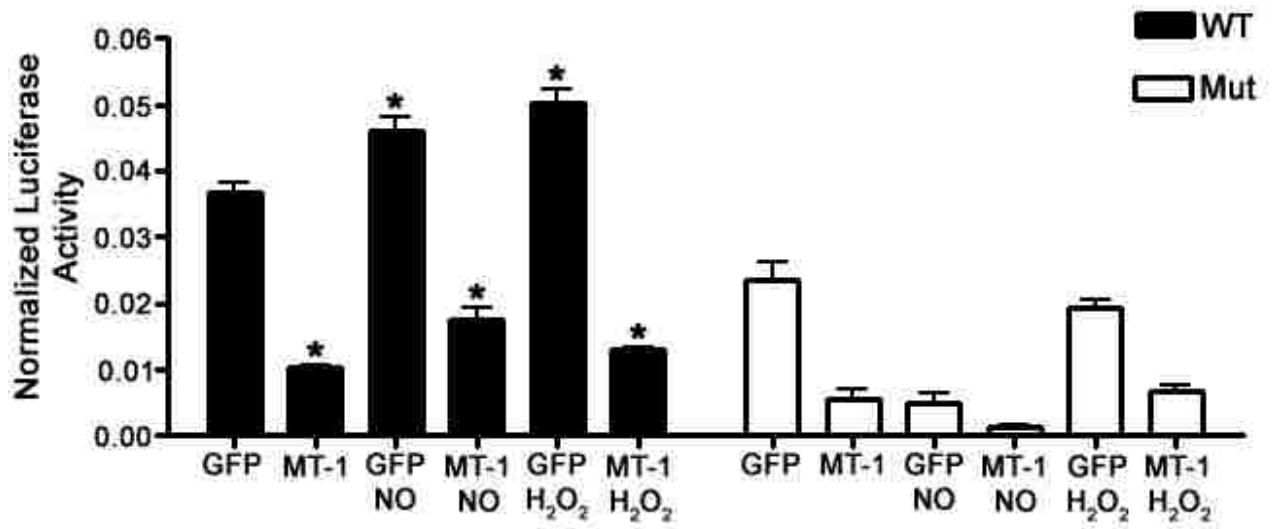
Wilham et al Fig. 6



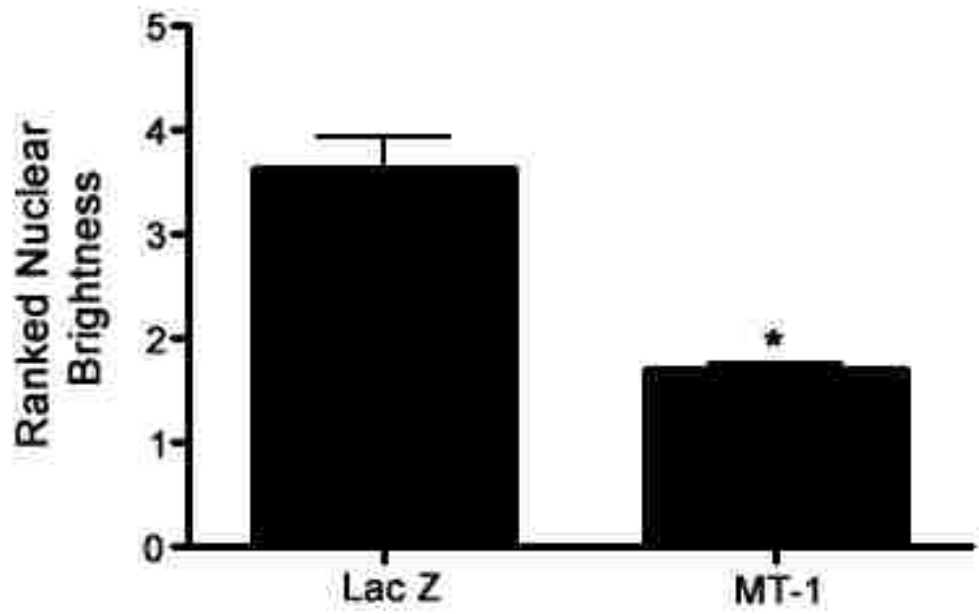
Wilham et al Fig. 7 A & B



Wilham et al Fig. 8 A & B

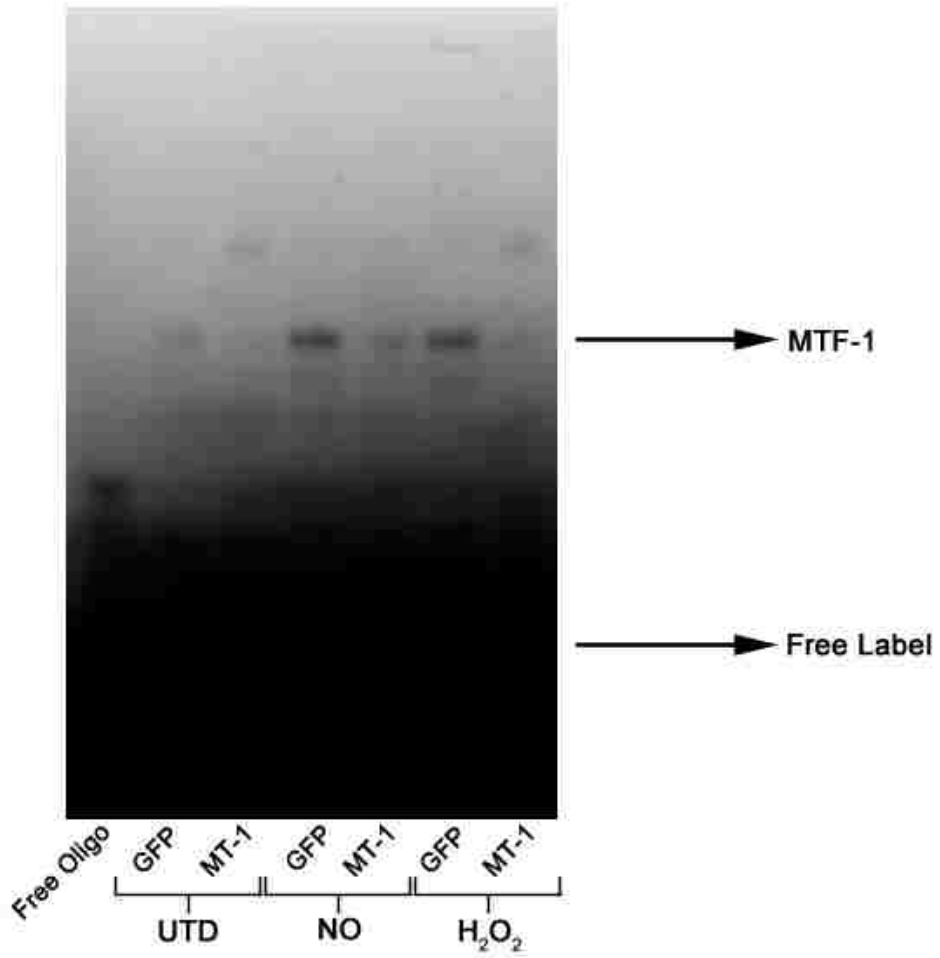


Wilham et al Fig. 9

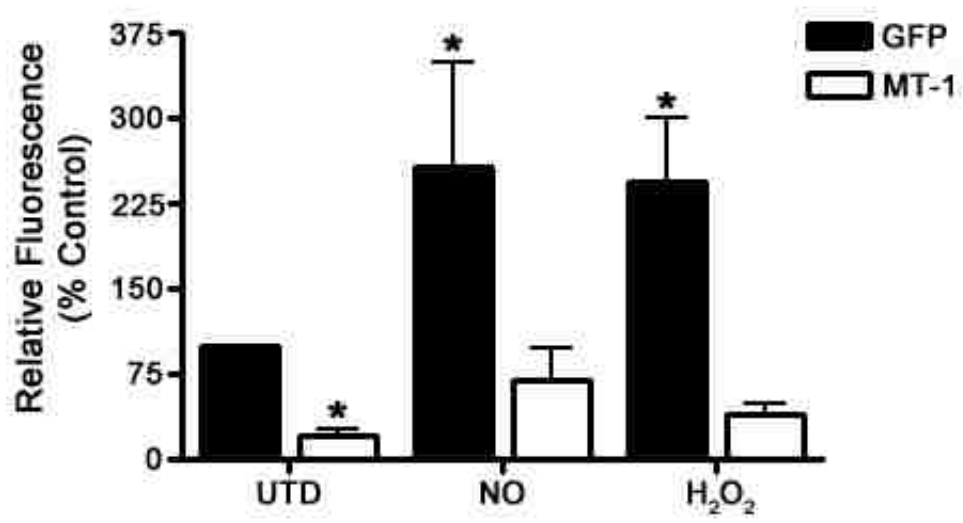


Wilham et al Fig. 10

A



B



Wilham et al Fig. 11 A & B

INHIBITION OF ENDOTHELIAL NITRIC OXIDE SYNTHASE BY
SUPEROXIDE INVOLVES ENZYME FRAGMENTATION

Jason Wilham¹

Dean Wiseman²

Lisa A. Brennan³

Stephen Wedgwood³

Stephen M. Black²

¹Department of Biomedical & Pharmaceutical Sciences,

The University of Montana, Missoula MT 59812,

²Vascular Biology Center, Medical College of Georgia, Augusta, GA 30912,

and

³Pediatrics, Northwestern University Medical School, Chicago, Illinois 60611-3008

ABSTRACT

A change in endothelial function is thought to play an important role in the development of pulmonary hypertension. We have previously demonstrated, in ovine models of pulmonary endothelial dysfunction, that there are changes in the synthesis and the activity of nitric oxide (NO). Hypertensive vasoconstriction is postulated to involve the degradation of NO by reactive oxygen species (ROS), especially the superoxide anion. The release of superoxide may be increased in the dysfunctional vascular endothelium. Antioxidant therapy has been proposed as a treatment regimen for pulmonary hypertension and other pathologies linked to endothelial dysfunction. Since the critical mediator of pulmonary vasorelaxation is generation of NO by the endothelial NOS (eNOS) protein we undertook a series of studies to determine the effects of pro-and anti-oxidants on eNOS function in ovine pulmonary arterial endothelial cells (PAECs). In initial studies we evaluated the effect of elevating superoxide levels in ovine PAECs by treating cells with the CuZnSOD inhibitor, diethyldithiocarbamate (DETC). Superoxide levels in cells were quantitated using fluorescent microscopy and the superoxide sensitive dye, dihydroethidium. After 4h of exposure, superoxide levels were elevated by 2.1-fold compared to untreated cells ($P < 0.05$). When eNOS activity was determined in DETC-treated cells, a 38% reduction in activity was detected compared to untreated cells ($P < 0.05$). Western Blot analysis revealed that eNOS protein levels were also decreased by 34.7% ($P < 0.05$). To investigate the mechanism for this decrease recombinant eNOS protein was exposed to a xanthine/xanthine oxidase superoxide generating system. Analysis of the eNOS protein indicated that superoxide induced fragmentation of the eNOS protein. Thus, we suggest that the activity of the eNOS

enzyme is sensitive to the cellular redox environment and that the increases in superoxide production thought to be associated with endothelial cell dysfunction result in the inhibition of the eNOS enzyme by inducing enzyme fragmentation.

INTRODUCTION

Published evidence suggests that normal pulmonary vascular reactivity and vascular smooth muscle cell proliferation is regulated by a complex interaction of vasoactive substances produced by the endothelium [1-3]. The development of hypertensive states in both the pulmonary and systemic circulatory systems is associated with increased vascular reactivity and the disruption of these regulatory mechanisms [4-9]. In most animal models of hypertension, there is impaired endothelium-dependent vaso-relaxation to agonists such as acetylcholine [10, 11], however, endothelial dysfunction has different characteristics depending on the model utilized [10]. Endothelial dysfunction may be defined as an imbalance between the synthesis, release or effect of endothelial factors capable of relaxing vascular smooth muscle or vasoconstrictor substances that can counteract these effects. This imbalance manifests itself as a reduction in endothelium-dependent vasodilatory response, or as an increased vasoconstrictor response [12]. Other functions of the endothelium may also be affected, such as the adhesion of platelets and leukocytes with the vascular wall and increased growth and migration of smooth muscle cells [12].

Nitric Oxide (NO) is an endothelium-derived relaxing factor synthesized by the oxidation of the guanidino nitrogen moiety of L-arginine following activation of nitric oxide synthase (NOS) [13]. After certain stimuli, such as shear stress and the receptor binding of specific vasodilators (endothelium-dependent vasodilators), NO is synthesized and released from the endothelial cell by the activation of endothelial NOS (eNOS) [14, 15]. Once released from endothelial cells, NO diffuses into vascular smooth muscle cells and activates soluble guanylate cyclase (sGC), a heterodimer with α_1 and β_1 subunits

which catalyzes production of guanosine-3',5'-cyclic monophosphate (cGMP) from guanosine-5'-triphosphate. cGMP induces vascular smooth muscle relaxation through activation of a cGMP-dependent protein kinase [16]. Endothelium-derived NO (and the resulting cGMP) is an important mediator of vascular tone and an inhibitor of platelet aggregation and smooth muscle mitogenesis [10, 17].

During the last several years it has become clear that oxidative inactivation of NO is likely to be important in the development of several pathologic conditions including atherosclerosis, hypercholesterolemia, hypertension, and diabetes [12]. Studies have shown that in the blood vessel, the balance existing between the steady state levels of NO and the superoxide anion appears to be disrupted resulting in a decrease in the bioavailability of NO [10, 12]. For example, large amounts of nitrogen oxides are released from vessels in an oxidatively degraded state in cholesterol-fed rabbits [18]. Treatment these rabbits with PEG-superoxide dismutase (SOD) dramatically increased endothelium-dependent vascular relaxation, suggesting a role for superoxide in oxidative inactivation of NO [19]. There is evidence that reactive oxygen species also diminish NO bioactivity in humans. For example, infusion of ascorbic acid improves vascular responses to acetylcholine in cigarette smokers [20]. In the endothelium, cyclooxygenase [21], xanthine oxidase [22], and NADPH oxidase [23] have been identified as significant producers of superoxide. More recent studies have indicated that NOS itself may also be a significant producer of superoxide during the development of nitrate tolerance [8]. Interestingly, the use of protein kinase C inhibitors was shown to decrease the production of superoxide in the tolerant vessels, suggesting that phosphorylation of eNOS by PKC may play a role in eNOS superoxide production [8]. NOS also produces superoxide

when the bioavailability of tetrahydrobiopterin or L-arginine are low [24]. Both superoxide and NO are free radicals (i.e., they contain an unpaired electron in their outer orbital). When exposed to each other, they undergo a facile radical-radical reaction that proceeds at a rate recently estimated to be $7 \times 10^9 \text{ mol}^{-1}\cdot\text{L}\cdot\text{s}^{-1}$ [25, 26]. This is approximately three times faster than the reaction rate for superoxide with either the Mn- or CuZn SOD. Thus, in a compartment in which both NO and SOD exist, there may be a propensity for superoxide to preferentially react with NO rather than SOD, depending on the relative concentrations of NO and SOD present.

It is unclear whether ROS can directly inhibit the eNOS enzyme or whether they exert their effects indirectly by scavenging the NO produced by the eNOS protein. Thus, the present study was undertaken to determine whether modulations in the cellular redox state in ovine PAECs would alter either the expression or activity of eNOS. The results obtained indicated that increasing superoxide levels (a pro-oxidant environment) decreased eNOS activity and protein levels.

MATERIALS AND METHODS

Cell Culture

Primary cultures of ovine pulmonary arterial endothelial cells (PAECs) were isolated as detailed previously [27]. Endothelial cell identity was confirmed by their typical cobblestone appearance, contact inhibition, specific uptake of 1,1'-dioctadecyl-1,3,3',3'-tetramethylindocarbocyanine perchlorate-labeled acetylated low-density lipoprotein (Molecular Probes, Eugene, OR), and positive staining for von Willebrand factor (Dako, Carpinteria, CA). PAECs were grown in Eagle DMEM containing 1g/l glucose and phenol red (MediaTech, Herndon, VA), supplemented with 10% fetal bovine serum (Hyclone, Logan, UT), antibiotic-antimycotic (MediaTech), basic fibroblast growth factor (bFGF 10ng/mL) (Sigma-Aldrich, St. Louis, MO). Cells were incubated in 21% O₂ and 5% CO₂ at 37°C. Cells were used at passage less than 10.

Analysis of Cellular Superoxide Generation

To determine the effect of DETC on cellular superoxide levels in PAECs, ovine PAECs were grown overnight in serum free DME-H16 with 1g/L glucose. Cultured PAECs were treated for 4h with DETC (1mM) or a vehicle control. PAECs were then loaded with the superoxide sensitive dye dihydroethidium (10μM) (Sigma-Aldrich, St. Louis, MO), for a further 15min, washed with PBS, and imaged live using a Nikon TE300 inverted fluorescent microscope. Dihydroethidium-stained cells were observed using excitation at 518nm and emission at 605nm. Fluorescent images were captured using a Nikon Cool-Snap digital camera and quantified using Metamorph software (Fryer) under identical imaging conditions. Statistical analyses between treatment groups

were carried out as detailed below. Specificity of dihydroethidium to detect superoxide was demonstrated by pre-incubating cells with PEG-SOD (50units) prior to the addition of DETC. Six separate experiments were performed and combined for the data in this experiment.

Assay for NOS Activity

NOS activity was determined by two methods: the Busch assay and NO_x probe (Apollo 4000 Free Radical Analyzer, World Precision Instruments, Inc.). Cultured PAECs were treated for 4h with DETC (1mM) or a vehicle control and then, NOS activity was measured. The first method, the Busch assay, measures the formation of ³H-citrulline from ³H-arginine as we have previously described [28-30]. Briefly, subcellular fractions (100μg) were incubated at 37°C for 45min in the presence of 1 mM NADPH, 14μM tetrahydrobiopterin, 5μM FAD, 1mM MgCl₂, 10μM unlabeled L-arginine, 0.1μCi [³H]-L-arginine, and in the presence or absence of other cofactors (calmodulin and calcium). The reaction was stopped by the addition of 4°C stop buffer (20 mM sodium acetate, pH 5, 1 mM L-citrulline, 2 mM EDTA, and 0.2 mM EGTA). Samples were applied to columns containing 1 ml of Dowex AG50W-X8 resin, Na⁺ form, pre-equilibrated with 1N NaOH. [³H]-citrulline was then quantitated by scintillation counting.

The second method measured NO_x production in the media with a NO_x specific probe. Briefly following treatment, media was collected and NO_x levels were measured. Potassium Nitrate solutions, made in media, were used to make a standard curve for determining NO_x levels.

Protein Extraction

Cultured PAECs were treated for 4h with DETC (1mM) or a vehicle control. Following treatment, cells were rinsed with DPBS (MediaTech) and RIPA lysis buffer added to each well. Cell were then collected and sheared with a 25-gauge needle 3X. Lastly, samples were spun at 14,000Xg for 10min and the supernatant was collected. Protein concentrations were analyzed using Bio-Rad protein assay (Bio-Rad, Hercules, CA) and Bovine Serum Albumin (BSA) for the protein standard curve.

Western Blotting

Western Blot analysis was performed as previously described [31]. Total protein extracts (~20µg) were resuspended in 5X Laemmli protein sample buffer and boiled for 5min. Total protein was then separated on a 4-20% Tris-SDS-HEPES polyacrylamide gel (Gradiopore, Frenchs Forest, Australia) and electrophoretically wet-transferred to a Hybond-PVDF membrane (Amersham, Arlington Hts., IL). The membranes were blocked with 5% nonfat dry milk in Tris buffered saline containing 0.1% Tween-20 (TBST) overnight at 4⁰C. After blocking, the membranes were incubated at room temperature for 2 hrs with the primary antibody (1:1,000 for α-eNOS, BD Biosciences), washed 3X with TBST, and incubated with a mouse anti-rabbit IgG-horseradish peroxidase conjugated secondary antibody (Pierce, Rockford, IL) for 1 hr. After washing, immunolabeled protein bands were visualized using chemiluminescence (SuperSignal West Fempto Substrate Kit, Pierce) on a Kodak Image Station 440CF with Kodak 1D Molecular Imaging Software and normalized to immunolabeled β-actin (1:1000, Sigma) on the same blot. To assure equal protein loading, duplicate

polyacrylamide gels were run, one normal and one stained with Coomassie blue. Four separate experiments were performed and combined for the data in this experiment.

Expression and Purification of eNOS

The poly-His-pCWeNOS vector ([source](#)) was transformed into the *E.coli* strain BL21 (DE3) plysS ([source](#)) for expression of recombinant human eNOS. LB cultures of poly-His-pCWeNOS, containing 100µg/ml of ampicillin, were grown until an OD₆₀₀ of 0.8 was reached. These cultures were then used to inoculate 6 liters of LB (pre-chilled to <15°C) split into four 2.8-litre Fernbach flasks. Induction of the bacterial promoter, [???](#), was then carried out by the addition of IPTG to a final concentration of 2mM. Cultures were then incubated at 18°C for 18h with a rotation rate of 220rpm prior to harvest by centrifugation.

Purification of recombinant human eNOS was carried out using Calmodulin-Sepharose as we previously described for preparation of recombinant neuronal NOS [32]. The only significant difference was that here, DTT was added to all purification buffers mentioned above at a concentration of 10µM.

To expose purified human recombinant eNOS (2µg) to superoxide, purified eNOS fractions (2µg) were exposed to both xanthine (0.5mM) (Sigma-Aldrich, St. Louis, MO) and xanthine oxidase (0.5 units) (Sigma-Aldrich, St. Louis, MO) for 20 min. Protein was then subjected to SDS-PAGE and stained with Coomassie blue. As a negative control, purified eNOS was also exposed to the NO donor, Spermine NONOate (50µM) (Cayman Chemical, Ann Arbor, MI) for 20min. The control groups were exposed to a vehicle

control for 20min. Four separate experiments were performed and combined for the data in this experiment.

Statistical Analysis

Values are expressed as the means \pm standard deviation from at least three experiments. Statistical analysis between experimental groups was performed unpaired T-test using the GB-STAT statistical analysis software program. A $p < 0.05$ was considered statistically significant.

RESULTS

Initially, experiments tested whether treating ovine PAECs with DETC could increase cellular superoxide levels. DETC-mediated increases in superoxide production by ovine PAECs were measured using dihydroethidium, a superoxide-sensitive fluorescent dye, and fluorescent microscopy (Figure 1). Results obtained demonstrated that exposure of ovine PAECs to DETC (1mM) for 4hrs resulted in a 105-fold increase in superoxide production (Figure 1 B, $p < 0.05$ vs Untreated), which was blocked in cells pre-incubated with PEG-SOD, an external SOD source (Figure 1, $p < 0.05$ vs DETC + PEG-SOD).

The next set of experiments determined whether the DETC-mediated increase in superoxide levels altered the activity of the eNOS enzyme in ovine PAECs. Exposure of PAECs to DETC *invitro* resulted in a 38% reduction in ^3H -arg to ^3H -citrulline conversion (Figure 2, $p < 0.05$ vs untreated control cells). We then examined eNOS protein levels in DETC treated and untreated PAECs using quantitative Western Blot analysis. The results obtained indicated that ENOS protein levels were also reduced, by 34.7% (Figure 3, $p < 0.05$ vs untreated cells).

The PAEC culture data suggested that superoxide inactivated eNOS, but we were uncertain whether an immediate component was involved. To determine whether superoxide directly inactivated eNOS, we exposed purified recombinant human ENOS to xanthine/xanthine oxidase (X/XO) superoxide generating system, or to the NO donor spermine NONOate. The results obtained (Figure 4) indicated that in the presence of X/XO the expected 135kD eNOS band was not observed. Rather two smaller fragments were now observed (marked as * in Figure 4). This effect was seen to be specific to

superoxide as this fragmentation was not observed when eNOS was exposed to the NO donor, spermineNONOate (Figure 4). Thus, the mechanism of ENOS inhibition induced by high levels of superoxide appears to be via an induction of ENOS fragmentation.

DISCUSSION

Controversy continues to exist over the possible alteration of NO synthesis in both pulmonary and systemic hypertensive patients and in animal models of these disease states. However, the development of hypertension is fundamentally linked with the reduction in NO signaling. As a consequence of the mechanical deformation of endothelial cells, there may be an increase in the production of free radicals such as the superoxide anion in hypertensive patients [33-35]. Normally, the concentration of superoxide remains low in physiological situations because the superoxide dismutase (SOD) enzyme reacts with it. However, increased superoxide production is possible from several sources within the endothelium, including cyclooxygenase [36], xanthine oxidase [22], NADPH oxidase [23], or even NOS, under specific conditions [8]. Whatever their source, the superoxide radical determines the viability of NO, as it can oxidize and de-activate NO thereby forming peroxynitrite (ONOO⁻) [25, 26]. Peroxynitrite is a strong oxidizing agent and can react with biological molecules, including protein and non-protein sulfhydryls, DNA, and membrane phospholipids [37]. Peroxynitrite is capable of nitrating free or protein-associated tyrosines and other phenolics [38]. Thus, a decrease in bio-available NO by its reaction with other free radicals could trigger the development of hypertensive states. In fact, in an ovine model of pulmonary hypertension we have found that pretreatment of vessels with membrane-permeable SOD or catalase enhanced calcium-ionophore-induced relaxations in pulmonary arteries from hypertensive but not control lambs [39]. These data indicate that superoxide and/or peroxynitrite formation may be involved in the impaired endothelium-dependent relaxations displayed in the hypertensive lambs. This model for PPHN

remained unclear, however, as to whether the mechanism of action of increased ROS generation, specifically superoxide, is due to its ability to react with NO or whether it can also directly inhibit eNOS activity. The latter would represent another mechanism to limit NO release. The results here showed that by directly exposing ovine PAECs to the CuZn SOD inhibitor, DETC, increased cellular oxidant stress in these cells by increasing superoxide levels. With DETC exposure, we found a significant decrease in the ability of eNOS to metabolize L-arginine within 4 hours of treatment. These results show that not only can superoxide react with NO to form peroxynitrite, thereby limit NO bioavailability; but also can also decrease eNOS activity.

However, the precise mode or mechanism of this inhibition was not clear. Our results showed that eNOS protein levels were reduced in the presence of DETC. Since the half-life of the eNOS protein is thought to be >24h, this suggested that perhaps superoxide has a direct effect on the protein itself. Exposing purified eNOS protein to superoxide produced a degradation of the eNOS protein into 2 fragments (approximate masses 70 and 60kD respectively), revealing that the mechanism for superoxide inhibition on eNOS occurs by enzyme fragmentation. It is still unclear whether superoxide levels can attain those needed to induce enzyme fragmentation *in vivo* since the short half-life, and high reactivity of superoxide would tend to limit the likelihood of eNOS and superoxide interacting. However, it is noteworthy that progressive endothelial dysfunction associated with advanced hypertension can be associated with increased free radical levels and lowered NO production and/or eNOS levels [40-43]. Superoxide induced degradation of eNOS demonstrated here could potentially be involved. It is also possible that because eNOS is a multi-enzyme complex with both oxidative and reductive

domains the superoxide anion may also interfere with electron transfer at the different active sites of the protein during the oxidation/reduction phase resulting in reduced enzymatic catalysis. Further studies will be needed to characterize the inhibitory mechanisms of superoxide on eNOS.

In conclusion, our results indicate that the NO-NOS system represents a complex bioregulated pathway whose regulation is tightly associated with the redox status of the cell. The high oxidant potential of NO suggests that its generation in a biological system must be tightly regulated. As demonstrated in our studies increasing superoxide levels within the cell (analogous to producing a more oxidized environment) resulted in a significant reduction in the catalytic capability of eNOS. Thus, the increases in ROS that may be involved in the development of endothelial dysfunction associated with a number of vascular diseases may cause a reduction in eNOS activity, possibly by inducing eNOS fragmentation, as well as increasing the destruction of NO by formation of other radicals.

ACKNOWLEDGMENTS

This research was supported in part by grants XXX from the American Heart Association Pacific Mountain Affiliates (to JW), HL60190 (to SMB), HL67841 (to SMB), HL072123 (to SMB), and HL070061 (to SMB) from the National Institutes of Health, and 0330292N from the American Heart Association National Office (to SW).

REFERENCES

1. Fineman, J.R., S.J. Soifer, and M.A. Heymann, *Regulation of pulmonary vascular tone in the perinatal period*. *Annu Rev Physiol*, 1995. **57**: p. 115-34.
2. Furgott, R.F., Vanhoutte, P.M., *Endothelium-derived relaxing and contracting factors*. *FASEB J.*, 1989(3): p. 2007-2018.
3. Wiklund, N.P., et al., *Modulatory role of endogenous nitric oxide in pulmonary circulation in vivo*. *Eur J Pharmacol*, 1990. **185**(1): p. 123-4.
4. Abman, S.H., P.F. Shanley, and F.J. Accurso, *Failure of postnatal adaptation of the pulmonary circulation after chronic intrauterine pulmonary hypertension in fetal lambs*. *J Clin Invest*, 1989. **83**(6): p. 1849-58.
5. Black, S.M., et al., *Increased endothelial NOS in lambs with increased pulmonary blood flow and pulmonary hypertension*. *Am J Physiol*, 1998. **275**(5 Pt 2): p. H1643-51.
6. Giaid, A. and D. Saleh, *Reduced expression of endothelial nitric oxide synthase in the lungs of patients with pulmonary hypertension*. *N Engl J Med*, 1995. **333**(4): p. 214-21.
7. Morin, F.C., 3rd, *Ligating the ductus arteriosus before birth causes persistent pulmonary hypertension in the newborn lamb*. *Pediatr Res*, 1989. **25**(3): p. 245-50.
8. Munzel, T., et al., *Effects of long-term nitroglycerin treatment on endothelial nitric oxide synthase (NOS III) gene expression, NOS III-mediated superoxide production, and vascular NO bioavailability*. *Circ Res*, 2000. **86**(1): p. E7-E12.
9. Ross, R., *The pathogenesis of atherosclerosis: a perspective for the 1990s*. *Nature*, 1993. **362**(6423): p. 801-9.
10. Boulanger, C.M., *Secondary endothelial dysfunction: hypertension and heart failure*. *J Mol Cell Cardiol*, 1999. **31**(1): p. 39-49.
11. Reddy, V.M., et al., *Altered endothelium-dependent responses in lambs with pulmonary hypertension and increased pulmonary blood flow*. *Am J Physiol*, 1996. **271**(2 Pt 2): p. H562-70.
12. Cai, H. and D.G. Harrison, *Endothelial dysfunction in cardiovascular diseases: the role of oxidant stress*. *Circ Res*, 2000. **87**(10): p. 840-4.
13. Moncada, S. and A. Higgs, *The L-arginine-nitric oxide pathway*. *N Engl J Med*, 1993. **329**(27): p. 2002-12.
14. Ignarro, L.J., et al., *Activation of purified soluble guanylate cyclase by endothelium-derived relaxing factor from intrapulmonary artery and vein: stimulation by acetylcholine, bradykinin and arachidonic acid*. *J Pharmacol Exp Ther*, 1986. **237**(3): p. 893-900.
15. Rubanyi, G.M., J.C. Romero, and P.M. Vanhoutte, *Flow-induced release of endothelium-derived relaxing factor*. *Am J Physiol*, 1986. **250**(6 Pt 2): p. H1145-9.
16. Ignarro, L.J., G. Ross, and J. Tillisch, *Pharmacology of endothelium-derived nitric oxide and nitrovasodilators*. *West J Med*, 1991. **154**(1): p. 51-62.
17. Sarkar, R. and R.C. Webb, *Does nitric oxide regulate smooth muscle cell proliferation? A critical appraisal*. *J Vasc Res*, 1998. **35**(3): p. 135-42.

18. Minor, R.L., Jr., et al., *Diet-induced atherosclerosis increases the release of nitrogen oxides from rabbit aorta*. J Clin Invest, 1990. **86**(6): p. 2109-16.
19. Mugge, A., et al., *Chronic treatment with polyethylene-glycolated superoxide dismutase partially restores endothelium-dependent vascular relaxations in cholesterol-fed rabbits*. Circ Res, 1991. **69**(5): p. 1293-300.
20. Heitzer, T., et al., *Tetrahydrobiopterin improves endothelium-dependent vasodilation in chronic smokers: evidence for a dysfunctional nitric oxide synthase*. Circ Res, 2000. **86**(2): p. E36-41.
21. Holland, J.A., et al., *Low-density lipoprotein stimulated peroxide production and endocytosis in cultured human endothelial cells: mechanisms of action*. Endothelium, 1997. **5**(3): p. 191-207.
22. Ratych, R.E., R.S. Chuknyiska, and G.B. Bulkley, *The primary localization of free radical generation after anoxia/reoxygenation in isolated endothelial cells*. Surgery, 1987. **102**(2): p. 122-31.
23. Griendling, K.K., D. Sorescu, and M. Ushio-Fukai, *NAD(P)H oxidase: role in cardiovascular biology and disease*. Circ Res, 2000. **86**(5): p. 494-501.
24. Vasquez-Vivar, J., et al., *Effect of redox-active drugs on superoxide generation from nitric oxide synthases: biological and toxicological implications*. Free Radic Res, 1999. **31**(6): p. 607-17.
25. Muijsers, R.B., et al., *Peroxynitrite: a two-faced metabolite of nitric oxide*. Life Sci, 1997. **60**(21): p. 1833-45.
26. Murphy, M.P., et al., *Peroxynitrite: a biologically significant oxidant*. Gen Pharmacol, 1998. **31**(2): p. 179-86.
27. Black, S.M., et al., *Ventilation and oxygenation induce endothelial nitric oxide synthase gene expression in the lungs of fetal lambs*. J Clin Invest, 1997. **100**(6): p. 1448-58.
28. Sheehy, A.M., M.A. Burson, and S.M. Black, *Nitric oxide exposure inhibits endothelial NOS activity but not gene expression: A role for superoxide*. Am. J. Physiol., 1998. **274**: p. L833-L841.
29. Black, S.M., et al., *Increased endothelial NOS in lambs with increased pulmonary blood flow and pulmonary hypertension*. Am J Physiol, 1998(275): p. H1643-H1651.
30. Black, S.M., et al., *Inhaled nitric oxide inhibits NOS activity in lambs: a potential mechanism for rebound pulmonary hypertension*. Am. J. Physiol., 1999. **277**: p. H1849-H1856.
31. Black, S.M., et al., *Ventilation and oxygenation induce endothelial nitric oxide synthase gene expression in the lungs of fetal lambs*. J. Clin. Invest, 1997. **100**: p. 1448-1458.
32. Black, S.M. and P.R. Ortiz de Montellano, *Characterization of rat neuronal nitric oxide synthase expressed in Saccharomyces cerevisiae*. DNA Cell Biol, 1995. **14**(9): p. 789-94.
33. Mattei, P., et al., *Endothelial function in hypertension*. J Nephrol, 1997. **10**(4): p. 192-7.
34. Nakazono, K., et al., *Does superoxide underlie the pathogenesis of hypertension?* Proc Natl Acad Sci U S A, 1991. **88**(22): p. 10045-8.

35. Panza, J.A., *Endothelial dysfunction in essential hypertension*. Clin Cardiol, 1997. **20**(11 Suppl 2): p. II-26-33.
36. Holland, J.A., et al., *Bradykinin induces superoxide anion release from human endothelial cells*. J Cell Physiol, 1990. **143**(1): p. 21-5.
37. Kooy, N.W. and J.A. Royall, *Agonist-induced peroxynitrite production from endothelial cells*. Arch Biochem Biophys, 1994. **310**(2): p. 352-9.
38. Ischiropoulos, H., et al., *Peroxyntirite-mediated tyrosine nitration catalyzed by superoxide dismutase*. Arch Biochem Biophys, 1992. **298**(2): p. 431-7.
39. Steinhorn, R.H., et al., *Altered endothelium-dependent relaxations in lambs with high pulmonary blood flow and pulmonary hypertension*. Am J Physiol Heart Circ Physiol, 2001. **280**(1): p. H311-7.
40. Huang, A., et al., *Superoxide released to high intra-arteriolar pressure reduces nitric oxide-mediated shear stress- and agonist-induced dilations*. Circ Res, 1998. **83**(9): p. 960-5.
41. Laursen, J.B., et al., *Role of superoxide in angiotensin II-induced but not catecholamine-induced hypertension*. Circulation, 1997. **95**(3): p. 588-93.
42. Rajagopalan, S., et al., *Angiotensin II-mediated hypertension in the rat increases vascular superoxide production via membrane NADH/NADPH oxidase activation. Contribution to alterations of vasomotor tone*. J Clin Invest, 1996. **97**(8): p. 1916-23.
43. Saugstad, O.D., *Mechanisms of tissue injury by oxygen radicals: implications for neonatal disease*. Acta Paediatr, 1996. **85**(1): p. 1-4.

FIGURE LEGENDS

Figure 1. *In situ* detection of superoxide in ovine pulmonary arterial endothelial cells.

Panel A. Representative fluorescent images of dihydroethidium (DHE)-treated ovine PAECs in response to the CuZnSOD inhibitor DETC (1mM). Conversion of DHE by superoxide to ethidium results in red nuclear fluorescence. Under identical imaging conditions more fluorescent cells were observed in the presence of DETC. Pre-incubation with PEG-SOD (50 units) reduced the ethidium signal, and indicates its specificity for superoxide.

Panel B. The fluorescent intensity of each image was quantified using Metamorph Imaging software and represented graphically. N=6. Values are mean \pm SD. * $p < 0.05$ vs Untreated, † $p < 0.05$ vs DETC + PEG-SOD.

Figure 2. Increased superoxide production inhibits eNOS activity in ovine pulmonary arterial endothelial cells. Ovine PAECs were treated for 4h with DETC (1mM) to inhibit CuZn SOD activity. Cell extracts were then prepared and the NOS activity was determined using ^3H -arginine to ^3H -citrulline conversion. Activities are presented as a percentage of untreated (no DETC exposure) cells. The data represents the mean \pm s.d of 4 separate experiments. * $p < 0.05$ vs untreated.

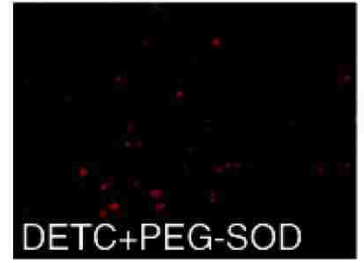
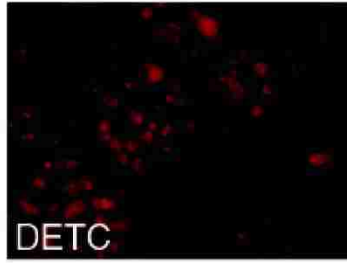
Figure 3. Increased superoxide production decreases eNOS protein levels in ovine pulmonary arterial endothelial cells.

Panel A. Protein extracts (25µg) from ovine PAECs, exposed or not to DETC (1mM) for 4h, were separated on a 7.5% SDS-polyacrylamide gel, electrophoretically transferred to Hybond membranes, and analyzed using a specific antiserum raised against eNOS. Untreated controls received vehicle only. A representative Western blot is shown.

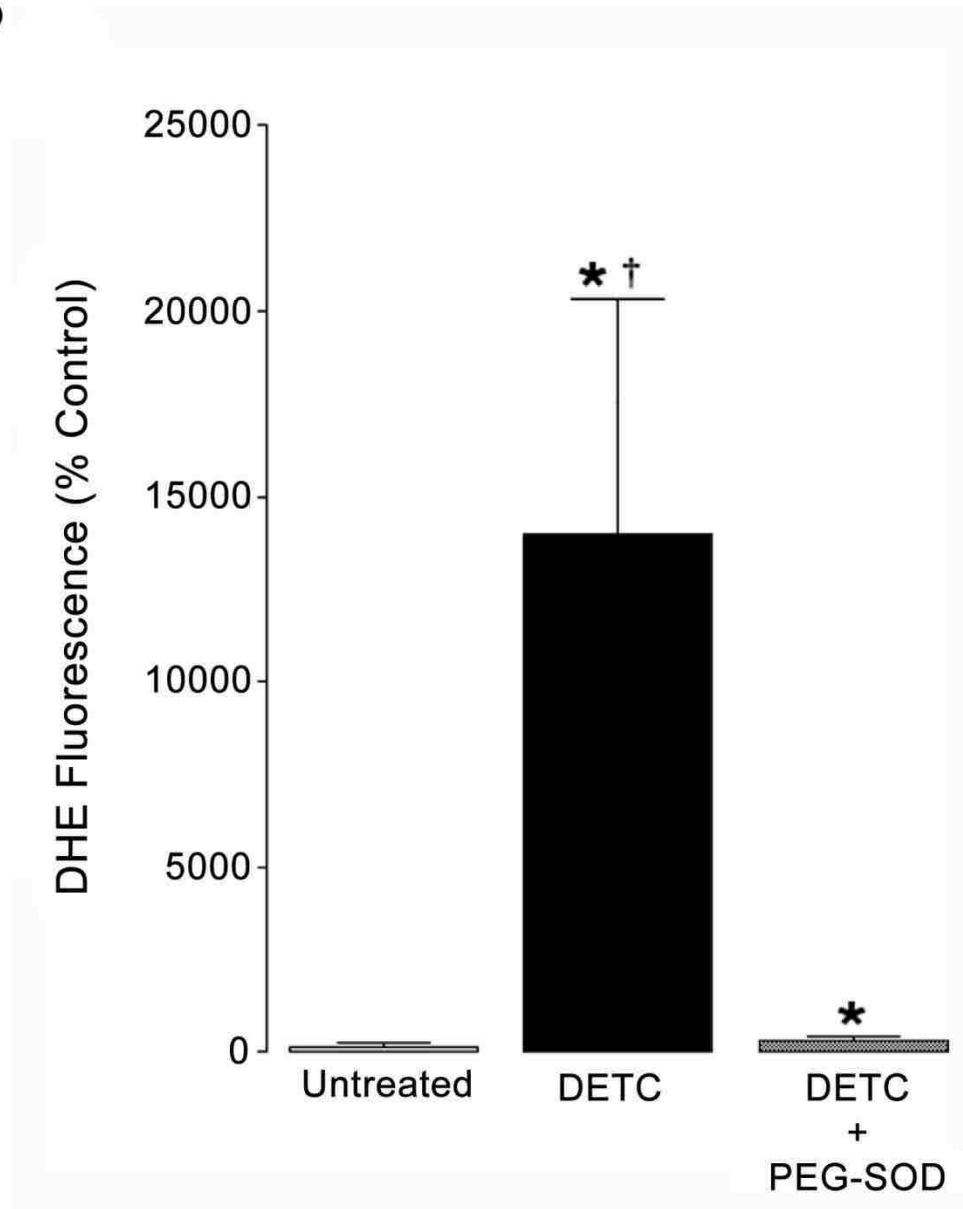
Panel B. The densitometric values for eNOS protein from ovine PAECs exposed or not to DETC (1mM) for 4h. eNOS Protein is decreased by 34.7% by DETC exposure. Values are mean ± standard deviation from 4 experiments. * $p < 0.05$ vs untreated.

Figure 4. Superoxide induces the degradation of eNOS. Purified human recombinant eNOS (2µg) was exposed for 20min to either: vehicle control, the superoxide (SO) generating system xanthine (0.5mM) and xanthine oxidase (0.5 units), or spermine NONOate (NO 50µM). In the presence of X/XO superoxide the eNOS protein is degraded into two fragments (marked by *). The gel is representative of 3 separate experiments.

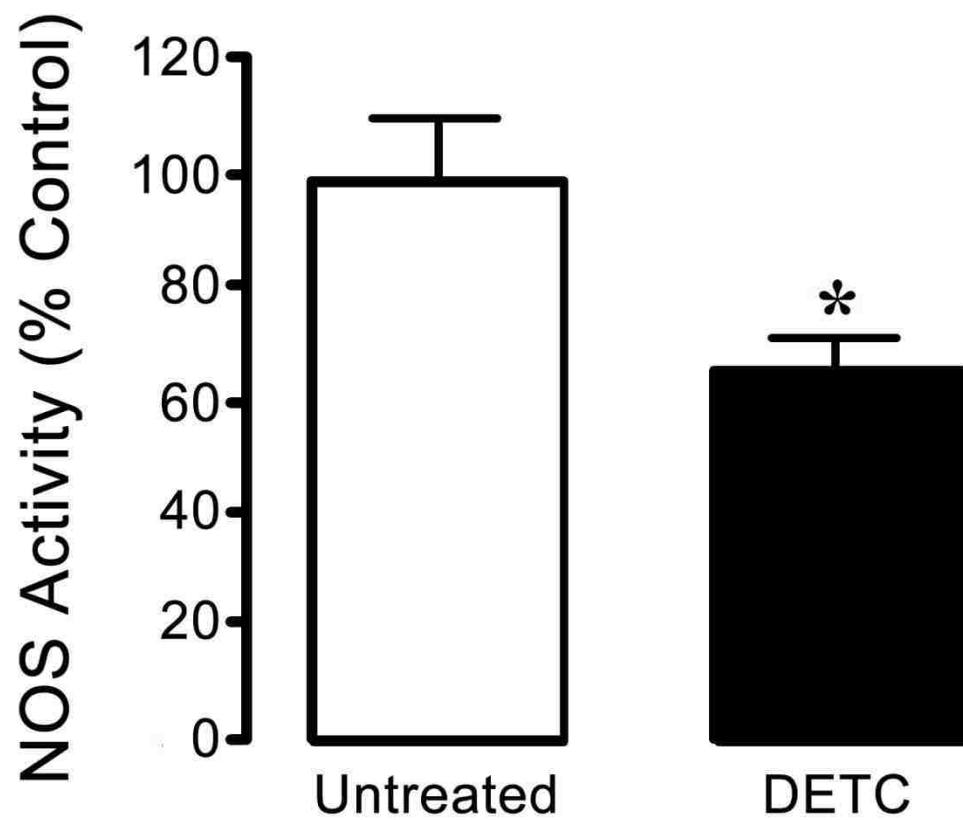
A



B



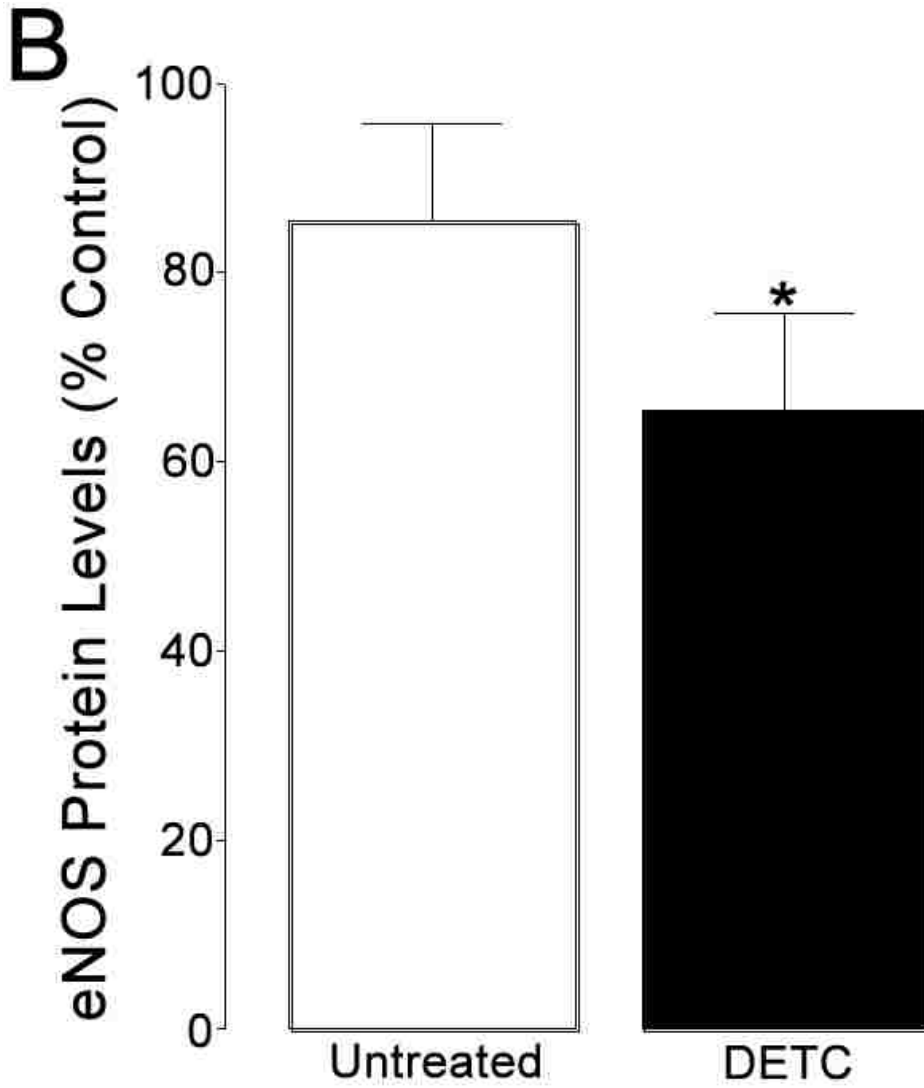
Wilham et al Fig. 1 A & B



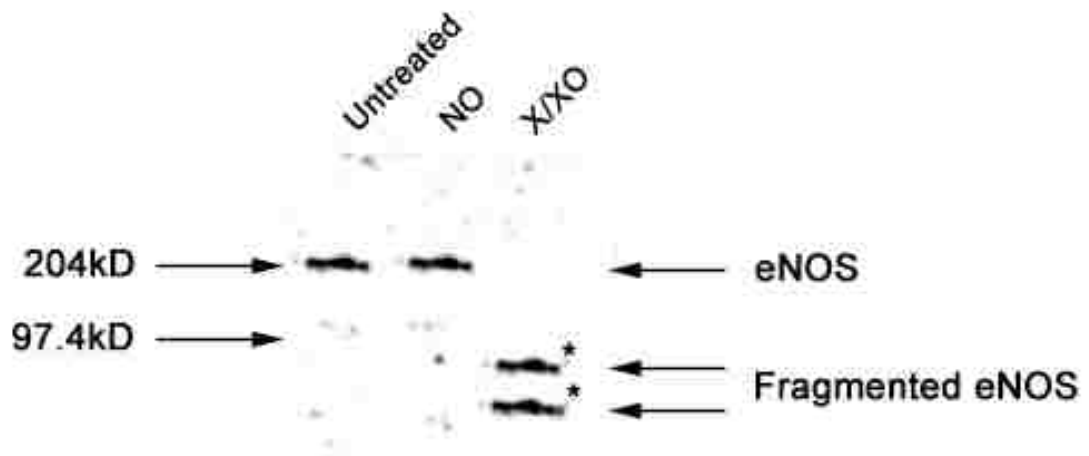
Wilham et al Fig. 2

A





Wilham et al Fig. 3 A & B



Wilham et al Fig. 4

ACTIVITY AND EXPRESSION OF ENOS IN ENDOTHELIAL CELLS IS
DEPENDENT ON THE ANTIOXIDANT ROLE OF TETRAHYDROBIOPTERIN

Jason Wilham¹

Dean Wiseman¹

Lisa A. Brennan²

Stephen Wedgwood²

Stephen M. Black¹

Department of ¹Biomedical & Pharmaceutical Sciences, The University of Montana,
Missoula MT 59812, and ²Pediatrics, Northwestern University Medical School, Chicago,
Illinois 60611-3008

Short Title: Antioxidant Role of BH₄ in eNOS Regulation

ABSTRACT

Newborns that do not survive persistent pulmonary hypertension of the newborn (PPHN) exhibit both an increase in the thickness of the smooth muscle cell (SMC) layer within pulmonary arterioles and an extension of this muscle to non-muscular arterioles. Oxidant production, associated with increased SMC growth, plays an important role both in the normal function of the vascular system as well as the pathogenesis of vascular disease. The production of nitric oxide (NO) in the vessel wall by the enzyme endothelial nitric oxide synthase (eNOS) is dependent on essential cofactors, including the most potent naturally occurring reducing agent, tetrahydrobiopterin (BH₄). Although BH₄ is thought to maintain the eNOS dimer, the exact mechanism of this maintenance is unknown. Utilizing NIH3T3 cells, a line with very low BH₄ levels, and bovine aortic endothelial cells (BAECs) our study set out to test the hypothesis that BH₄'s role in the regulation of eNOS is due to its high antioxidant potential. Our results in NIH3T3 cells demonstrate that catalase transduction decreases ROS levels, specifically H₂O₂, and increases eNOS total protein, dimer/monomer protein ratio and eNOS activity. In BAECs, the addition of BH₄ or L-sepiapterin, the substrate for the synthesis of BH₄, decreased ROS levels and increased eNOS dimer levels and activity. The addition of BH₄ to NIH3T3 cells also decreased ROS production. These results suggest that the association of BH₄ with eNOS may regulate eNOS protein levels and activity due to its high antioxidant potential.

INTRODUCTION

In persistent pulmonary hypertension of the newborn (PPHN), childbirth does not result in the normal decrease in pulmonary vascular resistance and coincident increase in pulmonary blood flow. PPHN affects 5 in 1000 births of term or near term infants each year. Newborns that die of PPHN exhibit both an increase in the thickness of the smooth muscle cell layer within pulmonary arterioles and an extension of this muscle to non-muscular arterioles [1]. The proliferation of smooth muscle cells has been strongly linked to the generation of reactive oxygen species (ROS), such as superoxide ($O_2^{\cdot-}$) and hydrogen peroxide (H_2O_2) [2-4].

Every cell type in the vascular wall, including fibroblasts [5], endothelial cells [6, 7], and smooth muscle cells [8], has been shown to produce and be regulated by ROS. This oxidant production plays an important role both in the normal function of the vascular system, as well as the pathogenesis of vascular disease.

The endothelium plays a major role in the modulation of vascular homeostasis. One key molecule produced by the endothelium is nitric oxide (NO), produced by the enzyme endothelial nitric oxide synthase (eNOS). eNOS catalyzes the oxidation reaction of L-arginine and molecular oxygen to L-citrulline and NO [9]. The production of NO in the vessel wall is dependent on essential cofactors, including the most potent naturally occurring reducing agent tetrahydrobiopterin (BH_4).

Biopterin metabolism is thought to be critical in the regulation of NOS activity. In the absence of sufficient levels of BH_4 , previous *in vitro* studies have found that eNOS becomes uncoupled, resulting in decreased NO production and increased superoxide ($O_2^{\cdot-}$) and hydrogen peroxide (H_2O_2) production [10, 11].

In a recent study by Wang, et. al., rats were supplemented with fructose in their diet, that is known to produce oxidative stress in vivo, and the results showed that endothelium-dependent relaxations were impaired [12]. Although, supplementing the fructose-fed rats with BH₄ in the water did not significantly increase the vascular content of BH₄, it did partially restore endothelium-dependent vascular relaxations and restore eNOS protein within the rat aortas [12].

Utilizing NIH3T3 cells, a line with very low BH₄ levels, and bovine aortic endothelial cells (BAECs), our study was designed to test the hypothesis that BH₄'s role in the regulation of eNOS is dependent on its high antioxidant potential. The experimental results supported the hypothesis showing that the association of BH₄ with eNOS regulated eNOS protein levels and activity.

MATERIALS AND METHODS

Cell culture

Primary cultures of Bovine pulmonary arterial endothelial cells (BAECs) were generously donated by Dr. J. Douglas Coffin at the University of Montana. Endothelial cell identity was confirmed by their typical cobblestone appearance, contact inhibition, specific uptake of 1,1'-dioctadecyl-1,3,3',3'-tetramethylindocarbocyanine perchlorate-labeled acetylated low-density lipoprotein (Molecular Probes, Eugene, OR), and positive staining for von Willebrand factor (Dako, Carpinteria, CA). BAECs were grown in Eagle DMEM containing 1g/l glucose and phenol red (MediaTech, Herndon, VA), supplemented with 10% fetal bovine serum (Hyclone, Logan, UT), and antibiotic-antimycotic (MediaTech). NIH3T3 cells were purchased from _____ (_____). These cells were grown in Eagle DMEM containing 1g/l glucose and phenol red (MediaTech, Herndon, VA), supplemented with 10% fetal calf serum (Hyclone, Logan, UT), and antibiotic-antimycotic (MediaTech). Prior to experimental treatment (unless otherwise noted) cells were trypsinized, counted with a hemacytometer and replated in a 6, 24-, or 96-well plate (Costar, Corning, NY) at densities of approximately $10^4/\text{cm}^2$ and allowed to adhere for at least 18hrs. Cells were incubated at 37°C in a humidified atmosphere of 95% air and 5% CO_2 .

Generation of Catalase and eNOS Adenoviral Expression Constructs

Adenoviral vectors that express either catalase or eNOS were constructed with the pAd/pENTR System (Invitrogen). Briefly, a pAd/CMV plasmid containing a catalase cDNA (cDNA purchased from ATCC, Manassas, VA) or eNOS cDNA (cDNA

purchased from ATCC, Manassas, VA) was created and transfected into 293A cells. A selected clone was propagated and viral lysates were collected and titered per the manufacturer's protocol. The titer for the AdV.catalase preparation was 1.0×10^{12} plaque-forming units per mL (pfu/mL) and the titer for the AdV.eNOS preparation was 1.0×10^{10} pfu/mL. Transductions of NIH3T3 cells were performed for 120min with virus diluted in normal DMEM for a multiplicity of infection (MOI) of 2000. An MOI=2000 yielded a transfection efficiency of 60%. Verification of transgene expression was performed using Western Blot analysis as previously described [13] using 20 μ g of total protein extracts probed with anti-catalase antibody (1:1000, QED, Malden, MA) or anti-eNOS antibody (1:1000, BD Biosciences) and normalized to concomitant immunostaining for β -actin (1:1000, Sigma) on the same blots.

Protein Extraction

NIH3T3 cells were grown in 6-well plates to 80% confluence. They were adenovirally transduced with eNOS alone for the control and eNOS + catalase for the treatment as stated in the previous section. Total protein was harvested after 36hrs.

BAECs were grown to confluence and treated for 24hrs with tetrahydro-L-Biopterin (BH₄) (Cayman Chemical, Ann Arbor, MI), L-sepiapterin, or a vehicle control. Following treatment, protein was harvested.

For harvesting, cells were rinsed with DPBS (MediaTech) and RIPA lysis buffer added to each well. Cells were then collected and sheared with a 25-gauge needle 3X. Lastly, samples were spun at 14,000Xg for 10min and the supernatant was collected.

Protein concentrations were analyzed using Bio-Rad protein assay (Bio-Rad, Hercules, CA) and Bovine Serum Albumin (BSA) for the protein standard curve.

Western blotting

Western Blot analysis was performed as previously described [14]. Total protein extracts (~20µg) were resuspended in 5X Laemmli protein sample buffer and boiled for 5min. Total protein was then separated on a 4-20% Tris-SDS-HEPES polyacrylamide gel (Gradiopore, Frenchs Forest, Australia) and electrophoretically wet-transferred to a Hybond-PVDF membrane (Amersham, Arlington Hts., IL). The membranes were blocked with 5% nonfat dry milk in Tris buffered saline containing 0.1% Tween-20 (TBST) overnight at 4⁰C. After blocking, the membranes were incubated at room temperature for 2 hrs with the primary antibody (1:1,000 for α-eNOS, BD Biosciences and 1:1000 α-metallothionein-I antibody, QED, Malden, MA), washed 3X with TBST, and incubated with a mouse anti-rabbit IgG-horseradish peroxidase conjugated secondary antibody (Pierce, Rockford, IL) for 1 hr. After washing, immunolabeled protein bands were visualized using chemiluminescence (SuperSignal West Fempto Substrate Kit, Pierce) on a Kodak Image Station 440CF with Kodak 1D Molecular Imaging Software and normalized to immunolabeled β-actin (1:1000, Sigma) on the same blot.

Low Temperature Poly Acrylamide Gel Electrophoresis (LT-PAGE)

LT-PAGE was used to analyze eNOS dimer levels. Briefly, NIH3T3 cells were transduced for 36hrs with eNOS alone for the control and eNOS + catalase for the treatment and BAECs were treated with BH₄, L-sepiapterin, or a vehicle control for

24hrs. Next, cells were rinsed 2X with DPBS. Total protein was harvested and concentrations measured as stated in the Western Blot section above. However, samples were not boiled as in a regular Western Blot prior to loading. Equal protein was loaded onto a denaturing polyacrylamide gel and run on ice at 30v for approximately 7hrs. Transfer, blocking, and immunoblotting were performed similar to the Western Blot method above.

Catalase Activity Assay

NIH3T3 cells were grown in 6-well plates to 80% confluence. They were adenovirally transduced with eNOS alone for the control and eNOS + catalase for the treatment as stated in the previous section. Total protein was harvested 36hrs post-transduction as described in the section above. Catalase activity was measured spectrophotometrically (Shimadzu Biospec) using 40µg of total protein extract from each sample. Briefly, 40µg sample + 99µL 0.05M Potassium Phosphate Buffer (pH=7.0) were combined and the spectrophotometer was auto zeroed. Then, 1µL 3% H₂O₂ was added to the mixture and the absorbance was followed at 240nm for 60sec. All reagents were used at room temperature.

Hydrogen Peroxide Levels

NIH3T3 cells were grown in 6-well plates to 80% confluence. They were adenovirally transduced with eNOS alone for the control and eNOS + catalase for the treatment as stated in the previous section. After 36hrs, plates were washed with DPBS and 1mL fresh media (700µL fresh media + 300µL conditioned media) was added to

each well. Media samples were collected over 4hrs (0, 30, 60, 120, 180, and 240 minutes) and an equal volume of fresh media was added to the well. Extracellular H₂O₂ levels were determined using an Amplex Red H₂O₂ detection kit (Invitrogen), following the manufacturer's instructions. A fluorescence plate reader (Fluoroscan) measured resorufin fluorescence at an excitation of 560nm and an emission of 590nm and a H₂O₂ standard curve (0-10μM H₂O₂) was used to determine its concentration. Background fluorescence was subtracted from all samples and standards.

Assay for NOS Activity

NOS activity was determined by measuring NO_x production in the media with a NO_x specific probe (Apollo 4000 Free Radical Analyzer, World Precision Instruments, Inc.). NIH3T3 cells were transduced for 24hrs with eNOS or eNOS + catalase and treated with BH₄ or a vehicle control for an additional 24hrs. BAECs were treated with L-sepiapterin, L-sepiapterin + NAS, or a vehicle control for 24hrs. NOS activity was determined in both NIH3T3 and BAECs following their respective treatments. Briefly, following treatment and a fresh media change, media was collected and either put on ice until analysis or frozen for later analysis. In one set of experiments, BAECs were sheared for 15min prior to media collection using a shear plate viscometer at 18v, which is comparable to shear forces seen in a blood vessel. NO_x levels were quantified and potassium nitrate standards were used to determine NO_x levels.

EPR Analysis

NIH3T3 cells were grown in 6-well plates to 80% confluence. They were adenovirally transduced with eNOS alone for the control and eNOS + catalase for the treatment. Twenty four hours post transduction, plates were rinsed with DPBS and treated with 100 μ M BH₄ for 24hrs. The cyclic hydroxylamine, CMH (Alexis Biochemicals), spin trap was diluted in EPR Buffer (25 μ M Dethferioxamine (Sigma-Aldrich) + 5 μ M Diethylcarbamate in DPBS without calcium and magnesium) at 5mg/250 μ L. For the last hour of treatment with BH₄, 80 μ L CMH spin trap and 2 μ L DMSO (Sigma) was added to each well. After 1hr, cells were rinsed with EPR buffer and then 1mL EPR buffer was added to each well. Cells were scraped into a new set of tubes and spun at 500 x g for 5min. Supernatant was removed and 35 μ L EPR buffer was added to each pellet. Cells were pulled through 25gauge needle to further break open cells and put on ice until analysis. Total protein concentrations were analyzed using Bio-Rad protein assay (Bio-Rad, Hercules, CA) and Bovine Serum Albumin (BSA) for the protein standard curve to normalize the EPR readings. The cell solution was then loaded into a 50 μ L capillary tube and EPR analysis was done with a MiniScope MS200 ESR (Magnettech, Berlin, Germany) at 40mW microwave power, 3,000mG modulation amplitude, and 100kHz modulation frequency. The EPR machine was set to average four readings. EPR spectra were analyzed and measured for amplitude using ANALYSIS version 2.02 software (Magnettech).

Measuring BH₄ and BH₂ Levels

BAECs were grown to confluence and treated for 24hrs with L-sepiapterin or BH₄. The cells were rinsed with DPBS and then 300 μ L of extraction buffer was added to

each well of the 6-well plates. The plates were snap frozen and thawed 3X by putting plates at -70°C for 20min and then back at room temperature for 3min. Then, the cells were scraped and spun in a microfuge tube for 10min at 4°C . The supernatant was put in a fresh tube and the pellet was discarded.

Standards of BH4 were prepared in dH_2O and run on the HPLC for standard curve. The HPLC column was washed with 5% methanol for 3min and 200 μL of each sample was loaded. Isocratic elution was done for 17min with 5% methanol. The column was cleaned for 8min with 100% methanol and re-equilibrated with 5% methanol for 3min before injecting another sample. The following parameters were used: Flow rate = 0.8mL/min. Fluorescence detector excitation/emission = 350/450nm, gain = 10, and attenuation = 1. Then, depending on column age, samples were eluted at 12-15min.

Statistical analysis

Values are expressed as the means \pm standard error of the mean from at least three experiments. Statistical analysis between experimental groups was performed by one way ANOVA or a T-test using the Graph Pad Prism 4.0 statistical analysis software program. A $P < 0.05$ was considered statistically significant.

RESULTS

Initially, we verified that the NIH3T3 cells used for these experiments expressed low levels of GTP cyclohydrolase, the rate limiting enzyme for the synthesis of tetrahydrobiopterin (BH₄). NIH3T3 cells were grown to confluence and protein was harvested. The control for this experiment was ovine lung tissue. Western blot analysis was used to analyze the amount of GTP cyclohydrolase protein. Results indicated that NIH3T3 cells have very low GTP Cyclohydrolase protein levels compared to lung tissue (Figure 1). This data is representative of four independent experiments.

Next, we determined the effect of catalase viral transduction on total catalase protein levels. NIH3T3 cells were grown to 80% confluence and transduced with endothelial nitric oxide synthase (eNOS) (control) or catalase + eNOS adenovirus at MOI=2000. 36hrs post transduction, protein was harvested and Western blot analysis was used to determine total catalase protein levels. Results indicated that catalase viral transduction at MOI=2000, gives a 20-fold increase in catalase protein levels compare to eNOS viral transduction alone (Figure 2). This data is representative of four independent experiments.

Viral transduction gave 20-fold increase in catalase protein, so then we looked at catalase activity levels. Once again, NIH3T3 cells were transduced with eNOS alone or eNOS + catalase. 36hrs later, protein was harvested and combined with a set amount of hydrogen peroxide (H₂O₂) to measure catalase's ability to dismutate the H₂O₂. Results found that a 20-fold increase in protein corresponded to a 6-fold increase in catalase activity (Figure 3). This data is representative of four independent experiments.

Following that, we determined whether the increases in catalase protein and activity would affect basal H₂O₂ levels in NIH3T3 cells. Once again, NIH3T3 cells were transduced with eNOS alone or eNOS + catalase. 36hrs later, cells were rinsed and fresh media was added. Media samples were collected over the next 4hrs and H₂O₂ levels were measured using the commercially available Amplex Red kit. There was nearly 30% less H₂O₂ in eNOS + catalase vs eNOS viral transduction alone (Figure 4). This data is representative of four independent experiments.

Knowing that the eNOS cofactor, BH₄, has very low expression in NIH3T3 cells, we decided to see what effect catalase transduction would have on total eNOS protein. NIH3T3 cells were virally transduced with eNOS alone or eNOS + catalase. Protein was harvested and western blot analysis was used to determine total eNOS protein levels. Results found nearly a 50% increase in total eNOS protein compared to eNOS transduction alone (Figure 5). This data suggests that a major role of BH₄ may be to act as an antioxidant to help maintain eNOS protein levels. This data is representative of four independent experiments.

eNOS is only active as a homodimer, therefore we looked at the effect of catalase transduction in NIH3T3 cells on eNOS monomer and dimer levels. Protein from the previous experiment was utilized for these studies. Protein was subjected to low temperature polyacrylamide gel electrophoresis to separate monomer and dimer eNOS proteins. Results are represented at a dimer to monomer ratio, so a higher ratio represents more of the active form of eNOS. There was nearly a 2-fold dimer to monomer ratio increase with catalase transduction (Figure 6). This further supports BH₄'s antioxidant role, not only in total eNOS protein maintenance, as seen in the previous experiment, but

also in maintaining the active dimeric form of eNOS. This data is representative of four independent experiments.

The next step was to look at the effect of catalase transduction on eNOS activity. NIH3T3 cells were grown to 80% confluence and virally transduced with eNOS or eNOS + catalase adenovirus. 24hrs later cells were treated for 24hrs with BH₄ or a vehicle control. Following this treatment, media from virally transduced NIH3T3 cells was collected and NO_x levels were analyzed using a NO_x-specific probe. A standard curve of various concentrations of potassium nitrate was used to determine the NO_x levels in the media. Results indicated that without BH₄ treatment, there was a nearly a 30% increase in eNOS activity with catalase transduction (Figure 7). However, with BH₄ treatment, there was no difference with catalase transduction (Figure 7). This data is representative of four independent experiments.

A series of experiments to look further at the role of BH₄ were done in bovine aortic endothelial cells (BAECs). BAECs have very high levels of BH₄ compared to the NIH3T3 cells. We hope that the direct addition of BH₄ or L-sepiapterin, which serves as a substrate for BH₄ synthesis through the pterin salvage pathway, independent of GTP cyclohydrolase, will give similar results compared to the catalase transduction.

In the first experiment, BAECs were grown to confluence and treated for 24hrs with various doses of BH₄ and L-sepiapterin. Media was collected and reactive oxygen species (ROS), specifically H₂O₂, were measured using the Amplex Red kit. Results demonstrate a dose dependent decrease in ROS levels with L-sepiapterin treatment. At 100μM BH₄, there is a significant decrease in ROS, but at 500μM, ROS is significantly

higher (Figure 8). At such a high level, this increase may be due to toxicity. This data is representative of four independent experiments.

Next, we looked at BH₄ and BH₂ levels in BAECs following L-sepiapterin or BH₄ treatment. BAECs were grown to confluence and treated with L-sepiapterin, BH₄, or a vehicle control for 24hrs. Protein was harvested and HPLC was used to measure BH₄ and BH₂ levels. Both L-sepiapterin and BH₄ treatment increased BH₄ and BH₂ levels, but to a greater extent with L-sepiapterin (Figure 9). This data is representative of four independent experiments.

Using the same spectrophotometric assay used to measure catalase activity, we next tested the direct addition of BH₄ on the dismutation rate of H₂O₂. We found about a 15-fold increase in H₂O₂ dismutation with BH₄ compared to a vehicle control (Figure 10). These results strongly support BH₄'s role as an antioxidant. This data is representative of four independent experiments.

BH₄ does have very strong antioxidant properties. Next, we looked at its effect on eNOS dimer levels. BAECs were grown to confluence and then treated with BH₄, L-sepiapterin, or a vehicle control for 24hrs. Similar to results in NIH3T3 cells following catalase transduction, BH₄ and L-sepiapterin increased eNOS dimer levels 10-15% (Figure 11). This data is representative of four independent experiments.

Lastly, we looked at the effect of BH₄ and L-sepiapterin on eNOS activity in BAECs. BAECs were grown to confluence and treated for 24hrs with L-sepiapterin, L-sepiapterin + N-acetyl-serotonin (NAS), or a vehicle control. L-sepiapterin caused a 30% increase in NO_x release (Figure 12), but this increase was abolished with the specific inhibitor of L-sepiapterin, NAS (Figure 12). The direct addition of BH₄ to BAECs did

not significantly increase eNOS activity (Figure 13). This may be because BH₄ levels and/or eNOS activity may already be maximal in these cells. However, exposing the cells to 20min of shear alone increased eNOS activity nearly 3-fold and with the addition of BH₄, increased it nearly 7-fold (Figure 13). This data is representative of four independent experiments.

Going back to the NIH3T3 cells, we decided to look at ROS production following catalase overexpression and BH₄ treatment. NIH3T3 cells were grown to 80% confluence and virally transduced with eNOS or eNOS + catalase. 24hrs later, cells were treated with BH₄ or a vehicle control for 24hrs. At 23hrs, the superoxide specific spin trap, CMH, was added to each well. Following treatment, cells were harvested in EPR buffer. EPR analysis indicated that catalase transduction significantly decreased ROS levels with or without BH₄ treatment (Figure 14). BH₄ treatment further decreased ROS levels in both eNOS and eNOS + catalase transduced samples. This data is representative of four independent experiments.

DISCUSSION

Endothelial nitric oxide synthase (eNOS) become uncoupled in persistent pulmonary hypertension of the newborn (PPHN), such that there is decreased production of the vasodilator, nitric oxide (NO) and increased production of cellular oxidants, such as hydrogen peroxide (H_2O_2) and superoxide ($O_2^{\cdot-}$). NOS enzymes do have the ability to secrete $O_2^{\cdot-}$ [15-17]. The four redox active prosthetic groups (FAD, FMN, heme, and BH_4) could potentially pass electrons to molecular oxygen (O_2). To prevent this uncoupling from NO synthesis, electron transfers in NOS enzymes are tightly regulated. A functional eNOS transfers electrons from NADPH through the flavins, FAD and FMN, in the carboxy-terminal reductase domain to the heme in the amino-terminal oxygenase domain. The reaction oxidizes L-arginine to L-citrulline and NO. If this electron flow is disturbed, superoxide is generated from the oxygenase domain instead of NO by dissociation of the ferrous dioxygen complex [18]. The production of nitric oxide (NO) in the vessel wall by the eNOS is dependent on essential enzyme cofactors, including the most potent naturally occurring reducing agent, tetrahydrobiopterin (BH_4). BH_4 is thought to maintain the eNOS homodimer, but we wanted to determine whether this was dimer maintenance was due to its high antioxidant capability.

This study utilized NIH3T3 cells, which express very low levels of GTP cyclohydrolase, which is the rate limiting enzyme for the synthesis of BH_4 , and do not express eNOS. These cells have high transduction efficiency and will lift shortly after reaching confluence; therefore all transductions were done at ~80% confluence and treatments/analysis done at confluence prior to cell lifting. After 36hrs, eNOS protein expressed very nicely compared to a transfection control, which contained no eNOS

(Data not shown). Catalase transduction resulted in a 20-fold increase in catalase protein (Figure 3) and was associated with a 6-fold increase in catalase activity (Figure 4).

Decreasing the basal oxidative environment in NIH3T3 cells by virally transducing with catalase (Figure 4) significantly increased total eNOS protein. These results suggest that without the antioxidant cofactor BH₄, eNOS may be vulnerable to even basal levels of cellular oxidants and support BH₄'s role as an antioxidant.

eNOS plays an important role in regulating vascular smooth muscle tone and blood pressure through its generation of NO, which also protects the intima of the vessels from platelet aggregation and leukocyte adhesion, and prevents proliferation of vascular smooth muscle [19, 20]. This enzyme is only active, however, as a homodimeric enzyme [21-23]. In the absence of adequate levels of BH₄, eNOS becomes uncoupled from the L-arginine oxidation and molecular oxygen is reduced to form superoxide [24]. eNOS uncoupling modulates endothelial dysfunction in various vascular disorders, including atherosclerosis [25], diabetes [26, 27], hypertension [28], and hypercholesterolemia [29]. It is now well established that BH₄ is important for the coupling of eNOS [30, 31]. The increased superoxide produced by an uncoupled eNOS reduces NO production and increased production of peroxynitrite, a production of superoxide reacting with available NO. Since BH₄ is thought to maintain the eNOS dimer, we tested whether decreasing the oxidative environment in NIH3T3 cells would increase eNOS dimer and did find a 2-fold increase in eNOS dimer/monomer ratio (Figure 6). With low BH₄ levels in NIH3T3 cells, these results suggest that BH₄'s antioxidant properties are important in eNOS dimer maintenance.

When in an active dimeric state and tightly coupled with sufficient cofactor levels, eNOS produces NO. In looking at the effect of catalase transduction on eNOS activity in the presence of low levels of BH₄, we found a 30% increase in NO_x release (Figure 7). The addition of BH₄ to these cells restored eNOS activity in the eNOS transduced only sample to the level of the eNOS/catalase dually transduced sample (Figure 7). This further supports our hypothesis that BH₄'s antioxidant properties are important for eNOS activity.

For the next series of experiments, we utilized a system with normal basal BH₄ levels, BAECs. The direct addition of BH₄ or L-sepiapterin, a substrate for BH₄ synthesis through the pterin salvage pathway, independent of GTP cyclohydrolase, gave us more insight into BH₄'s role in the regulation of eNOS and a comparison for the NIH3T3 eNOS/catalase dually transduced samples.

As expected, both BH₄ and L-sepiapterin significantly decreased ROS levels in BAECs (Figure 8), specifically H₂O₂, as measured by Amplex Red assay. However, at 500μM BH₄, ROS levels significantly increased (Figure 8). Too much antioxidant in the cell is most likely toxic. The addition of BH₄ to BAECs significantly increased cellular BH₂ levels, the oxidized inactive form of tetrahydrobiopterin, three-fold and BH₄ levels nearly six-fold (Figure 9). However, L-sepiapterin addition significantly increased cellular BH₂ levels about 20-fold and BH₄ levels nearly 150-fold (Figure 9).

Next, we measured the dismutation rate of H₂O₂ by BH₄ in BAECs and found about a 7-fold increase (Figure 10). These results were no surprise since it is known that BH₄ is the most potent naturally occurring reducing agent, but they do give a quantitative measurement of its reducing power.

BH₄ and L-sepiapterin had a similar effect on BAECs as did eNOS/catalase transduction in NIH3T3 cells, significantly increasing eNOS dimer levels 10-15% compared to a vehicle control. This does demonstrate that BH₄ is important in maintaining eNOS dimer levels, possible due to its antioxidant properties.

Even though L-sepiapterin increased BH₄ levels 150-fold (Figure 9), it only significantly increased eNOS activity about 30% compared to vehicle control BAECs (Figure 12). It also increased BH₂ levels 20-fold (Figure 9). Increased BH₂ can displace pre-bound BH₄ from its eNOS binding site in the oxygenase domain [32], which could enhance eNOS uncoupling, thus lowering eNOS activity and explaining this result.

The addition of BH₄ to BAECs interestingly did not result in a significant increase in eNOS activity (Figure 13). This may be due to the fact that it only increased intracellular BH₄ levels about six-fold and/or because BAEC eNOS is already quite active basally. Fluid shear stress is defined as the tractive force produced by moving a viscous fluid (blood) on a solid body (vessel wall), constraining its motion [33]. It is known to initiate diverse responses in endothelial cells, including increases in NOS activity, NO production, and eNOS mRNA/protein levels [34-41]. Our results indicated that shear significantly increased eNOS activity in BAECs and even further increased it with the addition of BH₄ (Figure 13).

Our last experiments went back to the NIH3T3 cells and looked at ROS production by EPR analysis in cells transduced with eNOS or eNOS/catalase and treated with BH₄ or a vehicle control. eNOS/catalase transduction significantly decreased ROS production three-fold compared to eNOS transduction alone (Figure 14). However, the addition of BH₄ to the eNOS transduced sample brought ROS levels back to that of

eNOS/catalase transduced (Figure 14). As expected, the eNOS/catalase transduced and treated with BH₄ resulted in the lowest ROS levels (Figure 14).

In conclusion, our results indicate that BH₄'s high antioxidant potential plays a major role in its regulation of eNOS protein levels and activity. NIH3T3 cells have very low BH₄ levels, which may not increase the overall oxidative environment, since cellular antioxidants tend to compensate for a lack of another antioxidant, but there would be less BH₄ available to associate with the transfected eNOS. Thus, eNOS may be more vulnerable as protected from the various oxidants present in the cell, leading to decreased protein and activity. By decreasing the oxidative environment with catalase transduction, we significantly increased eNOS total protein, dimer/monomer protein ratio, and activity. The direct addition of BH₄ to NIH3T3 cells significantly decreased ROS levels. Studies in BAECs, which contain much higher levels of BH₄ protein, further confirmed the previous results by demonstrating that the addition of BH₄ or L-sepiapterin significantly decreased the oxidative environment and increased eNOS dimer protein and activity levels. Further studies need to be done, especially on purified protein, to look further into BH₄'s antioxidant role in eNOS regulation. These studies do provide valuable insights into BH₄'s role in eNOS regulation and may help in the development of treatments for vascular diseases, such as PPHN, which are characterized by endothelial dysfunction.

ACKNOWLEDGMENTS

This research was supported in part by grants XXX from the American Heart Association Pacific Mountain Affiliates (to JW), HL60190 (to SMB), HL67841 (to SMB), HL072123 (to SMB), and HL070061 (to SMB) from the National Institutes of Health, and 0330292N from the American Heart Association National Office (to SW).

REFERENCES

1. Haworth, S.G. and L. Reid, *Persistent fetal circulation: Newly recognized structural features*. J Pediatr, 1976. **88**(4 Pt. 1): p. 614-20.
2. Brennan, L.A., et al., *Increased superoxide generation is associated with pulmonary hypertension in fetal lambs: a role for NADPH oxidase*. Circ Res, 2003. **92**(6): p. 683-91.
3. Sundaresan, M., et al., *Requirement for generation of H₂O₂ for platelet-derived growth factor signal transduction*. Science, 1995. **270**(5234): p. 296-9.
4. Wedgwood, S., R.W. Dettman, and S.M. Black, *ET-1 stimulates pulmonary arterial smooth muscle cell proliferation via induction of reactive oxygen species*. Am J Physiol Lung Cell Mol Physiol, 2001. **281**(5): p. L1058-67.
5. Meier, B., et al., *Human fibroblasts release reactive oxygen species in response to interleukin-1 or tumour necrosis factor-alpha*. Biochem J, 1989. **263**(2): p. 539-45.
6. Matsubara, T. and M. Ziff, *Increased superoxide anion release from human endothelial cells in response to cytokines*. J Immunol, 1986. **137**(10): p. 3295-8.
7. Matsubara, T. and M. Ziff, *Superoxide anion release by human endothelial cells: synergism between a phorbol ester and a calcium ionophore*. J Cell Physiol, 1986. **127**(2): p. 207-10.
8. Griendling, K.K., et al., *Angiotensin II stimulates NADH and NADPH oxidase activity in cultured vascular smooth muscle cells*. Circ Res, 1994. **74**(6): p. 1141-8.
9. Dawson, T.M. and S.H. Snyder, *Gases as biological messengers: nitric oxide and carbon monoxide in the brain*. J Neurosci, 1994. **14**(9): p. 5147-59.
10. Kwon, N.S., C.F. Nathan, and D.J. Stuehr, *Reduced biopterin as a cofactor in the generation of nitrogen oxides by murine macrophages*. J Biol Chem, 1989. **264**(34): p. 20496-501.
11. Reif, A., et al., *Tetrahydrobiopterin inhibits monomerization and is consumed during catalysis in neuronal NO synthase*. J Biol Chem, 1999. **274**(35): p. 24921-9.
12. Wang, X., et al., *Tetrahydrobiopterin prevents endothelial dysfunction and restores adiponectin levels in rats*. Eur J Pharmacol, 2007. **555**(1): p. 48-53.
13. Brennan, L.A., et al., *Nitric oxide activates p21ras and leads to the inhibition of endothelial NO synthase by protein nitration*. DNA Cell Biol, 2003. **22**(5): p. 317-28.
14. Black, S.M., et al., *Ventilation and oxygenation induce endothelial nitric oxide synthase gene expression in the lungs of fetal lambs*. J. Clin. Invest, 1997. **100**: p. 1448-1458.
15. Heinzl, B., et al., *Ca²⁺/calmodulin-dependent formation of hydrogen peroxide by brain nitric oxide synthase*. Biochem J, 1992. **281** (Pt 3): p. 627-30.
16. Pou, S., et al., *Generation of superoxide by purified brain nitric oxide synthase*. J Biol Chem, 1992. **267**(34): p. 24173-6.

17. Xia, Y., et al., *Superoxide generation from endothelial nitric-oxide synthase. A Ca²⁺/calmodulin-dependent and tetrahydrobiopterin regulatory process.* J Biol Chem, 1998. **273**(40): p. 25804-8.
18. Forstermann, U., *Endothelial NO synthase as a source of NO and superoxide.* Eur J Clin Pharmacol, 2006. **62 Suppl 1**: p. 5-12.
19. Furchgott, R.F. and J.V. Zawadzki, *The obligatory role of endothelial cells in the relaxation of arterial smooth muscle by acetylcholine.* Nature, 1980. **288**(5789): p. 373-6.
20. Ignarro, L.J., *Nitric oxide as a unique signaling molecule in the vascular system: a historical overview.* J Physiol Pharmacol, 2002. **53**(4 Pt 1): p. 503-14.
21. Ghosh, D.K., H.M. Abu-Soud, and D.J. Stuehr, *Domains of macrophage N(O) synthase have divergent roles in forming and stabilizing the active dimeric enzyme.* Biochemistry, 1996. **35**(5): p. 1444-9.
22. Rodriguez-Crespo, I. and P.R. Ortiz de Montellano, *Human endothelial nitric oxide synthase: expression in Escherichia coli, coexpression with calmodulin, and characterization.* Arch Biochem Biophys, 1996. **336**(1): p. 151-6.
23. Venema, R.C., et al., *Subunit interactions of endothelial nitric-oxide synthase. Comparisons to the neuronal and inducible nitric-oxide synthase isoforms.* J Biol Chem, 1997. **272**(2): p. 1276-82.
24. Adlam, D., et al., *Relationships between nitric oxide-mediated endothelial function, eNOS coupling and blood pressure revealed by eNOS-GTP cyclohydrolase 1 double transgenic mice.* Exp Physiol, 2007. **92**(1): p. 119-26.
25. Kawashima, S., *The two faces of endothelial nitric oxide synthase in the pathophysiology of atherosclerosis.* Endothelium, 2004. **11**(2): p. 99-107.
26. Pannirselvam, M., et al., *Cellular basis of endothelial dysfunction in small mesenteric arteries from spontaneously diabetic (db/db -/-) mice: role of decreased tetrahydrobiopterin bioavailability.* Br J Pharmacol, 2002. **136**(2): p. 255-63.
27. Shinozaki, K., et al., *Abnormal biopterin metabolism is a major cause of impaired endothelium-dependent relaxation through nitric oxide/O₂- imbalance in insulin-resistant rat aorta.* Diabetes, 1999. **48**(12): p. 2437-45.
28. Landmesser, U., et al., *Oxidation of tetrahydrobiopterin leads to uncoupling of endothelial cell nitric oxide synthase in hypertension.* J Clin Invest, 2003. **111**(8): p. 1201-9.
29. Stroes, E., et al., *Tetrahydrobiopterin restores endothelial function in hypercholesterolemia.* J Clin Invest, 1997. **99**(1): p. 41-6.
30. Vasquez-Vivar, J., B. Kalyanaraman, and P. Martasek, *The role of tetrahydrobiopterin in superoxide generation from eNOS: enzymology and physiological implications.* Free Radic Res, 2003. **37**(2): p. 121-7.
31. Vasquez-Vivar, J., et al., *Superoxide generation by endothelial nitric oxide synthase: the influence of cofactors.* Proc Natl Acad Sci U S A, 1998. **95**(16): p. 9220-5.
32. Vasquez-Vivar, J., et al., *The ratio between tetrahydrobiopterin and oxidized tetrahydrobiopterin analogues controls superoxide release from endothelial nitric oxide synthase: an EPR spin trapping study.* Biochem J, 2002. **362**(Pt 3): p. 733-9.

33. Nerem, R.M. and P.R. Girard, *Hemodynamic influences on vascular endothelial biology*. Toxicol Pathol, 1990. **18**(4 Pt 1): p. 572-82.
34. Korenaga, R., et al., *Laminar flow stimulates ATP- and shear stress-dependent nitric oxide production in cultured bovine endothelial cells*. Biochem Biophys Res Commun, 1994. **198**(1): p. 213-9.
35. Kuchan, M.J. and J.A. Frangos, *Role of calcium and calmodulin in flow-induced nitric oxide production in endothelial cells*. Am J Physiol, 1994. **266**(3 Pt 1): p. C628-36.
36. Kuchan, M.J., H. Jo, and J.A. Frangos, *Role of G proteins in shear stress-mediated nitric oxide production by endothelial cells*. Am J Physiol, 1994. **267**(3 Pt 1): p. C753-8.
37. Nishida, K., et al., *Molecular cloning and characterization of the constitutive bovine aortic endothelial cell nitric oxide synthase*. J Clin Invest, 1992. **90**(5): p. 2092-6.
38. Noris, M., et al., *Nitric oxide synthesis by cultured endothelial cells is modulated by flow conditions*. Circ Res, 1995. **76**(4): p. 536-43.
39. Ranjan, V., Z. Xiao, and S.L. Diamond, *Constitutive NOS expression in cultured endothelial cells is elevated by fluid shear stress*. Am J Physiol, 1995. **269**(2 Pt 2): p. H550-5.
40. Uematsu, M., et al., *Regulation of endothelial cell nitric oxide synthase mRNA expression by shear stress*. Am J Physiol, 1995. **269**(6 Pt 1): p. C1371-8.
41. Vane, J.R., E.E. Anggard, and R.M. Botting, *Regulatory functions of the vascular endothelium*. N Engl J Med, 1990. **323**(1): p. 27-36.

FIGURE LEGENDS

Fig. 1. NIH3T3 cells have very little GTP Cyclohydrolase protein levels compared to lung tissue. Protein was harvested from NIH3T3 cells and lung tissue. Western blot analysis was used to analyze GTP Cyclohydrolase protein levels. All values are mean \pm SEM (n=4). * $P < 0.05$ vs. Lung Tissue.

Fig. 2. Catalase protein levels in NIH3T3 cells after transduction with catalase adenovirus increases expression 20-fold. NIH3T3 cells were co-transduced with catalase and eNOS adenoviruses at MOI=1000. 36hrs later, cell protein was harvested. Western blot analysis was used to analyze human catalase levels. All values are mean \pm SEM (n=4). * $P < 0.05$ vs. eNOS.

Fig. 3. Catalase activity increases 6-fold in catalase transduced NIH3T3 cells. NIH3T3 cells were co-transduced with catalase and eNOS adenoviruses at MOI=1000. 36hrs later, catalase activity was measured using spectrophotometric assay. All values are mean \pm SEM (n=4). * $P < 0.05$ vs. eNOS.

Fig. 4. Hydrogen peroxide levels decrease nearly 30% in catalase transduced NIH3T3 cells. NIH3T3 cells were co-transduced with catalase and eNOS adenoviruses at MOI=1000. 36hrs later, H₂O₂ levels were measured using DCF-DA and reading on a multiscan at 360nm. All values are mean \pm SEM (n=4). * $P < 0.05$ vs. eNOS.

Fig. 5. eNOS protein levels in NIH3T3 cells after transduction with eNOS and catalase adenovirus increases expression nearly 50%. NIH3T3 cells were co-transduced with catalase and eNOS adenoviruses at MOI=1000. 36hrs later, cell protein was harvested. Western blot analysis was used to analyze eNOS protein levels. All values are mean \pm SEM (n=4). * $P<0.05$ vs. eNOS.

Fig. 6. Catalase transduction leads to a dimer shift in NIH3T3 cells. NIH3T3 cells were co-transduced with catalase and eNOS adenoviruses at MOI=1000. 36hrs later, cell protein was harvested. LT-PAGE and Western blot analysis was used to analyze eNOS dimer/monomer protein levels. All values are mean \pm SEM (n=4). * $P<0.05$ vs. eNOS.

Fig. 7. Catalase transduction leads to an increase in eNOS activity. NIHT3 cells were co-transduced with catalase and eNOS adenoviruses at MOI=1000. 24hrs later, cells were treated for 24hrs with 100mM BH₄. Media was collected and NO_x levels were measured using an NO_x specific probe. All values are mean \pm SEM (n=4). * $P<0.05$ vs. eNOS.

Fig. 8. Treating BAECs with either BH₄ or L-Septiapterin leads to decreases in ROS levels in cells. BAECs were grown to confluence and treated with BH₄ or L-Septiapterin. Media was collected and Amplex Red assay was performed. All values are mean \pm SEM (n=4). * $P<0.05$ vs. 0.

Fig. 9. Both L-Sepiapterin and BH4 cause increases in BH4 and BH2 levels in BAECs. BAECs were grown to confluence and treated with L-Sepiapterin or BH4. Cellular protein was harvested and HPLC was used to analyze BH2 (A) and BH4 (B) levels. All values are mean \pm SEM (n=4). * $P < 0.05$ vs. Untreated.

Fig. 10. BH4 causes the rate of H2O2 dismutation to increase nearly 15-fold from baseline. Solutions of hydrogen peroxide were analyzed for dismutation rates with or without BH4. All values are mean \pm SEM (n=4). * $P < 0.05$ vs. Untreated.

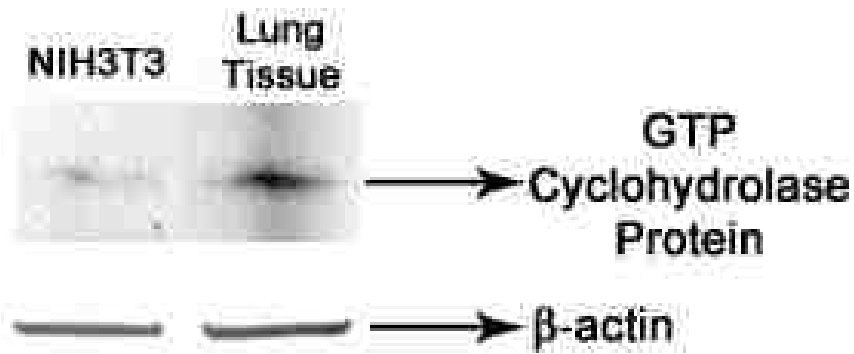
Fig. 11. Both BH4 and L-Sepiapterin cause increases in eNOS dimer levels. BAECs were grown to confluence and treated with BH4 or L-Sepiapterin. Cellular protein was harvested and eNOS dimer levels were measured using LT-PAGE. All values are mean \pm SEM (n=4). * $P < 0.05$ vs. Untreated.

Fig. 12. L-Sepiapterin causes increases in eNOS activity in BAECs. BAECs were grown to confluence and treated with L-Sepiapterin +/- N-acetyl-serotonin (blocks conversion of L-sepiapterin to BH4). All values are mean \pm SEM (n=4). * $P < 0.05$ vs. Untreated.

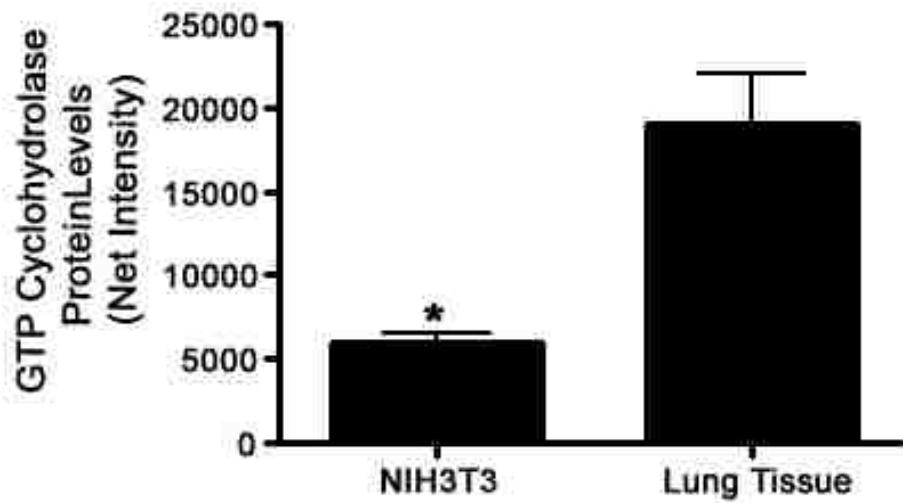
Fig. 13. BH₄ and Shear in combination cause increases in eNOS activity over shear alone. BAECs were grown to confluence and treated or not with BH₄. Cells were then exposed with shear forces with a shear plate viscometer for 20 minutes. Media was collected and analyzed for NO_x levels using an NO specific probe. All values are mean \pm SEM (n=4). * $P < 0.05$ vs. Untreated.

Fig. 14. BH₄ causes decreases in ROS levels in virally transduced NIH3T3 cells. NIH3T3 cells were grown to 80% confluence and virally transduced with eNOS or eNOS+Catalase. After 36hrs, cells were harvested and EPR was run using the CMH spin trap. All values are mean \pm SEM (n=6). * $P < 0.05$ vs. eNOS.

A

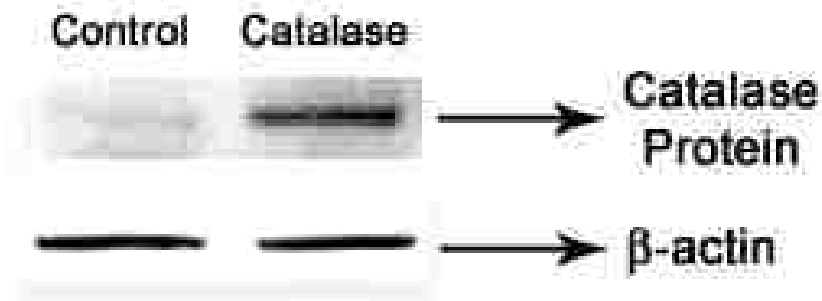


B

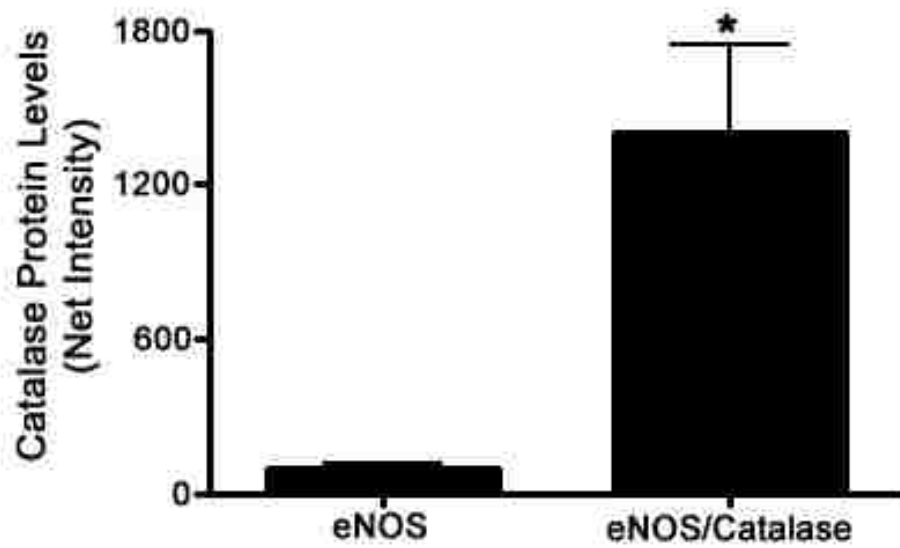


Wilham et al Fig. 1 A & B

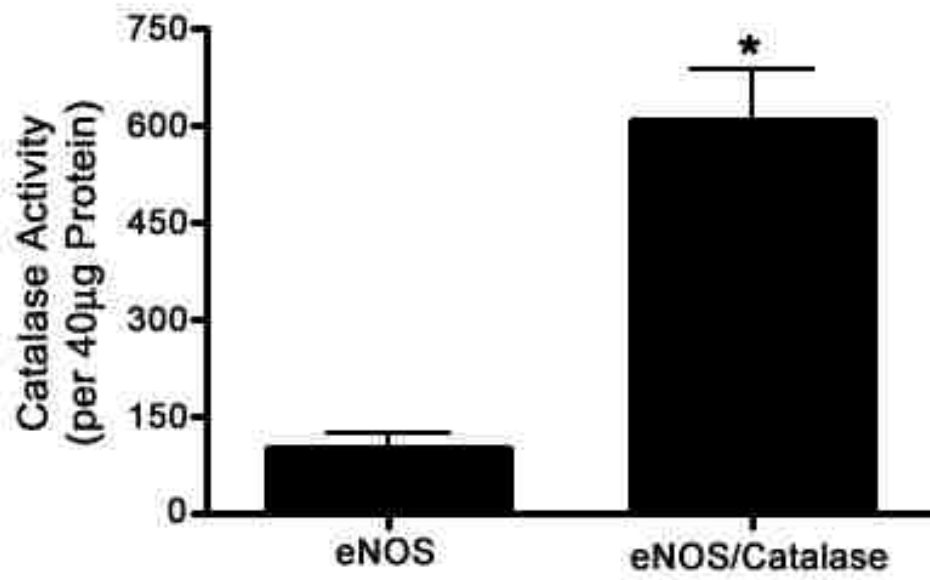
A



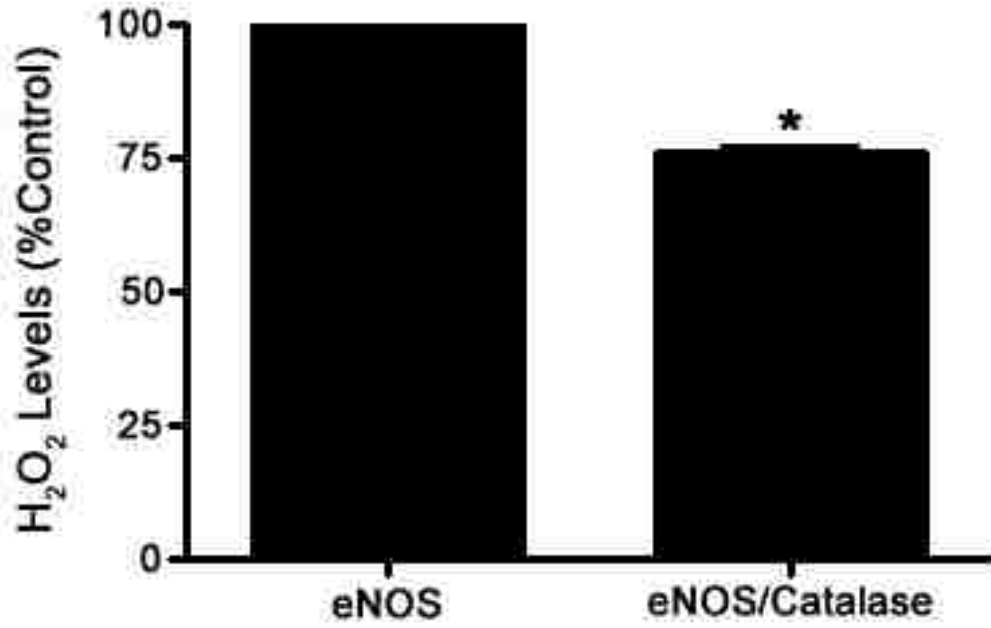
B



Wilham et al Fig. 2 A & B

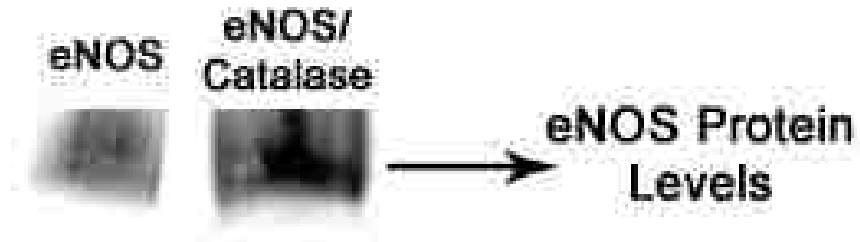


Wilham et al Fig. 3

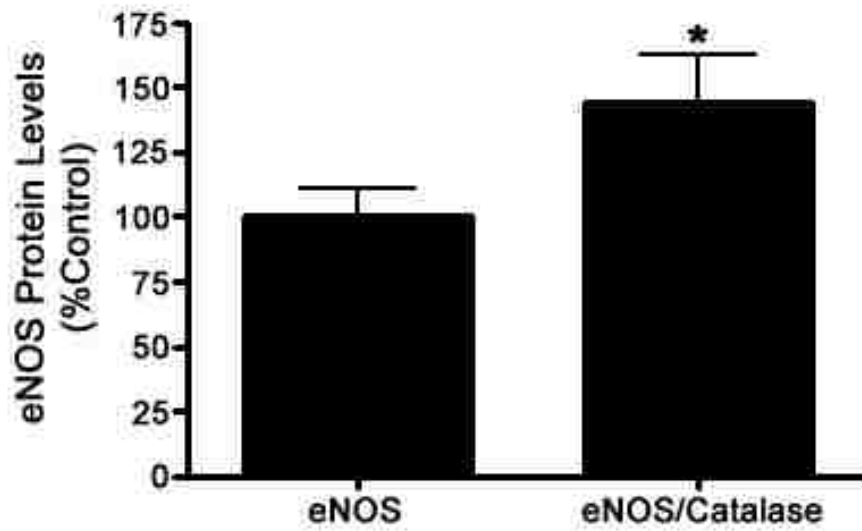


Wilham et al Fig. 4

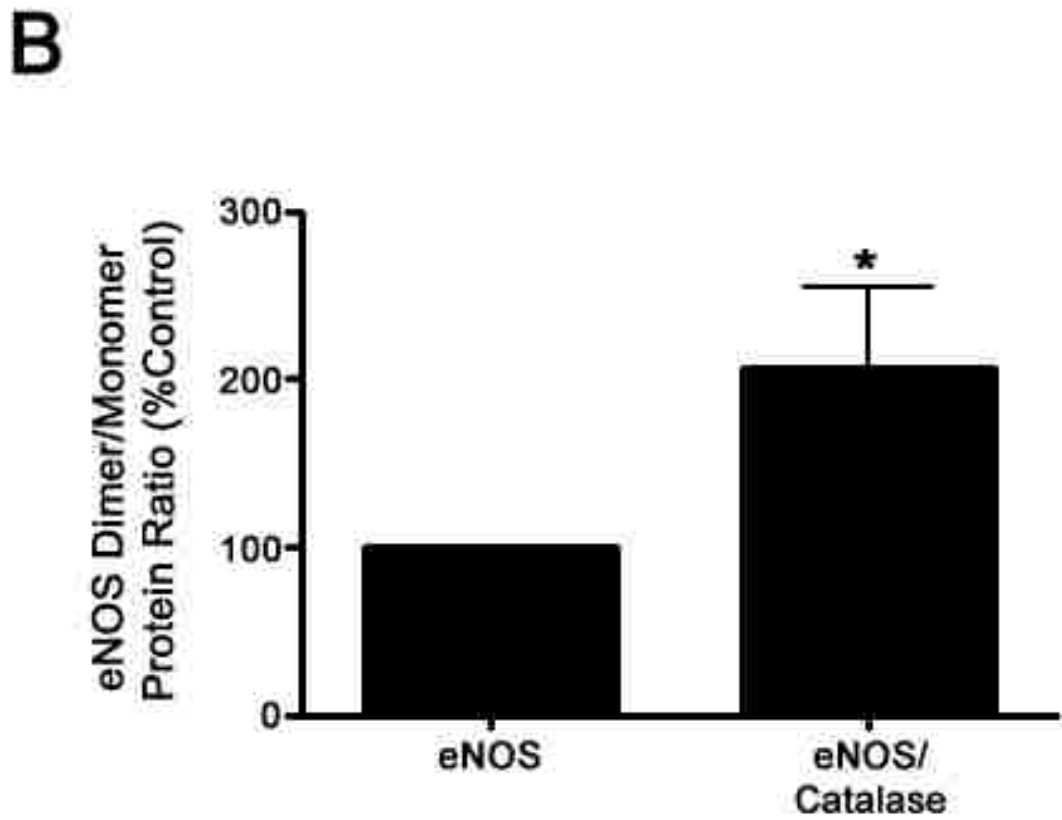
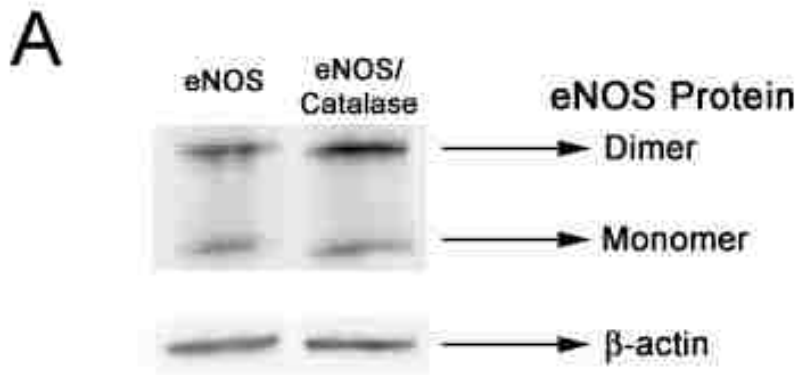
A



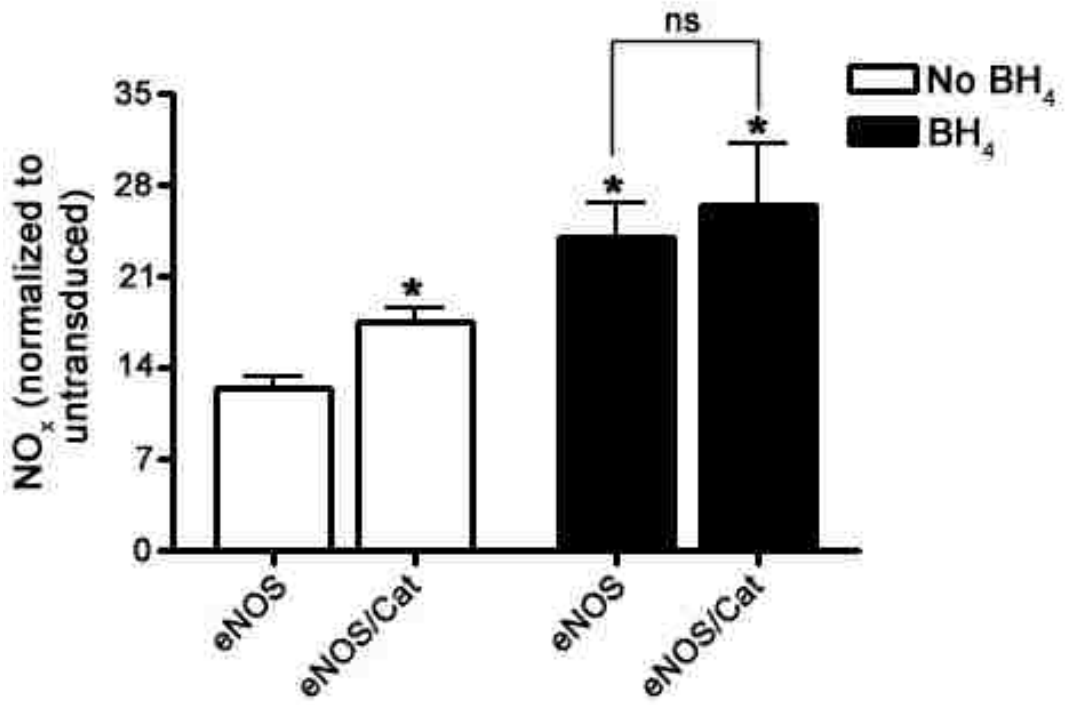
B



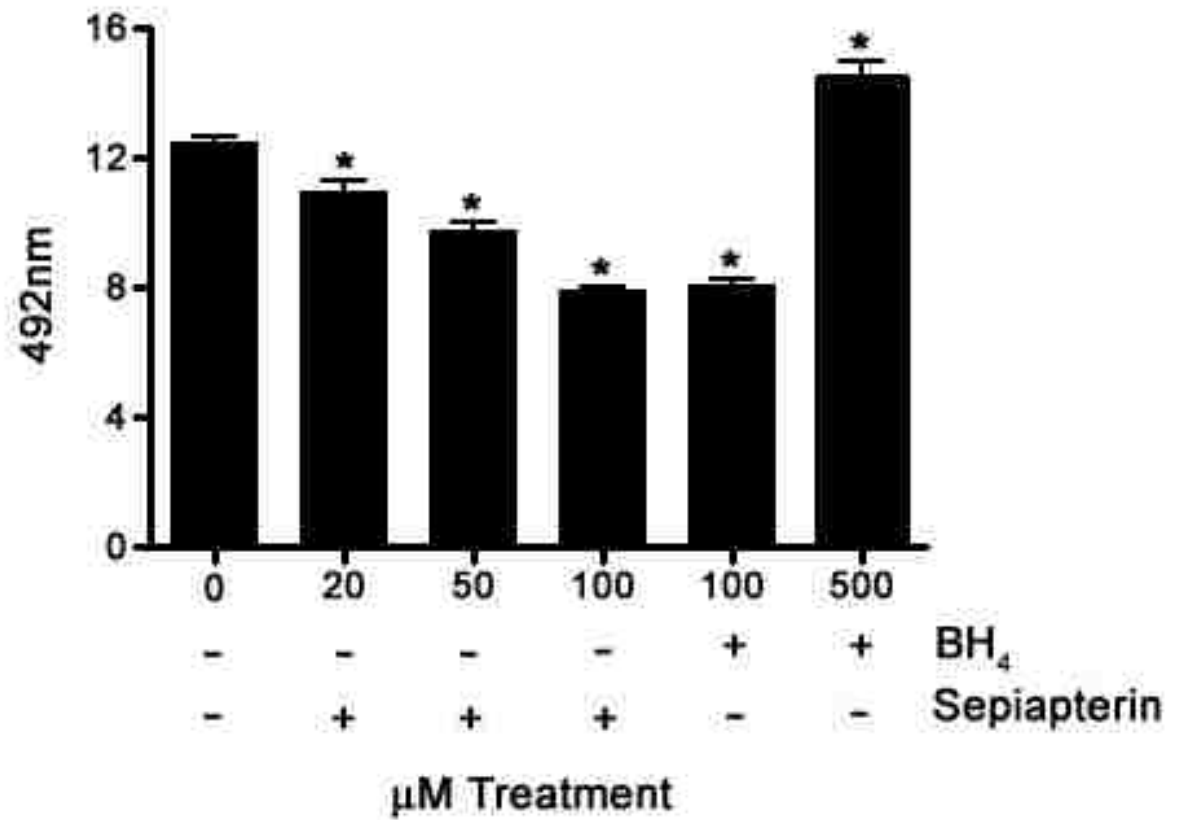
Wilham et al Fig. 5 A & B



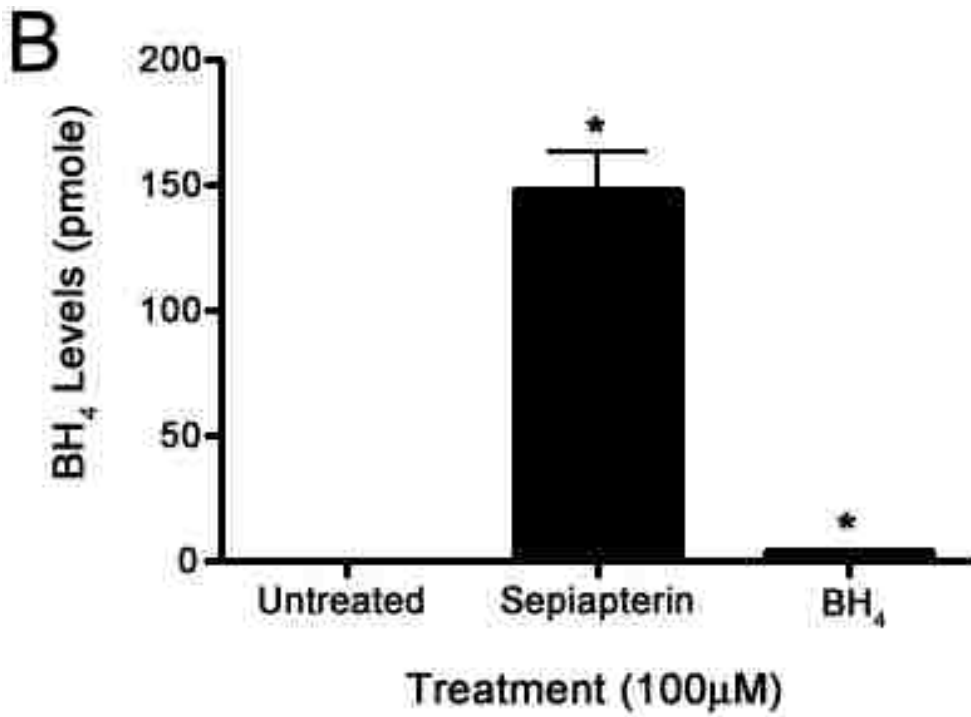
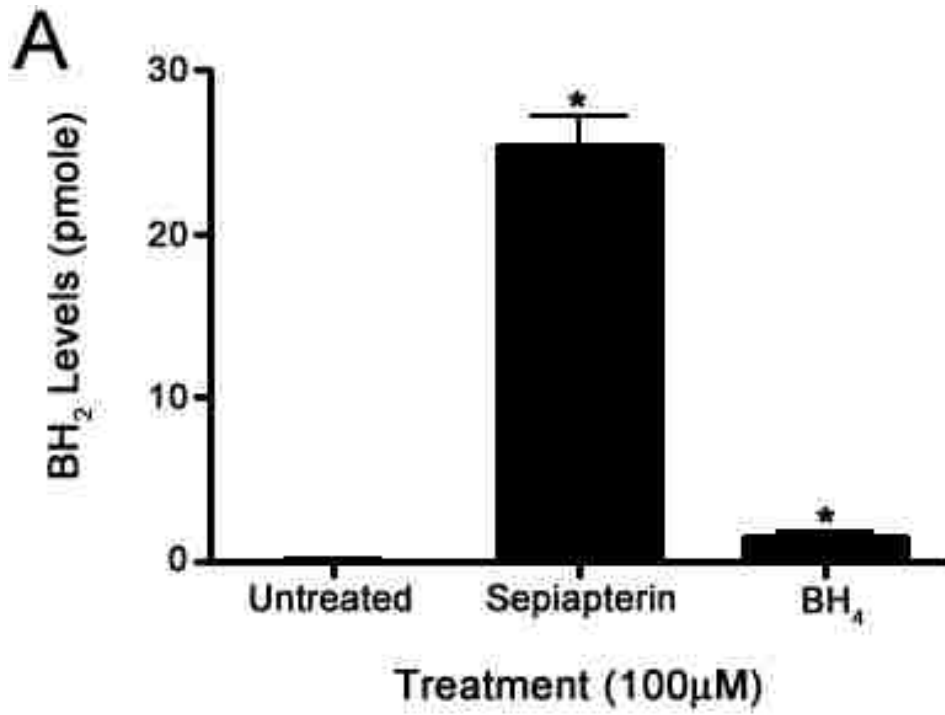
Wilham et al Fig. 6 A & B



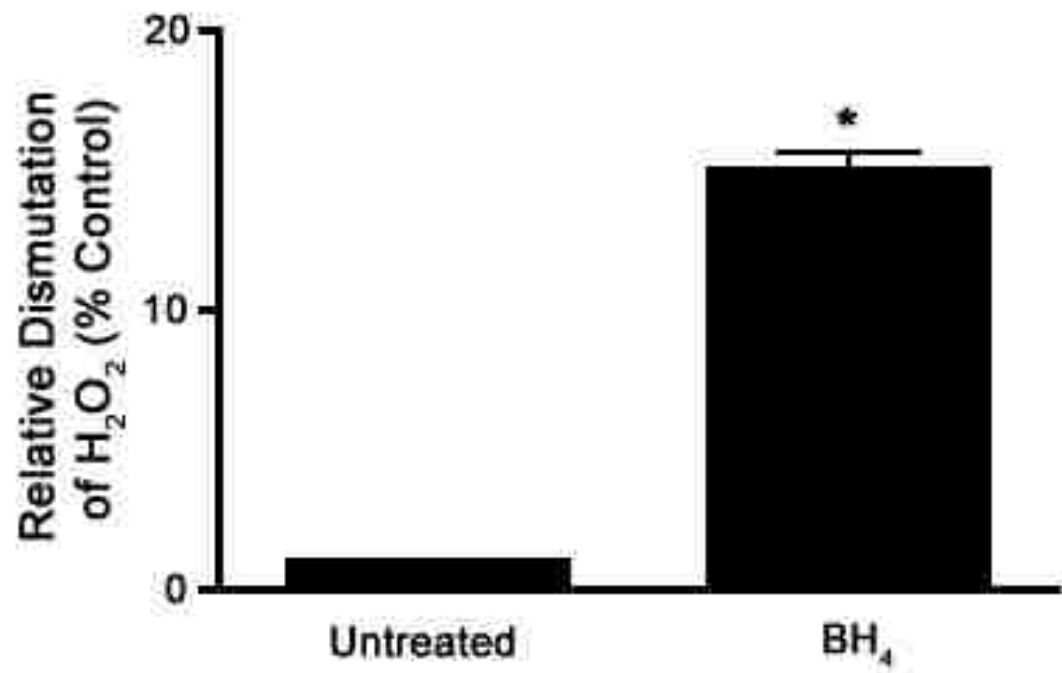
Wilham et al Fig. 7



Wilham et al Fig. 8

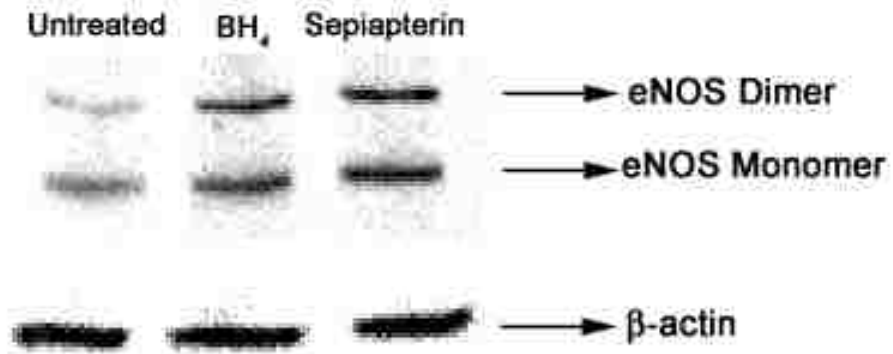


Wilham et al Fig. 9 A & B

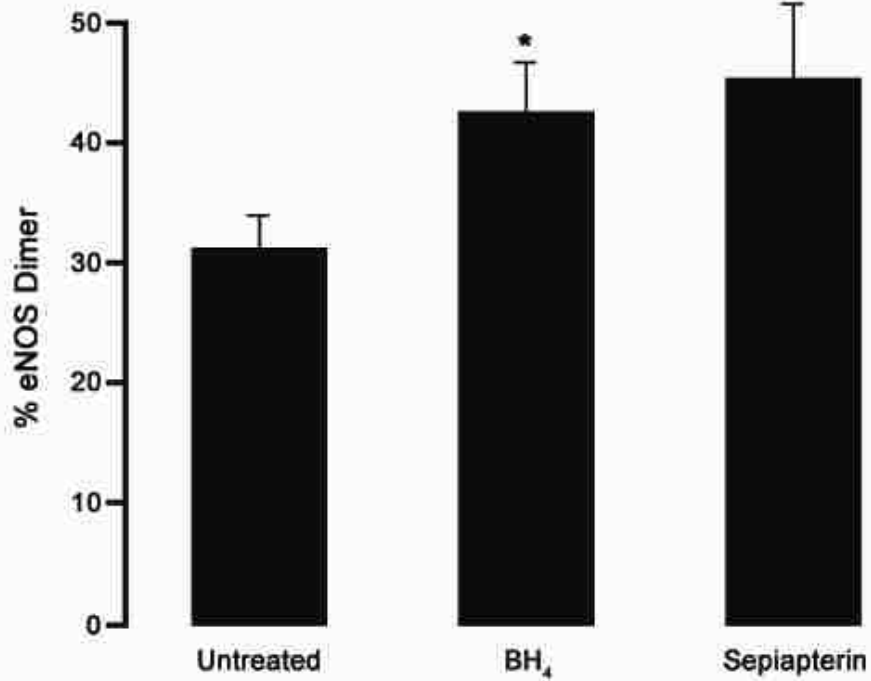


Wilham et al Fig. 10

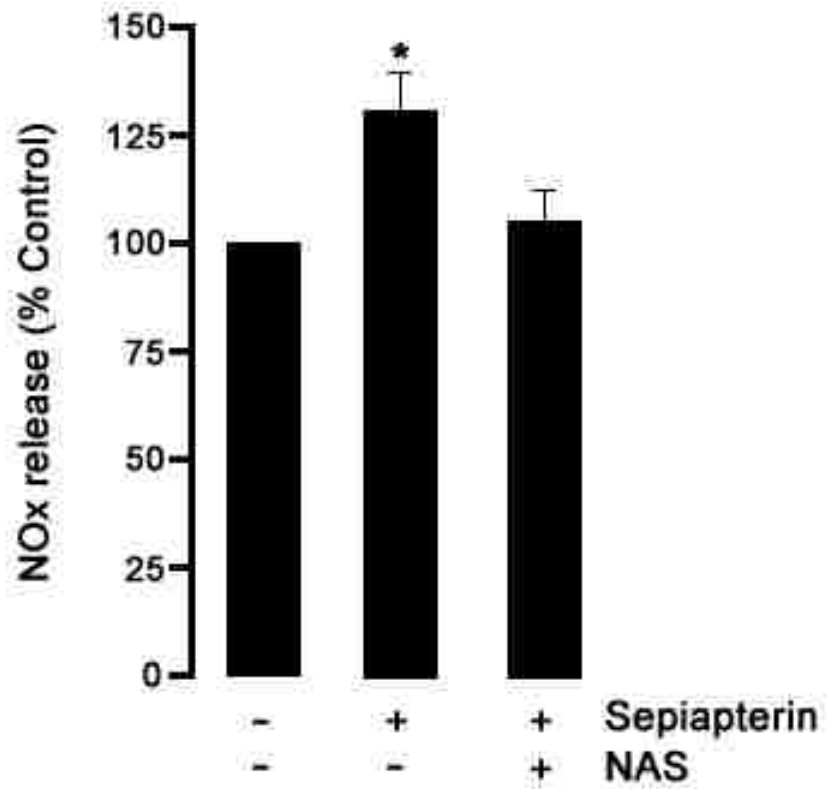
A



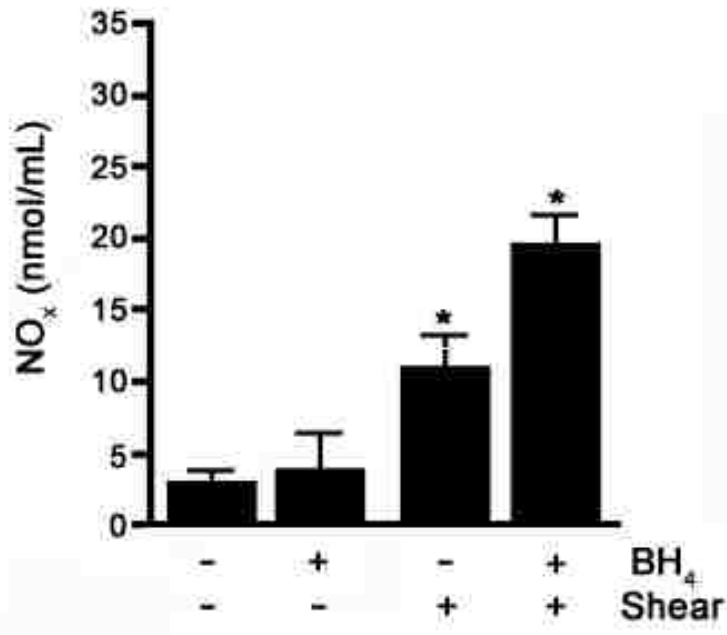
B



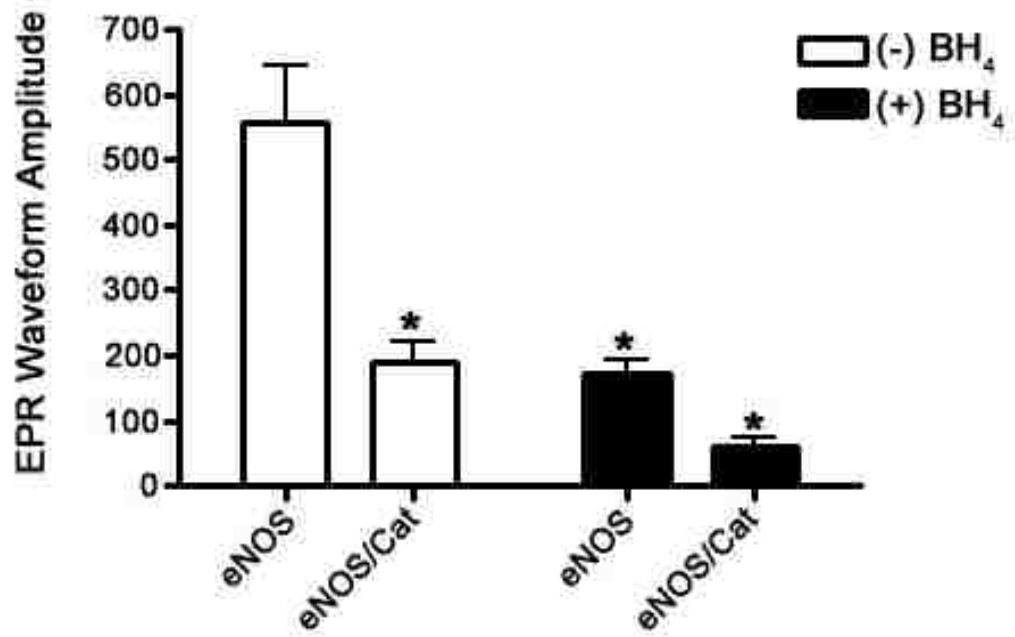
Wilham et al Fig. 11 A & B



Wilham et al Fig. 12



Wilham et al Fig. 13



Wilham et al Fig. 14

COMMON CONCLUSIONS

These studies furthered the understanding of the regulation of endothelial nitric oxide synthase (eNOS) at the transcriptional and post-translational levels. The development of persistent pulmonary hypertension of the newborn (PPHN), a very serious disease affecting nearly 5 in 1000 newborns each year [5] and is associated with a decrease in the activity and expression of eNOS. Our hypothesis was proven correct such that eNOS is regulated by nitric oxide (NO) and reactive oxygen species (ROS), specifically hydrogen peroxide (H₂O₂) through an increase in intracellular zinc (Zn), thus activating the heavy metal responsive transcription factor 1 (MTF-1), which binds to the 5' flanking region of the eNOS promoter. These novel studies and future work may help to identify new targets and novel therapies for PPHN.

Chapter 1

Some early developmental endothelial cell studies in our lab indicated that increases in eNOS expression and activity correlated with increases in cellular levels of labile zinc (Zn) (Figures 3 & 4). We also analyzed the eNOS promoter and found the presence of a heavy metal response element (HRE) located at -899/-893 in the 5'-flanking sequence of the human eNOS gene. Therefore, in our first study, we set out to define the mechanism by which zinc mediated eNOS expression at the transcriptional level and eNOS activity at the post-translational level. We hypothesized that the addition of zinc to fetal pulmonary aortic endothelial cells (FPAECs) would activate heavy metal responsive transcription factor 1 (MTF-1) causing nuclear translocation and binding to the HRE in the 5'-flanking region of the eNOS gene. This in turn would lead to

increased in eNOS protein expression. Since zinc holds the eNOS homo-dimer together, we also hypothesized that the addition of zinc would induce increased in eNOS activity as measured by a release of NO.

Our hypothesis was proven correct in that the addition of low micro-molar levels of zinc to FPAECs increased eNOS dimer protein, total protein, and eNOS promoter-luciferase activity. It also significantly increased MTF-1 nuclear translocation and binding to the eNOS MRE. Zinc depletion studies yielded results contrary to our expectations, however, they did not affect eNOS dimer levels, indicating that once the

eNOS dimer is formed it remains tightly bound.

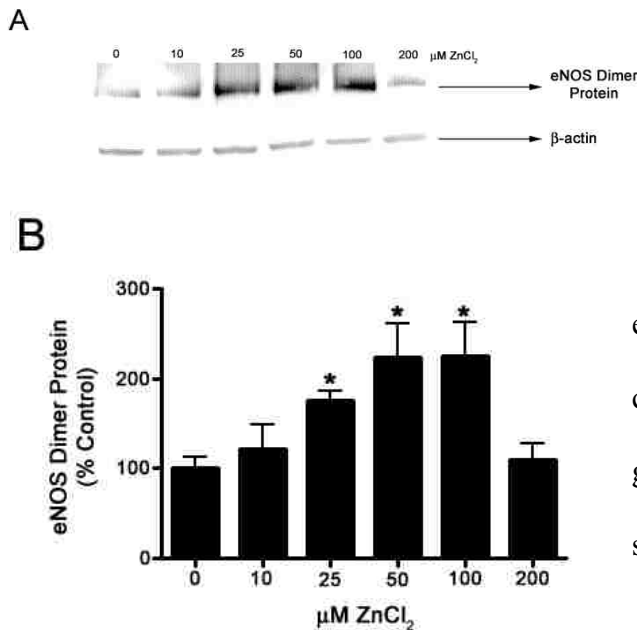


Fig. 6. eNOS dimer levels dose dependently increase with ZnCl_2 treatment up to $100\mu\text{M}$ and then decrease at $200\mu\text{M}$. BAECs were treated with ZnCl_2 for 4hrs. Protein was harvested and LT-PAGE was used to separate eNOS dimer and blots were probed with eNOS Ab. All values are mean \pm SEM (n=4). * $P < 0.05$ vs. $0\mu\text{M ZnCl}_2$.

Chapter 2

PPHN is associated with endothelial dysfunction, and endothelial cells have been shown to increase their generation of hydrogen peroxide and superoxide both from the “uncoupling”

of endothelial nitric oxide synthase (eNOS) and from the activation of nicotinamide adenine dinucleotide phosphate-oxidase (NADPH) complex. Both eNOS mRNA and protein levels

are decreased in PPHN, contributing to decreased levels of NO production. Under normal *in vivo* conditions, endothelial cells are continually exposed to low amounts of nitric oxide (NO) and H₂O₂. Previous *in vitro* data from our lab indicated that high levels of NO and H₂O₂ can actually break up the eNOS dimer [99-101]. However, our preliminary studies for this chapter indicated that low levels of these oxidants increased eNOS expression. Also, both NO and H₂O₂ are known to s-nitrosylate metallothionein (MT-1), thus increasing cellular free zinc [72-74]. Therefore, our second study investigated whether the addition of NO and H₂O₂ increased eNOS expression and activity by increasing cellular free zinc levels. We hypothesized that low micro-molar levels of NO and H₂O₂ increase eNOS expression and activity by increasing cellular free zinc.

Our hypothesis was proven correct such that both NO and H₂O₂ increased cellular levels of labile zinc. It also increased eNOS mRNA, total protein, and promoter-luciferase activity. Both NO and H₂O₂ caused significantly higher zinc dependent nuclear translocation and binding of the eNOS promoter by MTF-1. Findings from this study demonstrate a pathway of eNOS activation by low dose NO and H₂O₂

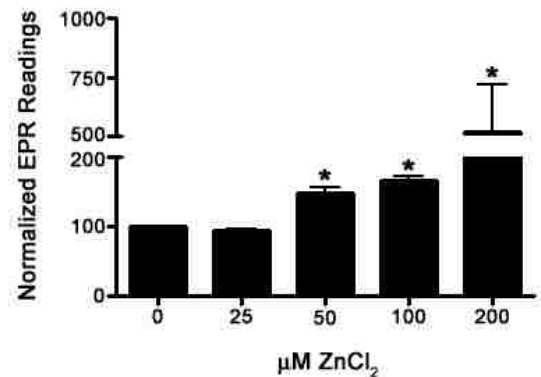


Fig. 7. 4hr Zinc treatments of 50uM and greater lead to increased ROS production in BAECs. BAECs were treated for 4hrs with ZnCl₂. At 3.5hrs, CMH spin trap was added to the cells. EPR analysis was performed on the samples. All values are mean ± SEM (n=4). * P<0.05 vs. 0μM ZnCl₂.

through free zinc release and heavy metal responsive transcription factor 1 (MTF-1) activation.

Chapter 3

Hypertensive vasoconstriction is postulated to involve the degradation of NO by reactive oxygen species (ROS), especially the superoxide anion. Antioxidant therapy has been proposed as a treatment regimen for pulmonary hypertension and other pathologies linked to endothelial dysfunction. Results from the first two chapters indicated that low levels of zinc, NO, or H₂O₂ can actually stimulate eNOS, however, when at higher levels, this stimulation was abolished. Using electron paramagnetic resonance (EPR), we looked at ROS production in endothelial cells following exposure to increasing, non-toxic doses of zinc (Figure 7). ROS levels were much lower in exposures that stimulated eNOS compared to the ROS levels in exposures to higher levels of zinc that did not stimulate eNOS (Figure 6 & 7). Since the critical mediator of pulmonary vasorelaxation is generation of NO by eNOS, we wanted to determine the effect of ROS, specifically superoxide (O₂⁻) on eNOS function in ovine pulmonary arterial endothelial cells (PAECs).

Therefore, we set out to establish whether modulating the cellular redox state in endothelial cells would alter eNOS expression and/or activity. We hypothesized that high levels of O₂⁻ would indirectly inhibit eNOS by scavenging NO since NO readily reacts with O₂⁻ to produce peroxynitrite. Results indicate that our hypothesis was proven at least partially incorrect. At high levels, O₂⁻ decreased eNOS protein levels and the

catalytic capability of the enzyme. Some $O_2^{\cdot-}$ may be directly inactivating NO, however, at the levels used in these experiments, $O_2^{\cdot-}$ actually caused eNOS fragmentation.

These experiments suggest that NO-NOS system represents a complex bioregulated pathway whose regulation is tightly associated with the redox status of the cell. Thus, the increases in ROS that may be involved in the development of endothelial dysfunction, which is associated with a number of vascular diseases, may cause a reduction in eNOS activity, possibly by inducing eNOS fragmentation and directly interacting with NO to form more reactive radicals.

Chapter 4

Persistent pulmonary hypertension of the newborn (PPHN) is associated with increased ROS production. Oxidant production plays an important role both in the normal functioning of the vascular system as well as the pathogenesis of vascular disease. As we saw in chapters 2 & 3, eNOS is dynamically regulated by the redox status of the cell. The production of nitric oxide (NO) in the vessel wall by the eNOS is dependent on essential enzyme cofactors, including the most potent naturally occurring reducing agent, tetrahydrobiopterin (BH_4). In a study by Wang, et al., rats were supplemented with fructose in their diet, which is known to produce oxidative stress in vivo, and it was found that endothelium-dependent relaxations were impaired [102]. Supplementing the fructose-fed rats with BH_4 in the water partially restored endothelium-dependent vascular relaxations and eNOS protein levels within the rat aortas [102]. Although BH_4 is thought to maintain eNOS dimer, the exact mechanism of this maintenance is unknown.

To look further into the regulation of eNOS by ROS, we explored the role of BH₄. Utilizing NIH3T3 cells, a line with very low BH₄ levels, and bovine aortic endothelial cells (BAECs), we hypothesized that BH₄'s role in the regulation of eNOS was due to its high antioxidant potential. Our results in NIH3T3 cells, which have very low levels of BH₄, demonstrate that catalase transduction decreased ROS levels, specifically H₂O₂, and increased eNOS total protein, dimer/monomer protein ratio, and eNOS activity. In BAECs, the addition of BH₄ or L-sepiapterin, the substrate for the synthesis of BH₄, decreased ROS levels and increased eNOS dimer levels and activity. The addition of BH₄ to NIH3T3 cells also decreased ROS production. The results supported the hypothesis such that the association of BH₄ with eNOS regulates eNOS protein levels and activity mainly due to its high antioxidant potential.

Summary/Future Studies

In summary, these studies establish a link in endothelial cells between the oxidative environment, cellular zinc homeostasis and eNOS protein and activity. Maintaining certain dietary levels of zinc could be important in retaining healthy endothelial function and zinc supplementation during pregnancy may help minimize symptoms PPHN by increasing eNOS levels and activity prior to birth.

The regulation of the NO-NOS system is complex and does involve many factors. It would be interesting to look further into the involvement of other zinc-finger transcription factors, such as SP-1 and AP-1, in the regulation of eNOS. Other eNOS cofactors and associated proteins, such as HSP90 may also play important roles in eNOS regulation. Certain hormones, such as estrogen, play an important role in the fetal-to-

newborn transition and it would be interesting to explore their role in the cellular oxidative environment, zinc homeostasis, and eNOS regulation. Continuing to further the understanding of eNOS regulation may help to identify new pathways and novel therapies for cardiovascular diseases such as PPHN.

LITERATURE CITED

1. Dawes, G.S., et al., *Changes in the lungs of the new-born lamb*. J Physiol, 1953. **121**(1): p. 141-62.
2. Iwamoto, H.S., D. Teitel, and A.M. Rudolph, *Effects of birth-related events on blood flow distribution*. Pediatr Res, 1987. **22**(6): p. 634-40.
3. Rudolph, A.M., *Fetal and neonatal pulmonary circulation*. Annu Rev Physiol, 1979. **41**: p. 383-95.
4. Petros, A.J. and C.M. Pierce, *The management of pulmonary hypertension*. Paediatr Anaesth, 2006. **16**(8): p. 816-21.
5. Hooper, W.C., et al., *Vascular endothelium summary statement V: Pulmonary hypertension and acute lung injury: Public health implications*. Vascul Pharmacol, 2006.
6. Konduri, G.G., et al., *Early inhaled nitric oxide therapy for term and near-term newborn infants with hypoxic respiratory failure: neurodevelopmental follow-up*. J Pediatr, 2007. **150**(3): p. 235-40, 240 e1.
7. Kirsch, E.A., et al., *Estrogen acutely stimulates endothelial nitric oxide synthase in H441 human airway epithelial cells*. Am J Respir Cell Mol Biol, 1999. **20**(4): p. 658-66.
8. German, Z., et al., *Molecular basis of cell-specific endothelial nitric-oxide synthase expression in airway epithelium*. J Biol Chem, 2000. **275**(11): p. 8183-9.
9. Drummond, G.R., et al., *Transcriptional and posttranscriptional regulation of endothelial nitric oxide synthase expression by hydrogen peroxide*. Circ Res, 2000. **86**(3): p. 347-54.
10. Fleming, I. and R. Busse, *Molecular mechanisms involved in the regulation of the endothelial nitric oxide synthase*. Am J Physiol Regul Integr Comp Physiol, 2003. **284**(1): p. R1-12.
11. Fulton, D., J.P. Gratton, and W.C. Sessa, *Post-translational control of endothelial nitric oxide synthase: why isn't calcium/calmodulin enough?* J Pharmacol Exp Ther, 2001. **299**(3): p. 818-24.
12. Govers, R. and T.J. Rabelink, *Cellular regulation of endothelial nitric oxide synthase*. Am J Physiol Renal Physiol, 2001. **280**(2): p. F193-206.
13. Li, H., T. Wallerath, and U. Forstermann, *Physiological mechanisms regulating the expression of endothelial-type NO synthase*. Nitric Oxide, 2002. **7**(2): p. 132-47.
14. Searles, C.D., *Transcriptional and posttranscriptional regulation of endothelial nitric oxide synthase expression*. Am J Physiol Cell Physiol, 2006. **291**(5): p. C803-16.
15. Tai, S.C., G.B. Robb, and P.A. Marsden, *Endothelial nitric oxide synthase: a new paradigm for gene regulation in the injured blood vessel*. Arterioscler Thromb Vasc Biol, 2004. **24**(3): p. 405-12.
16. Bloch, K.D., et al., *Pulmonary soluble guanylate cyclase, a nitric oxide receptor, is increased during the perinatal period*. Am J Physiol, 1997. **272**(3 Pt 1): p. L400-6.
17. Sanchez, L.S., et al., *Cyclic-GMP-binding, cyclic-GMP-specific phosphodiesterase (PDE5) gene expression is regulated during rat pulmonary development*. Pediatr Res, 1998. **43**(2): p. 163-8.

18. Shaul, P.W., *Ontogeny of nitric oxide in the pulmonary vasculature*. Semin Perinatol, 1997. **21**(5): p. 381-92.
19. Shaul, P.W., M.A. Farrar, and R.R. Magness, *Pulmonary endothelial nitric oxide production is developmentally regulated in the fetus and newborn*. Am J Physiol, 1993. **265**(4 Pt 2): p. H1056-63.
20. Xue, C., P.R. Reynolds, and R.A. Johns, *Developmental expression of NOS isoforms in fetal rat lung: implications for transitional circulation and pulmonary angiogenesis*. Am J Physiol, 1996. **270**(1 Pt 1): p. L88-100.
21. Parker, T.A., et al., *Developmental changes in endothelial nitric oxide synthase expression and activity in ovine fetal lung*. Am J Physiol Lung Cell Mol Physiol, 2000. **278**(1): p. L202-8.
22. Shaul, P.W., *Regulation of vasodilator synthesis during lung development*. Early Hum Dev, 1999. **54**(3): p. 271-94.
23. Loesch, A. and G. Burnstock, *Ultrastructural localization of nitric oxide synthase and endothelin in rat pulmonary artery and vein during postnatal development and ageing*. Cell Tissue Res, 1996. **283**(3): p. 355-65.
24. Marsden, P.A., et al., *Structure and chromosomal localization of the human constitutive endothelial nitric oxide synthase gene*. J Biol Chem, 1993. **268**(23): p. 17478-88.
25. Rairigh, R.L., et al., *Role of inducible nitric oxide synthase in regulation of pulmonary vascular tone in the late gestation ovine fetus*. J Clin Invest, 1998. **101**(1): p. 15-21.
26. Liu, S., *Nitric oxide-dependent pro-oxidant and pro-apoptotic effect of metallothioneins in HL-60 cells challenged with cupric nitrilotriacetate*. Biochemical Journal, 2001. **354**(Pt 2): p. 397-406.
27. Pearce, L.L., *Metallothionein, nitric oxide and zinc homeostasis in vascular endothelial cells*. Journal of Nutrition, 2000. **130**(5S Suppl): p. 1467S-70S.
28. Pitt, B.R., *Overexpression of metallothionein decreases sensitivity of pulmonary endothelial cells to oxidant injury*. American Journal of Physiology, 1997. **273**(4 Pt 1): p. L856-65.
29. Pearce, L.L., *Role of metallothionein in nitric oxide signaling as revealed by a green fluorescent fusion protein*. Proceedings of the National Academy of Sciences of the United States of America, 2000. **97**(1): p. 477-82.
30. Sherman, T.S., et al., *Nitric oxide synthase isoform expression in the developing lung epithelium*. Am J Physiol, 1999. **276**(2 Pt 1): p. L383-90.
31. Venema, R.C., et al., *Organization of the bovine gene encoding the endothelial nitric oxide synthase*. Biochim Biophys Acta, 1994. **1218**(3): p. 413-20.
32. Teichert, A.M., et al., *Characterization of the murine endothelial nitric oxide synthase promoter*. Biochim Biophys Acta, 1998. **1443**(3): p. 352-7.
33. Karantzoulis-Fegaras, F., et al., *Characterization of the human endothelial nitric-oxide synthase promoter*. J Biol Chem, 1999. **274**(5): p. 3076-93.
34. Fineman, J.R., S.J. Soifer, and M.A. Heymann, *Regulation of pulmonary vascular tone in the perinatal period*. Annu Rev Physiol, 1995. **57**: p. 115-34.
35. Furgott, R.F., Vanhoutte, P.M., *Endothelium-derived relaxing and contracting factors*. FASEB J., 1989(3): p. 2007-2018.

36. Wiklund, N.P., et al., *Modulatory role of endogenous nitric oxide in pulmonary circulation in vivo*. Eur J Pharmacol, 1990. **185**(1): p. 123-4.
37. Ghosh, D.K., H.M. Abu-Soud, and D.J. Stuehr, *Domains of macrophage N(O) synthase have divergent roles in forming and stabilizing the active dimeric enzyme*. Biochemistry, 1996. **35**(5): p. 1444-9.
38. Rodriguez-Crespo, I. and P.R. Ortiz de Montellano, *Human endothelial nitric oxide synthase: expression in Escherichia coli, coexpression with calmodulin, and characterization*. Arch Biochem Biophys, 1996. **336**(1): p. 151-6.
39. Venema, R.C., et al., *Subunit interactions of endothelial nitric-oxide synthase. Comparisons to the neuronal and inducible nitric-oxide synthase isoforms*. J Biol Chem, 1997. **272**(2): p. 1276-82.
40. Dawson, T.M. and S.H. Snyder, *Gases as biological messengers: nitric oxide and carbon monoxide in the brain*. J Neurosci, 1994. **14**(9): p. 5147-59.
41. Ignarro, L.J., G. Ross, and J. Tillisch, *Pharmacology of endothelium-derived nitric oxide and nitrovasodilators*. West J Med, 1991. **154**(1): p. 51-62.
42. Boulanger, C.M., *Secondary endothelial dysfunction: hypertension and heart failure*. J Mol Cell Cardiol, 1999. **31**(1): p. 39-49.
43. Sarkar, R. and R.C. Webb, *Does nitric oxide regulate smooth muscle cell proliferation? A critical appraisal*. J Vasc Res, 1998. **35**(3): p. 135-42.
44. Abman, S.H., P.F. Shanley, and F.J. Accurso, *Failure of postnatal adaptation of the pulmonary circulation after chronic intrauterine pulmonary hypertension in fetal lambs*. J Clin Invest, 1989. **83**(6): p. 1849-58.
45. Black, S.M., et al., *Increased endothelial NOS in lambs with increased pulmonary blood flow and pulmonary hypertension*. Am J Physiol, 1998. **275**(5 Pt 2): p. H1643-51.
46. Giaid, A. and D. Saleh, *Reduced expression of endothelial nitric oxide synthase in the lungs of patients with pulmonary hypertension*. N Engl J Med, 1995. **333**(4): p. 214-21.
47. Morin, F.C., 3rd, *Ligating the ductus arteriosus before birth causes persistent pulmonary hypertension in the newborn lamb*. Pediatr Res, 1989. **25**(3): p. 245-50.
48. Munzel, T., et al., *Effects of long-term nitroglycerin treatment on endothelial nitric oxide synthase (NOS III) gene expression, NOS III-mediated superoxide production, and vascular NO bioavailability*. Circ Res, 2000. **86**(1): p. E7-E12.
49. Ross, R., *The pathogenesis of atherosclerosis: a perspective for the 1990s*. Nature, 1993. **362**(6423): p. 801-9.
50. Anderson, T.J., *Nitric oxide, atherosclerosis and the clinical relevance of endothelial dysfunction*. Heart Fail Rev, 2003. **8**(1): p. 71-86.
51. Feron, O., et al., *Hypercholesterolemia decreases nitric oxide production by promoting the interaction of caveolin and endothelial nitric oxide synthase*. J Clin Invest, 1999. **103**(6): p. 897-905.
52. Goligorsky, M.S., et al., *Relationships between caveolae and eNOS: everything in proximity and the proximity of everything*. Am J Physiol Renal Physiol, 2002. **283**(1): p. F1-10.
53. Morio, H., et al., *Effect of modified LDL on the release of NO and PGI2 from rat peritoneal macrophages*. J Atheroscler Thromb, 1995. **2**(1): p. 41-5.

54. Cai, H. and D.G. Harrison, *Endothelial dysfunction in cardiovascular diseases: the role of oxidant stress*. *Circ Res*, 2000. **87**(10): p. 840-4.
55. Minor, R.L., Jr., et al., *Diet-induced atherosclerosis increases the release of nitrogen oxides from rabbit aorta*. *J Clin Invest*, 1990. **86**(6): p. 2109-16.
56. Mugge, A., et al., *Chronic treatment with polyethylene-glycolated superoxide dismutase partially restores endothelium-dependent vascular relaxations in cholesterol-fed rabbits*. *Circ Res*, 1991. **69**(5): p. 1293-300.
57. White, C.R., et al., *Circulating plasma xanthine oxidase contributes to vascular dysfunction in hypercholesterolemic rabbits*. *Proc Natl Acad Sci U S A*, 1996. **93**(16): p. 8745-9.
58. Heitzer, T., et al., *Tetrahydrobiopterin improves endothelium-dependent vasodilation in chronic smokers: evidence for a dysfunctional nitric oxide synthase*. *Circ Res*, 2000. **86**(2): p. E36-41.
59. Holland, J.A., et al., *Low-density lipoprotein stimulated peroxide production and endocytosis in cultured human endothelial cells: mechanisms of action*. *Endothelium*, 1997. **5**(3): p. 191-207.
60. Ratych, R.E., R.S. Chuknyiska, and G.B. Bulkley, *The primary localization of free radical generation after anoxia/reoxygenation in isolated endothelial cells*. *Surgery*, 1987. **102**(2): p. 122-31.
61. Griendling, K.K., D. Sorescu, and M. Ushio-Fukai, *NAD(P)H oxidase: role in cardiovascular biology and disease*. *Circ Res*, 2000. **86**(5): p. 494-501.
62. Vasquez-Vivar, J., et al., *Effect of redox-active drugs on superoxide generation from nitric oxide synthases: biological and toxicological implications*. *Free Radic Res*, 1999. **31**(6): p. 607-17.
63. Muijsers, R.B., et al., *Peroxynitrite: a two-faced metabolite of nitric oxide*. *Life Sci*, 1997. **60**(21): p. 1833-45.
64. Murphy, M.P., et al., *Peroxynitrite: a biologically significant oxidant*. *Gen Pharmacol*, 1998. **31**(2): p. 179-86.
65. Meier, B., et al., *Human fibroblasts release reactive oxygen species in response to interleukin-1 or tumour necrosis factor-alpha*. *Biochem J*, 1989. **263**(2): p. 539-45.
66. Matsubara, T. and M. Ziff, *Increased superoxide anion release from human endothelial cells in response to cytokines*. *J Immunol*, 1986. **137**(10): p. 3295-8.
67. Matsubara, T. and M. Ziff, *Superoxide anion release by human endothelial cells: synergism between a phorbol ester and a calcium ionophore*. *J Cell Physiol*, 1986. **127**(2): p. 207-10.
68. Griendling, K.K., et al., *Angiotensin II stimulates NADH and NADPH oxidase activity in cultured vascular smooth muscle cells*. *Circ Res*, 1994. **74**(6): p. 1141-8.
69. Wiseman, D.A., et al., *Alterations in zinc homeostasis underlie endothelial cell death induced by oxidative stress from acute exposure to hydrogen peroxide*. *Am J Physiol Lung Cell Mol Physiol*, 2007. **292**(1): p. L165-77.
70. Wiseman, D.A., et al., *Endothelial response to stress from exogenous Zn²⁺ resembles that of NO-mediated nitrosative stress, and is protected by MT-1 overexpression*. *Am J Physiol Cell Physiol*, 2006. **291**(3): p. C555-68.

71. Boulden, B.M., et al., *Early determinants of H₂O₂-induced endothelial dysfunction*. Free Radic Biol Med, 2006. **41**(5): p. 810-7.
72. Zhang, B., et al., *Activity of metal-responsive transcription factor 1 by toxic heavy metals and H₂O₂ in vitro is modulated by metallothionein*. Mol Cell Biol, 2003. **23**(23): p. 8471-85.
73. Pearce, L.L., et al., *Metallothionein, nitric oxide and zinc homeostasis in vascular endothelial cells*. J Nutr, 2000. **130**(5S Suppl): p. 1467S-70S.
74. St Croix, C.M., et al., *Nitric oxide-induced changes in intracellular zinc homeostasis are mediated by metallothionein/thionein*. Am J Physiol Lung Cell Mol Physiol, 2002. **282**(2): p. L185-92.
75. Spahl, D.U., et al., *Regulation of zinc homeostasis by inducible NO synthase-derived NO: nuclear metallothionein translocation and intranuclear Zn²⁺ release*. Proc Natl Acad Sci U S A, 2003. **100**(24): p. 13952-7.
76. Ignarro, L.J., *Heme-dependent activation of soluble guanylate cyclase by nitric oxide: regulation of enzyme activity by porphyrins and metalloporphyrins*. Semin Hematol, 1989. **26**(1): p. 63-76.
77. Stamler, J.S., et al., *S-nitrosylation of proteins with nitric oxide: synthesis and characterization of biologically active compounds*. Proc Natl Acad Sci U S A, 1992. **89**(1): p. 444-8.
78. Liu, S., et al., *Nitric oxide-dependent pro-oxidant and pro-apoptotic effect of metallothioneins in HL-60 cells challenged with cupric nitrilotriacetate*. Biochem J, 2001. **354**(Pt 2): p. 397-406.
79. Pearce, L.L., et al., *Role of metallothionein in nitric oxide signaling as revealed by a green fluorescent fusion protein*. Proc Natl Acad Sci U S A, 2000. **97**(1): p. 477-82.
80. Berendji, D., et al., *Nitric oxide mediates intracytoplasmic and intranuclear zinc release*. FEBS Lett, 1997. **405**(1): p. 37-41.
81. Tang, Z.L., et al., *Role of zinc in pulmonary endothelial cell response to oxidative stress*. Am J Physiol Lung Cell Mol Physiol, 2001. **281**(1): p. L243-9.
82. Nyborg, J.K. and O.B. Peersen, *That zinging feeling: the effects of EDTA on the behaviour of zinc-binding transcriptional regulators*. Biochem J, 2004. **381**(Pt 3): p. e3-4.
83. Heuchel, R., et al., *The transcription factor MTF-1 is essential for basal and heavy metal-induced metallothionein gene expression*. Embo J, 1994. **13**(12): p. 2870-5.
84. Otsuka, F., et al., *Purification and characterization of a protein that binds to metal responsive elements of the human metallothionein IIA gene*. J Biol Chem, 1994. **269**(38): p. 23700-7.
85. Radtke, F., et al., *Cloned transcription factor MTF-1 activates the mouse metallothionein I promoter*. Embo J, 1993. **12**(4): p. 1355-62.
86. Balamurugan, K., et al., *Metal-responsive transcription factor (MTF-1) and heavy metal stress response in Drosophila and mammalian cells: a functional comparison*. Biol Chem, 2004. **385**(7): p. 597-603.
87. Lichtlen, P. and W. Schaffner, *The "metal transcription factor" MTF-1: biological facts and medical implications*. Swiss Med Wkly, 2001. **131**(45-46): p. 647-52.

88. Hamer, D.H., *Metallothionein*. Annu Rev Biochem, 1986. **55**: p. 913-51.
89. Radtke, F., et al., *Functional domains of the heavy metal-responsive transcription regulator MTF-1*. Nucleic Acids Res, 1995. **23**(12): p. 2277-86.
90. Giedroc, D.P., X. Chen, and J.L. Apuy, *Metal response element (MRE)-binding transcription factor-1 (MTF-1): structure, function, and regulation*. Antioxid Redox Signal, 2001. **3**(4): p. 577-96.
91. Palmiter, R.D., *Regulation of metallothionein genes by heavy metals appears to be mediated by a zinc-sensitive inhibitor that interacts with a constitutively active transcription factor, MTF-1*. Proc Natl Acad Sci U S A, 1994. **91**(4): p. 1219-23.
92. Langmade, S.J., et al., *The transcription factor MTF-1 mediates metal regulation of the mouse ZnT1 gene*. J Biol Chem, 2000. **275**(44): p. 34803-9.
93. Lichtlen, P., et al., *Target gene search for the metal-responsive transcription factor MTF-1*. Nucleic Acids Res, 2001. **29**(7): p. 1514-23.
94. Moellering, D., et al., *The induction of GSH synthesis by nanomolar concentrations of NO in endothelial cells: a role for gamma-glutamylcysteine synthetase and gamma-glutamyl transpeptidase*. FEBS Lett, 1999. **448**(2-3): p. 292-6.
95. Mueller, P.R., S.J. Salser, and B. Wold, *Constitutive and metal-inducible protein: DNA interactions at the mouse metallothionein I promoter examined by in vivo and in vitro footprinting*. Genes Dev, 1988. **2**(4): p. 412-27.
96. Searle, P.F., *Zinc dependent binding of a liver nuclear factor to metal response element MRE-a of the mouse metallothionein-I gene and variant sequences*. Nucleic Acids Res, 1990. **18**(16): p. 4683-90.
97. Stuart, G.W., P.F. Searle, and R.D. Palmiter, *Identification of multiple metal regulatory elements in mouse metallothionein-I promoter by assaying synthetic sequences*. Nature, 1985. **317**(6040): p. 828-31.
98. Gunes, C., et al., *Embryonic lethality and liver degeneration in mice lacking the metal-responsive transcriptional activator MTF-1*. Embo J, 1998. **17**(10): p. 2846-54.
99. Black, S.M., et al., *Inhaled nitric oxide inhibits NOS activity in lambs: potential mechanism for rebound pulmonary hypertension*. Am J Physiol, 1999. **277**(5 Pt 2): p. H1849-56.
100. Ravi, K., et al., *S-nitrosylation of endothelial nitric oxide synthase is associated with monomerization and decreased enzyme activity*. Proc Natl Acad Sci U S A, 2004. **101**(8): p. 2619-24.
101. Sheehy, A.M., M.A. Burson, and S.M. Black, *Nitric oxide exposure inhibits endothelial NOS activity but not gene expression: a role for superoxide*. Am J Physiol, 1998. **274**(5 Pt 1): p. L833-41.
102. Wang, X., et al., *Tetrahydrobiopterin prevents endothelial dysfunction and restores adiponectin levels in rats*. Eur J Pharmacol, 2007. **555**(1): p. 48-53.